GULLY EROSION IN THE SANDSPRUIT CATCHMENT, WESTERN CAPE, WITH A FOCUS ON THE DISCONTINUOUS SPLIT GULLY SYSTEM AT MALANSDAM

by

GEORGE OLIVIER

Thesis presented in partial fulfilment of the requirements for the degree of Master of Science at Stellenbosch University

Supervisor: Dr WP de Clercq

Department of Soil Sciences

Co-Supervisor: Mr BHA Schloms

Department of Geography and Environmental Sciences

December 2013

Declaration

By submitting this thesis electronically, I declare that the entirety of the work contained therein is my own, original work, that I am the sole author thereof (save to the extent explicitly otherwise stated), that reproduction and publication thereof by Stellenbosch University will not infringe any third party rights and that I have not previously in its entirety or in part submitted it for obtaining any qualification

December 2013

ABSTRACT

Gully erosion is a major environmental problem not only having direct influences on site but also indirect influences felt further down the catchment. Combating gully erosion has proven to be elusive due to the difficulty in finding the causal factors and developing mechanisms involved. Soil is the medium in which gully erosion occurs yet few research have investigated it as a driving factor behind gully development and those that have has done it in a very elementary way.

The first aim of this project was to physically and chemically characterise and classify the discontinuous gully system at Malansdam to establish the relationship between landscape hydrology and geomorphologic gully development with a focus on control factors. This was done by field observations, physical measurements and spatial and hydrological analyses with a Geographical Information System (GIS). The Malansdam gully system was the first ever recorded Strahler stream order (SSO) 5 classical gully system with the most active region being in the upper reaches where a steeper slope is experienced. Although piping was observed the V-shape channels and SAR data from traditional wet analysis indicated runoff to be the dominant formation process. A duo of factors, consisting of one anthropogenic and one natural factor respectively, was found that the major control factors behind the gully formation. A unique anthropogenic factor that has never been published beforehand was found to be the anthropogenic driving factor namely the ploughed contour cultivation technique employed by the farmers in the Sandspruit catchment. The ploughed contours act as channels firstly collecting and secondly moving water that would have drained naturally downwards in the valley to one exit point in the gully system. This allows increased erosive energy because of the larger volumes of water entering one single point in the upper reaches of the gully system where a steeper slope is experienced. The driving factor in the natural group was determined to be weak soil structure due to an abundant amount of exchangeable Mg^{2+} cations occupying the exchange sites on the clay fraction. This would cause soil to disperse in the presence of water even with a low amount of exchangeable Na^{+}. Combat methods would accordingly exist in the form of rectifying the soil structure and finding an alternative to the ploughed contour system currently employed, but also planting vegetation especially grass or wheat in the gully channels.

The second aim of this project was to determine the capability of Near Infrared (NIR) spectrometry, with wavenumbers 12 500 – 4 000 cm-1, to predict indicators used in soil science to establish the dispersive nature of a soil. These indices included the Exchangeable Sodium Percentage (ESP), Sodium Absorption Ratio (SAR), Magnesium Saturation Percentage (MS%), Electrical Conductivity (EC), Potential Hydrogen (pH) as well as the four main exchangeable cations namely calcium (Ca^{2+}), potassium (K^{+}), sodium (Na^{+}) and magnesium (Mg^{2+}). Surface and subsurface soil samples were collected from active gully heads. These samples were minimally pre-processed thus only dried, milled and sieved. Thereafter it was subject to NIR analysis making use of the Bruker multi-purpose

FT-NIR Analyser (MPA; Bruker Optik GmbH, Germany) with a spectral range of 12 500cm-1 to 4000cm-1 which is. Partial Least Square Regression (PLSR) models were built for each index and the exchangeable cations making use of QUANT 2 utility of OPUS 6.5 (MPA; Bruker Optik GmbH, Germany) software. Five different regrssion statistics namely the coefficient of determination (r^2), Root Mean Square Error of Cross Validation (RMSECV), Ratio of Performance to Deviation (RPD), Bias and the Ratio of Performance of Quartiles (RPIQ) were used to assess the legitimacy of each PLSR model. Upon validation all the PLSR models performed in line with previously published work and in certain cases better. The only exception was MS% which would require further investigation. NIR thus possess the capability to predict a soil's dispersive nature in a fast, reliable, inexpensive and non- destructive way, thus implying whether or not it contributes to gully erosion at a significant level or only minimally.

Keywords and Phrase: Electrical Conductivity, exchangeable cations (Calcium, Potassium, Sodium and Magnesium), Exchangeable Sodium Percentage, Geographical Information System, Gully, Hydrology, Magnesium Saturation Percentage, Near Infrared, OPUS 6.5, Partial Least Square Regression models, Ploughed contours, Potential Hydrogen, Slope, Sodium Absorption Ratio, Strahler Stream Order.

OPSOMMING

Donga erosie is 'n groot omgewingsprobleem. Dit het nie net ‘n direkte invloed op die area waar dit geleë is nie, maar het ook ‘n indirekte invloed wat elders in die opvangsgebied ervaar word. Bekamping van donga erosie is moeisaam aangesien die faktore wat aanleiding gee tot die vorming en dryf daarvan moeilik is om te bepaal. Grond is die medium waarin erosie plaasvind, maar daar is nogtans steeds min navorsing wat grond ondersoek het as ‘n moontlike faktor aanleiding gee tot donga erosie. Die wat dit al wel ingesluit het, het dit slegs op n baie elemntêre manier ondersoek.

Die eerste doel van hierdie projek was om die diskontinue donga stelsel fisies en chemise te karakteriseer en klassifiseer om soedoende die verhouding tussen die landskap hidrologie en geomorfologiese donga ontwikkeling te bepaal met n fokus op die faktore wat dit dryf. Dit was gedoen deur middel van observasies gedoen terwyl veldwerk uitgerig was, fisiese metings asook ruimtelike en hidrologiese analises deur gebruik te maak van n Geografiese Inligting Stelsel (GIS). Die klassieke Malansdam donga stelsel is ‘n Strahler stroomorde (SSO) van 5 toegeken en is die eerste een ooit wat dit behaal het. Die mees aktiefste area was in die bolope waar die steilste helling ervaar was. Alhoewel ondergrondse pyp formasie waargeneem was het die V-vormige donga kanale en SAR data van die tradisionele nat analise aangedui dat afloop die dominante vorming proses was. Daar was gevind dat 'n duo van faktore, wat bestaan uit een menslike en een natuurlike faktor onderskeidelik, die faktore was wat donga ontwikkeling in die area dryf. 'n Unieke menslike faktor wat nog nie vantevore gepubliseer is, was bevind as die menslike faktor wat aanleiding gee tot donga erosie. Hierdie faktor is die bewerkiingsmetode wat in die Sandspruit opvangsgebied gebruik word naamlik geploegde kontoerbewerking. Die geploegde kontoere tree op as kanale om eerstens water te versamel en tweedens om die vloeirigting daarvan te wysig. Water wat onder natuurlike toestande afwaarts sou dreineer tot in die vallei word vasgevang deur die kontoere en gekanaliseer na een invloei punt in die donga. Hierdie proses verhoog die erosiekrag van die water aangesien groter volumes by 'n enkele punt in die steiler bolope van die donga stelsel invloei. Die dryf faktor in die natuurlike groep was swak grond struktuur. Die oorsaak hiervan was die besetting van ‘n grootmaat uitruilbare Mg^{2+} katione op die uitruil plekke van die kleifraksie. Dit sou veroorsaak dat grond in die teenwoordigheid van water maklik sou dispergeer, selfs in die teenwoordigheid van 'n lae hoeveelheid uitruilbare Na^{+} katione. Metodes om donga erosie te bekamp sal dienooreenkomstig bestaan uit die herstel van die grondstruktuur en die toepassing van 'n alternatiewe gondbewerkings stelsel. Die aanplanting van plantegroei, veral gras en koring binne die donga kanale sal verder help met die veg tot bekamping

Die tweede doel van hierdie projek was om te bepaal indien naby infrarooi (NIR) spektrometrie (met golfnommer van 12 500 – 4 000cm-1) oor die vermoë beskik om aanwysers wat traditioneel in grondkunde gebruik word om die dispergering van grond te meet te voorspel. Hierdie aanwysers sluit

vyf indekse in naamlik die Veranderlike Natrium Persentasie (ESP), Natrium Absorpsie Verhouding (SAR), Magnesium Versadiging Persentasie (MS%), Elektriese Geleidingsvermoë (EC) en die Potensiële Waterstof (pH) sowel as die vier hoof uitruilbare katione naamlik kalsium (Ca^{2+}) , kalium (K^{+}), natrium (Na^{+}) en magnesium (Mg^{2+}). Oppervlak en ondergrondse grondmonsters is ingesamel by die punt van oorsprong by aktiewe dongas. Hierdie monsters is minimaal voorberei, dus slegs gedroog, gemaal en gesif. Daarna was dit onderworpe aan die NIR analise. Die Bruker meerdoelige FT-NIR Analiseerder (MPA; Bruker Optik GmbH, Duitsland) met 'n spektrale omvang van 12 500cm 1 4000cm-1 is hiervoor gebruik. Parsiële kleinste kwadraat regressie (PLSR) modelle is gebou vir elke indeks asook die uitruilbare katione deur gebruik te maak van die nutsprogram Quant 2 van die OPUS 6.5 (MPA; Bruker Optik GmbH, Duitsland) sagteware. Vyf verskillende regressie statistieke naamlik die bepalingskoëffisiënt (r^2), vierkantswortel fout tydens kruis validasie (RMSECV), verhouding van prestasie teenoor voorspellingsafwyking (RPD), sydigheid en die verhouding van prestasie van kwartiele (RPIQ) was gebruik om die geldighied van elke PLSR model te asseseer. Alle PLSR modelle het goed presteer, behalwe vir MS% wat verdere navorsing vereis. NIR beskik dus oor die vermoë om die aard van dispergering van grond te bepaal op 'n vinnige, betroubare, goedkoop en nie afbrekende manier. Dit kan dus effektief aangewend word as ‘n substitusie vir die traditionele metodes om te bepaal as grond a beduidende faktor is of nie.

Trefwoorde en frases: Donga, Elektriese Geleidingsvermoë, Geografiese Inligting Stelsel, Geploegde kontoere, Hidrologie, Naby Infrarooi, Magnesium Versadiging Persentasie, Natrium Absorpsie Verhouding, OPUS 6.5, Parsiële kleinste kwadraat regressie modelle, Potensiële Waterstof, Strahler Stroomorde, Uitruilbare katione (kalsium, kalium, natrium, magnesium), Veranderlike Natrium Persentasie.

CONTENTS

FIGURES

TABLES

APPENDICES

LIST OF ABBREVIATIONS

Ca^{2+}: Calcium cation

CAF: Central Analytical Facility

CEC: Cation Exchange Capacity

CGA: Centre of Geographical Analysis

CH_3COONH_4: Ammonium Acetate

DEM: Digital Elevation Model

DRDLR: Department of Rural Development and Land Reform

EC: Electrical Conductivity

ECEC: Effective Cation Exchange Capacity

ESP: Exchangeable Sodium Percentage

GIS: Geographical Information System

GPS: Global Positioning System

K^+: Potassium cation

KCL: Potassium Chloride

M: Molar

Mg^{2+}: Magnesium cation

MIR: Mid Infrared

MS%: Magnesium Saturation Percentage

MSC: Multiplicative Scattering Correction

Na^+: Sodium cation

NGI: National Geo-spatial Information

NIR: Near Infrared

pH: Potential Hydrogen

PLSR: Partial Least Squares Regression

r^2: Coefficient of Determination

RPD: Ratio of Performance to Deviation

RPIQ: Ratio of Performance of Quartiles

RPM: Revolutions per Minute

RMSECV: Root Mean Square Error of Cross Validation

RMSEP: Root Mean Square Error of Prediction

RSA: Republic of South Africa

SAR: Sodium Absorption Ratio

SD: Standard Deviation

SNV: Vector Normalisation

SOM: Soil Organic Matter

SSE: Sum of Squared Errors

SSO: Strahler Stream Order

ACKNOWLEDGEMENTS

I would like to thank the following people, whom without, this project would not have become a reality:

- Dr. Willem de Clercq for his insight and guidance throughout the span of the project.

- Nicolette du Toit, not only as editor, but an understanding loving fiancée always being supportive and willing to listen to daily mini progress reports as well as problems, however big or small.

- Family and friends for always showing an interest in this project and who kept me motivated to keep going.

- Prof. John Clemens for allowing me to take time off work in order to conduct field work thus allowing the project to progress smoothly and reach a timeous conclusion.

- Prof. Alex Kisters and Dr. Daniel Mikes who had advice on hand from their experience in the academic environment.

- Matt Gordon and Herchille Achilles for their analytical work.

- Farmers from Malansdam and Kasteelberg who allowed for this research to be conducted on the gully systems in their area without any restrictions.

- Hélène Nieuwoudt and Eric Mashimbe for providing training on the Bruker MPA FT-NIR Analyser and OPUS 6.5 software and also in providing guidance in analysing the NIR spectra.

- Anton Kunneke for taking time in his busy schedule to help with the 3D scan of the gully network in the study area.

- Carisa Minnie and Jacques Snyman for their humorous quips during hard times; the “wors” and DONG will be fondly remembered.

- Mrs Annatjie French for helping me with various administrative tasks as well as her continual friendliness.

- The CGA team at the Geography and Environmental studies Department, especially Theo Pauw, for his help with various ArcGIS issues.

1 TO DIFFRENTIATE GULLY EROSION FROM WATER EROSION OR NOT…

1.1 NEED FOR GULLY SPECIFIC EROSION RESEARCH

Soil erosion is a major environmental problem in the Republic of South Africa (RSA). This is not a recent revelation as perhaps the first step towards soil conservation (although very limited scope) was the obligation imposed upon landowners in 1682. This stated that all watercourses and furrows were to be kept free from any obstacles in order to prevent soil erosion occurring on cultivated lands during the rainy season (Verster *et al* 2009). If this point, though infantile in nature, could be considered as the starting point of RSA's battle against soil erosion it has had a long history and it is indicative of how serious the nature of this problem is.

Since this early inception against soil erosion, various studies have been conducted on soil erosion. Defining soil erosion is quite straightforward: it is the detachment of soil by water or wind and the displacement thereof (Morgan 2005). However, discovering the control factors driving the process is much more complex and ranges from anthropogenic to physical factors. The range of studies that have been conducted in RSA thus far, has addressed the definition *per se, via* defining the process at work and compiling reports of soil erosion occurrences, thus doing a spatial analysis of soil erosion (Talbot 1947). Yet fewer studies have investigated the full range of control factors causing this (Champion 1933) and quantifying the amount of sediment lost due to it.

With regards to addressing the process and spatial occurrences, the main stream research area has been on soil erosion caused by water. This seems sensible due to only the coastal regions of RSA being prone to soil erosion by wind which amounts to approximately 25%, (Hoffman & Todd 2000) therefore leaving water to be the dominant agent causing soil erosion in RSA (Laker 2004; Le Roux *et al* 2008). The processes linked to water erosion are well known; they are rill, sheet and gully erosion and have all been observed.

In terms of exploring the control factors causing water erosion much of the discussion in RSA has surrounded anthropogenic factors linking land degradation to European colonisation, especially in the Karoo (Rienks *et al* 2000; Boardman 2003; Keay-Bright & Boardman 2009). This is important as soil erosion can be an indicator of soil and land degradation, but can also cause it. Soil erosion thus aggravates soil and land degradation and *vice versa* (Lal 2001). It has long been known that human activities can be the cause of soil erosion or elevate the levels of current soil erosion. The majority of soil erosion studies in RSA have focussed on exactly this. It has an historical outlook of how European colonisation has played a role in land degradation through water erosion due the removal of vegetation and other incorrect agricultural activities such as overgrazing and the removal of natural

vegetation for cropland coupled with climate change (Acocks 1953; Bond *et al* 1994; Hoffman *et al* 1999b; Kakembo 2001; Boardman *et al* 2003). The conclusion is that the majority of soil erosion research focussing on RSA has thus been confined to investigating control factors in the anthropogenic group. Yet, soil erosion is a natural process occurring by means of interaction with water and soil. Therefore, it is unusual that so few studies have investigated the influence of physical factors on gully erosion. Evidence from recent research suggests that this purely humanistic approach could well be erroneous. "A recent general survey of degradation notes the need to redress this balance by giving more attention to soil and water issues" (Hoffman *et al* 1999b in Boardman *et al* 2003: 165). "The possibility that intrinsic variables linked to the erosion system are more significant influences than human interference alone has been suggested" (Garland and Broderick 1992; Cobban and Weaver 1993; Boucher and Powell 1994 cited in Rienks *et al* 2000: 12).

An apparent deficiency thus exists with regards to exploring the control factors driving soil erosion by water yet another shortage in the same avenue is noticeable. In terms of water erosion, concentrated flow in the form of gully and rill erosion significantly contribute to total soil loss (Poesen *et al* 2003). Quantification data on these two aspects vary according to spatial and temporal scale and through research done in different parts of the world it was indicated that "soil loss rates by gully erosion represent from a minimal 10% up to 94% of total sediment yield caused by water erosion" (Poesen *et al* 2003:96). The sediment yield increase as the occurrences of gullies increase in a catchment (Poesen *et al* 2002). This is further supported by Armstrong and Mckenzie (2002) where sediment yields were at least one order of magnitude higher in catchments containing gullies compared to ungullied catchments. Verstraeten *et al* (2003) also indicated that gullies and vegetation cover had the greatest impact on sediment yield. It is evident that gully erosion as a specific entity should be studied as the contribution of gully erosion to soil loss and sediment yield and therefore its environmental impact cannot be ignored.

Gully erosion however is an area that has long been avoided. This is due to the difficulty in understanding this phenomenon (Valentin *et al* 2005). The reason may be that it "is a threshold-dependant process controlled by a wide range of factors" (Valentin *et al* 2005: 136) and "gully erosion is mostly a systemic threshold rather than a single factor threshold phenomenon. This means that all the factors influencing gully erosion hold the system close to equilibrium. When this equilibrium is disturbed, a response which might be gullying, is induced which will operate until the system is in equilibrium again" (Van Zijl 2010: 10). Various factors can contribute to the system approaching equilibrium and even a seemingly insignificant change in the system can be responsible for the threshold to be crossed (Nordstrom 1988). Therefore, a significant amount of factors may drive gully erosion at any given time and the study of gully systems therefore cannot rely on a singular factor approach. A multiple factor approach needs to be followed in order to identify all possible factors influencing gully erosion and understand the whole system at work.

Two voids have come to the fore with research in the field of soil erosion by water. Firstly, several studies conform to examining control factors in the anthropogenic group whilst research on the control factors in the natural group remains limited. If this trend continues an important constituent in terms of establishing soil erosion might be neglected. Secondly, many authors investigating gully erosion examine a single control factor in isolation. This particular approach will cause the outcome to be warped or too narrow therefore not portraying the full picture. A multifactor approach needs to be followed with the investigation, hence integrating factors from both anthropogenic and natural groups. Once this emerges, an understanding to answering two important questions which are the following: "Why is this happening?" and "How can it be controlled?" may be explained. This will further enhance the capability of predicting areas prone to gully erosion. This is important as Kosov *et al* (1978 in Sidorchuk 1999) found that in the first 5% of a gully's lifetime 90% of a gully's length, 60% of the area and 35% of its volume is eroded.

1.2 PROBLEM STATEMENT

Gully erosion has been linked to land degradation worldwide. It causes large soil losses that contribute to the overall sediment yield. It has negative direct influence (on-site), but also further indirect influences (off site) (Valentin *et al* 2005). Direct on-site influences include an economic burden on farmers potentially threatening the sustainability of agriculture in a number of ways: the removal of fertile top soil, breaking agricultural field units into smaller fields, adding to cultivation costs as farmers need to manoeuvre around the gully system, impacting a soil's water holding capacity, and furthermore lowering perched water tables, therefore reducing the availability of water livestock and cultivation. Off-site influences include silting up of reservoirs and rivers, causing a decline in water quality, and also flooding. "Gully erosion has long been neglected because it is difficult to study and to predict" (Valentin *et al* 2005: 133). Recently gully erosion has attracted growing interest. The main reason for this occurrence is the heightened concern for off-site impacts.

The severity of this problem has also been recognised in RSA. Researchers consequently followed suite with this trend and a spate of recent studies focussing on this area emerged (Recent publications in this area include: Rienks *et al* 2000; Kakembo 2001; Boardman *et al* 2003; Meadows 2003; Meadows & Hoffman 2003; Sonneveld *et al* 2005; Le Roux *et al* 2008; Kakembo *et al* 2009; Keay-Albright & Boardman 2009 and Van Zijl 2010). Even though this trend has been followed in RSA, it is still infantile in nature and requires further attention.

1.3 RESEARCH PROBLEM

In a RSA context soil erosion is regarded as one of the most significant environmental problems. This is highlighted by various recent studies (Watson 2000; Sonneveld *et al* 2005; Keay-Bright & Boardman 2007; Kakembo *et al* 2009). These studies however, have focussed on Kwazulu-Natal, the Karoo area and RSA's home lands namely Lesotho and Swaziland.

The South-western cape has a unique climate in RSA. It is the only province that is semi-arid and has a Mediterranean climate. This climate type is associated with a strong seasonal winter rainfall regime. Talbot (1947) and Meadows (2003) indicated that this area is highly susceptible to significant levels of water erosion. Poesen and Hooke (1997) were also of opinion that gully erosion plays an essential role in soil and land degradation in Mediterranean climates. The contribution that gully erosion makes to sediment yield cannot be overlooked, especially in a Mediterranean climate (Poesen *et al* 1996; Oostwoud Wijdenes *et al* 2000; Poesen *et al* 2002). This opinion is thus widely accepted, yet studies in this particular area in RSA remain scarce.

Given the extent of the problems associated with gully formation, little information is available in the Western Cape with regards to its occurrence as well as the root causes of its formation. This area needs to be placed under scrutiny, in order to find the factors driving gully formation by investigating both the anthropogenic group and the neglected physical group, especially the soil factor. Soil cannot be overlooked, as the physio-chemical properties of a soil play an important role in its structure and thus susceptibility to water and gully erosion. Soil is the medium in which soil erosion occurs and it cannot be justifiably ignored or only investigated on a basic nature.

Once this information is obtained it can be useful to land owners, especially famers and enable them to make informative decisions on gully prevention and control.

1.4 AIMS & OBJECTIVES

The aim for this Masters in Science research study is twofold:

PHASE 1 aim: Physical and chemical characterisation and classification of the gully system structure to establish the relationship between landscape hydrology and geomorphologic development of the gully system.

The below objectives need to be reached to accomplish the aim for Phase 1:

- Review the applicable literature with regards to gully erosion
- Literature review to find suitable measures and indices related to soil erosion
- Obtain high resolution stereo images to identify a gully system to serve as study site

- Collect soil samples from active gully heads within the study area for chemical characterisation
- Pre-treat and treat soil samples in order to determine the values of the indicators identified in the literature review
- Acquire 1.5m Digital Elevation Model (DEM) for the study site
- Create order and structure within the gully system to plan physical measurement stations
- Construction and installation of sediment traps and erosion pins
- Obtained rainfall data for the area for the duration of the physical measurement cycle
- Integration of physical measurements and rainfall events
- Construct a conceptual model as to the control factors of gully formation on the area and how gully erosion influences hydrology and geomorphology of the study area

PHASE 2 aim: Capturing a Near Infrared (NIR) trend to establish the potential for the usage of NIR reflectance spectroscopy to determine the probability of soil dispersion.

The objectives that need to be fulfilled in order to reach the aim for Phase 2 partly overlap those mentioned in Phase 1. Nevertheless, they are as follow:

- Literature review on NIR application in Soil Science
- Determination of suitable soil dispersion indices by means of literature review
- Attainment of high resolution stereo images to identify a study area
- Collect soil samples from active gully heads within the study area
- Pre-treat and treat soil samples in order to determine the real values of the dispersive indicators identified in the review
- Acquire a diffuse reflectance graph for the samples via spectrophotometer
- Calibrate and build a predictive Partial Least Squares Regression (PLSR) model by combining the real values obtained via traditional methods and those indicated by the diffuse reflectance graph
- Validate the predictability of the PLSR model
- Research airborne and satellite sensors to investigate the possibility of using the predictive PLSR models developed in conjunction with remote sensing

1.5 RESEARCH DESIGN

A flow diagram has been constructed to depict the workflow for both Phases from infant stage through to the final product. Figure 1.1 below illustrates the research design for both Phase 1 and 2.

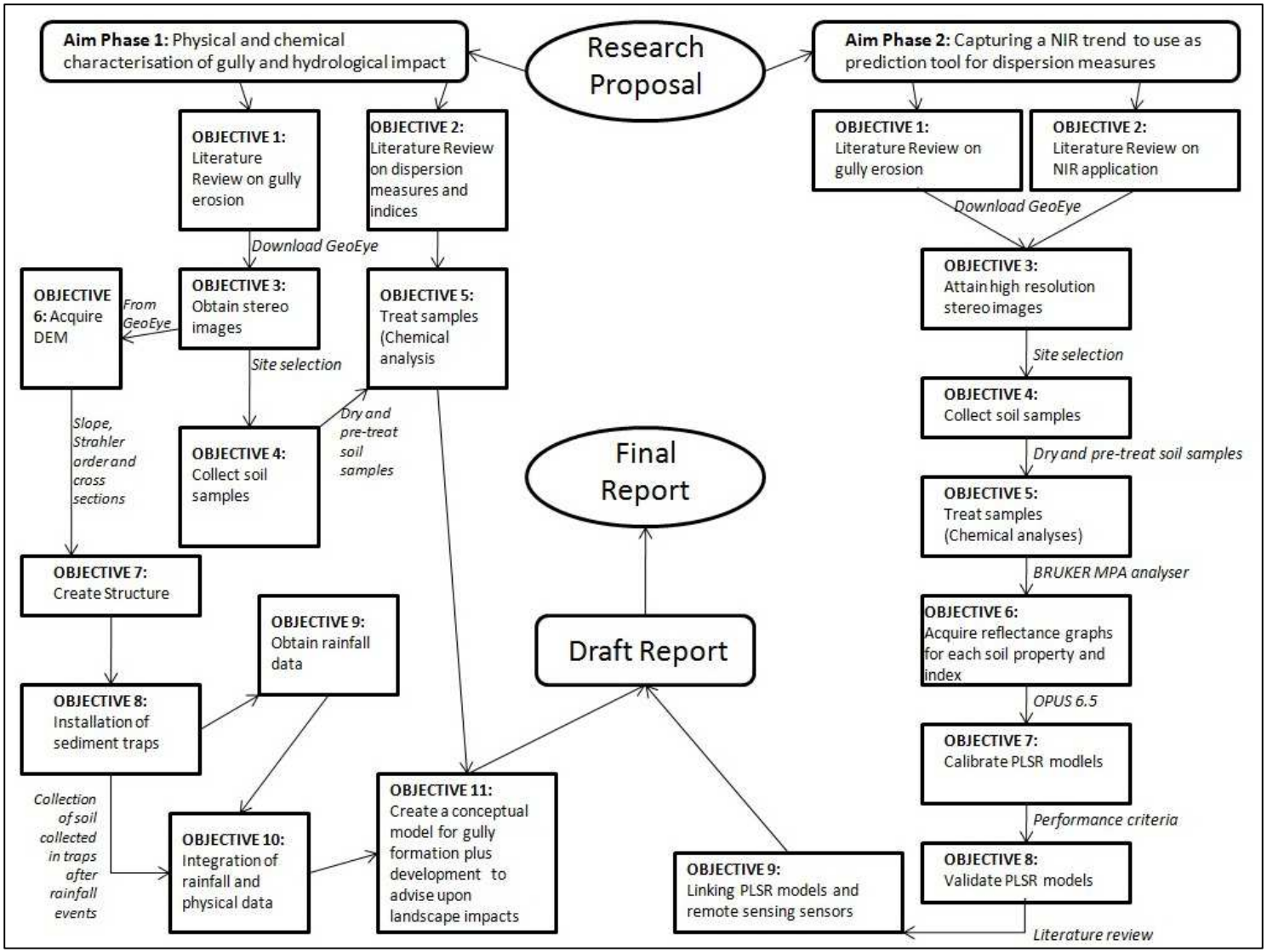

Figure 1.1 Work flow diagram for phases 1 and 2

1.6 STUDY AREA

The study area is the Sandspruit catchment which is approximately 120km² in extent (Figure 1.2). It is situated in the Swartland region of the Western Cape of RSA. The Sandspruit is a tributary of the Berg River and the two rivers join approximately 25km downstream of the Voëlvlei dam ($33^0$09'34.75"S and $18^0$53'44.75"E) which forms the northern most point of the catchment with its southern most point extending to Riebeek Wes. Figure 1.2 indicates the exact location of the axe shaped catchment. The landform consists of gentle undulating hills with the only prominent mountain being Kasteelberg at the southern most part. The height above mean sea level ranges from 64m at its lowest and 254m above mean sea level being the highest point. The slopes in the area are relatively gentle with the exception of Kasteelberg with approximately 61% of the areas slope being between 0° - 4° and 27% between 4° and 7°. The underlying geology consists of Malmesbury shale which was deposited during the pre-Cambrian time period.

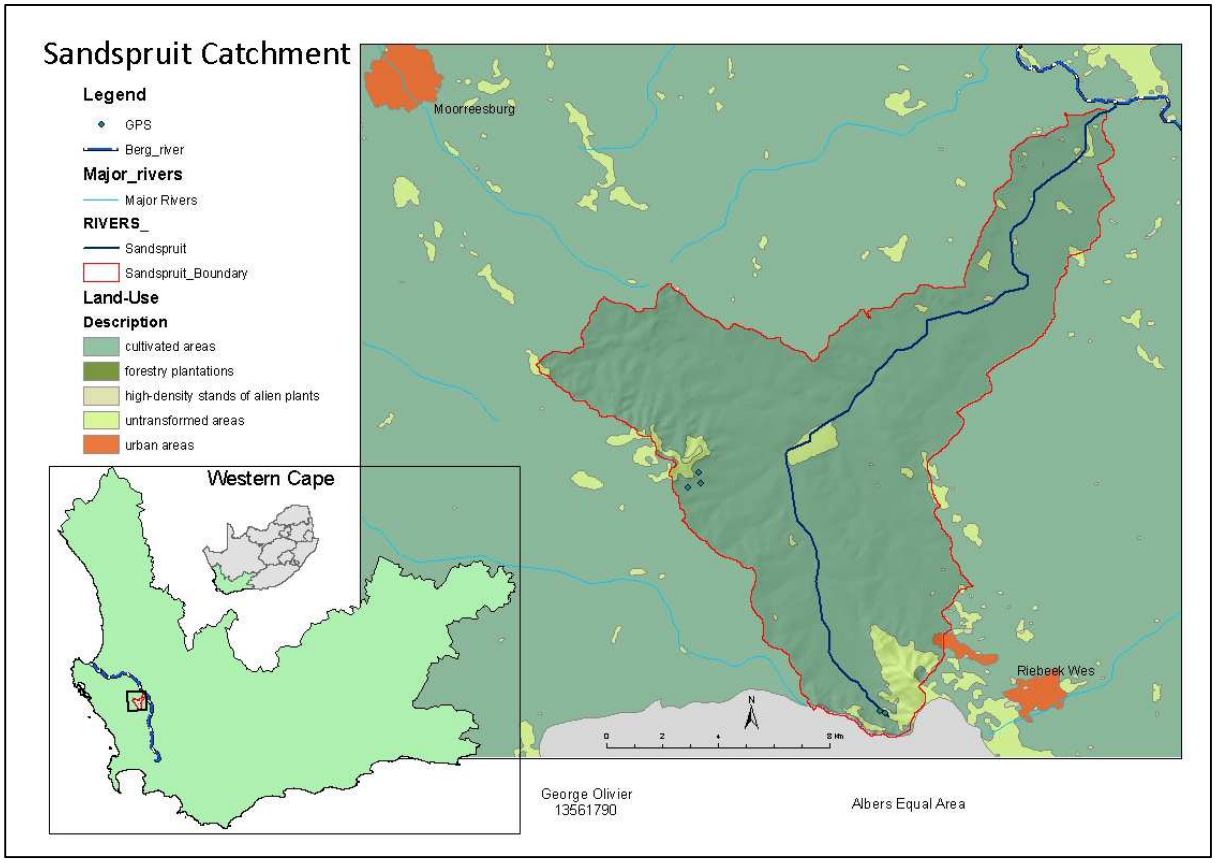

Figure 1.2 Sandspruit catchment orientation map

The area has a Mediterranean type climate with a winter rainfall that is associated with frontal depressions due to the shifting of the global pressure systems to the north. Summer aridity is experienced as a result of the influence of the cold Benguela stream that flows at the West coast of RSA. The mean annual rainfall for Moorreesburg is 315mm and 479mm for Riebeek Wes (SA Explorer 2010). There is a large variation between summer and winter temperatures; with the midday

average temperatures in July (winter) being 17°C and February (summer) 29.2°C for Moorreesburg and Riebeek Wes with an average July midday temperature of 16.9°C and February 29.8°C (SA Explorer 2010). The area is extensively used for agriculture. Wheat produce is the dominant type of agriculture in the area interspersed by vineyards and olive plantations. A few farmers also keep livestock, mainly sheep, on their farms. The natural vegetation that occurs in the area is unique to the Western Cape and consists of the fynbos and renosterveld.

1.7 THESIS FLOW

Due to the twofold nature of this project, the thesis flow will be different to a conventional thesis. Each Chapter will encompass the flow of the whole phase of investigation that is a short introductory section followed by the methodology pursued, results achieved, discussion thereof and a brief conclusion. The only chapter not adopting this structure is Chapter 2 which will serve as a literature review.

Following this introductory Chapter, is Chapter 2. This will consist of firstly, a concise literature review on the geomorphology of gully erosion. The term, gully, will firstly be clarified by defining it followed by a discussion on the formation processes. Attention will then shift to factors causing and driving gully erosion. Factors from both the natural and anthropogenic groups will be discussed. Thereafter NIR will be introduced indicating its relevance to gully erosion research.

Chapter 3 will investigate the Malansdam gully system as a whole. It will focus on how the agricultural activity currently employed in the Malansdam area affects the hydrology response and gully erosion.

Chapter 4 will physically characterise the discontinuous gully system at Malansdam. Field observations at the Malansdam gully system will also be evaluated. Thereafter, the methodologies applied at the Malansdam test site will be explained followed by the results achieved. These results will be discussed with a brief conclusion.

Chapter 5 investigates whether the chemistry of the soil plays a part in driving gully erosion at Malansdam. It will also serve as the final step in the characterisation process of the discontinuous gully system at Malansdam.

Chapter 6 will assess the usage of NIR reflectance spectroscopy as a prediction tool for soil variables used to examine soil dispersion. The results will be discussed, concluding with a few remarks surrounding the second phase of this project.

Chapter 7 will be a concise conclusion of the study, reflecting on the thesis as a whole. Furthermore, shortfalls and successes of this project will be discussed whilst also identifying potential areas of study for future projects.

2 GULLY GEOMORPHOLOGY

2.1 A GULLY DEFINED

"A gully can be defined as a deep channel on a hillside, generally cut by running water, and often not containing perennial flow" (Kirkby & Bracken 2009: 1841). This relatively simple definition provides a starting point as to establish what a gully is but requires further detail. Firstly, it does not include size limitations. A cut-off value is required to establish where rills stop and where gullying begins. Secondly, it confines gully erosion to hillsides. Gully erosion can occur on valley floors, especially in areas where deposited sediment results in unstable soils (Laker 2004).

The following improves Kirkby and Bracken's (2009) definition by starting to differentiate with size limits although betraying it in terms of agricultural activities. "Gullies that develop in agricultural lands are divided into two groups: (1) Classic gullies that are channels too deep to be erased with ordinary tillage equipment with its depth ranging from 0.5m to 30m" (Foster 1986: 91) and (2) "ephemeral gullies are small and continuous channels eroded by overland flow that can be easily filled by normal tillage, only to reform again in the same places during the next rain season" (Casalf *et al* 2006: 128). Due to differing tillage methods the above definition for an ephemeral gully is fairly open, still making it difficult to differentiate between rills and ephemeral gullies. Hauge (1977) proposed a gully to be defined as a channel with a critical cross-sectional area of 929 cm^2 and various authors have employed this as their definition of an ephemeral gully (Poesen *et al* 1996; Vandaele *et al* 1996; Svoray & Markovitch 2009). According to Souchère (1995) this is also the threshold value of channels influencing the manoeuvrability of farming machinery across cultivated fields. Also, Vandaele *et al* (1996) and Laflen *et al* (1985) indicated that the cross sectional area are normally wide relative to its depth lending further sustenance to Souchère (1995).

The Malansdam gully system does occur in cultivated land, therefore the distinction should be made between classical and ephemeral gullies. This will however only be the case when differentiating between the two sizes is pertinent in order to make a certain point. In such cases the explicit terms namely classical (depth of 0.5m and up) or ephemeral (cross sectional area of 929cm^2) will be used. In all other cases the term gully will encapsulate both groups, which means a gully will be defined as channels incised into the landscape with a minimum cross sectional area of 929cm^2.

2.2 FORMATION SYSTEMS

Gully formation can be classified into two separate formation systems. Firstly, gullies can form due to concentrated overland flow and secondly due to sub-surface water flow (Kirkby & Bracken 2009).

2.2.1 Concentrated overland flow

According to Morgan (1995), gullies that form due to concentrated overland flow occur in a complex process. The formation process can be seen in Figure 2.1 below.

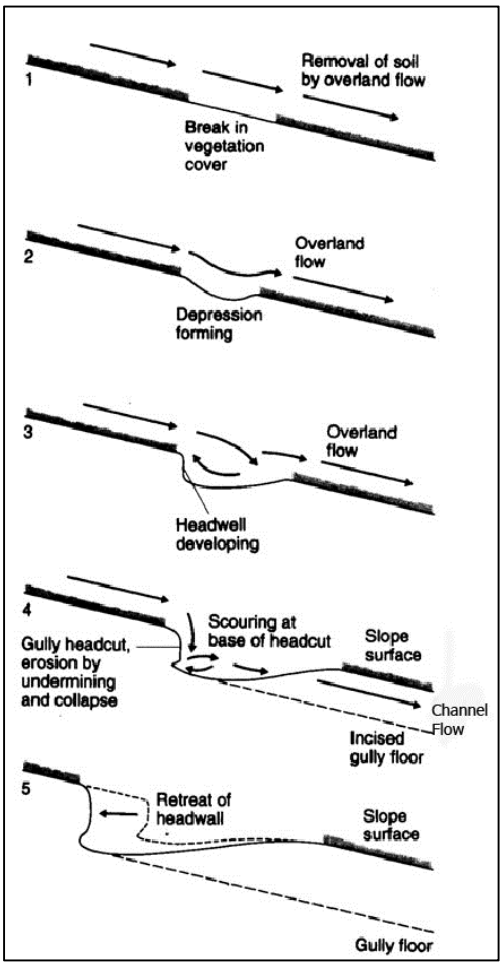

Source: Morgan 1995

Figure 2.1 Concentrated overland flow gully formation process

A "depression forms for example because of a loss in vegetation cover due to overgrazing or a fire. Water concentrates in these depressions enlarging it. Erosion is concentrated at the heads of the depression where near vertical scarps develop over which flow occurs. Some of the soil particles are detached by this flow of water, but most of the erosion occurs with scouring at the base of the scarp which results in deepening of the channel and also undermining of the headwall, leading to collapse and thus further retreat. Sediment is produced further down the gully" (Morgan 1995: 19).

2.2.2 Sub-surface flow

In addition to this process, gullies can also develop via piping (Soil Science Society of America 2013). This differs to the concentrated overland flow formation process as it occurs through sub-surface water flow. This type of flow leads to the formations of pipes or tunnels in the sub soil. When the size of these tunnels or pipes reach a critical size and cannot carry the weight of the soil above it,

it will collapse. Thereafter the process described in section 2.2.1 will take over the role as dominant process due to the depression occurring at the surface as observed by Faulkner *et al* (2004).

Piping arises "in duplex soils where infiltration rate is governed by the B horizon, rather than the faster infiltration rate of the A horizon. During a rainfall event water quickly infiltrates the A and E horizon, but not the B horizon. A subsurface flow will now occur at the contact between the E and the B horizons causing tunnelling/ piping" (Van Zijl 2010: 10) as indicated in Figure 2.2. When soils are dispersive this effect is aggravated (Rooyani 1985).

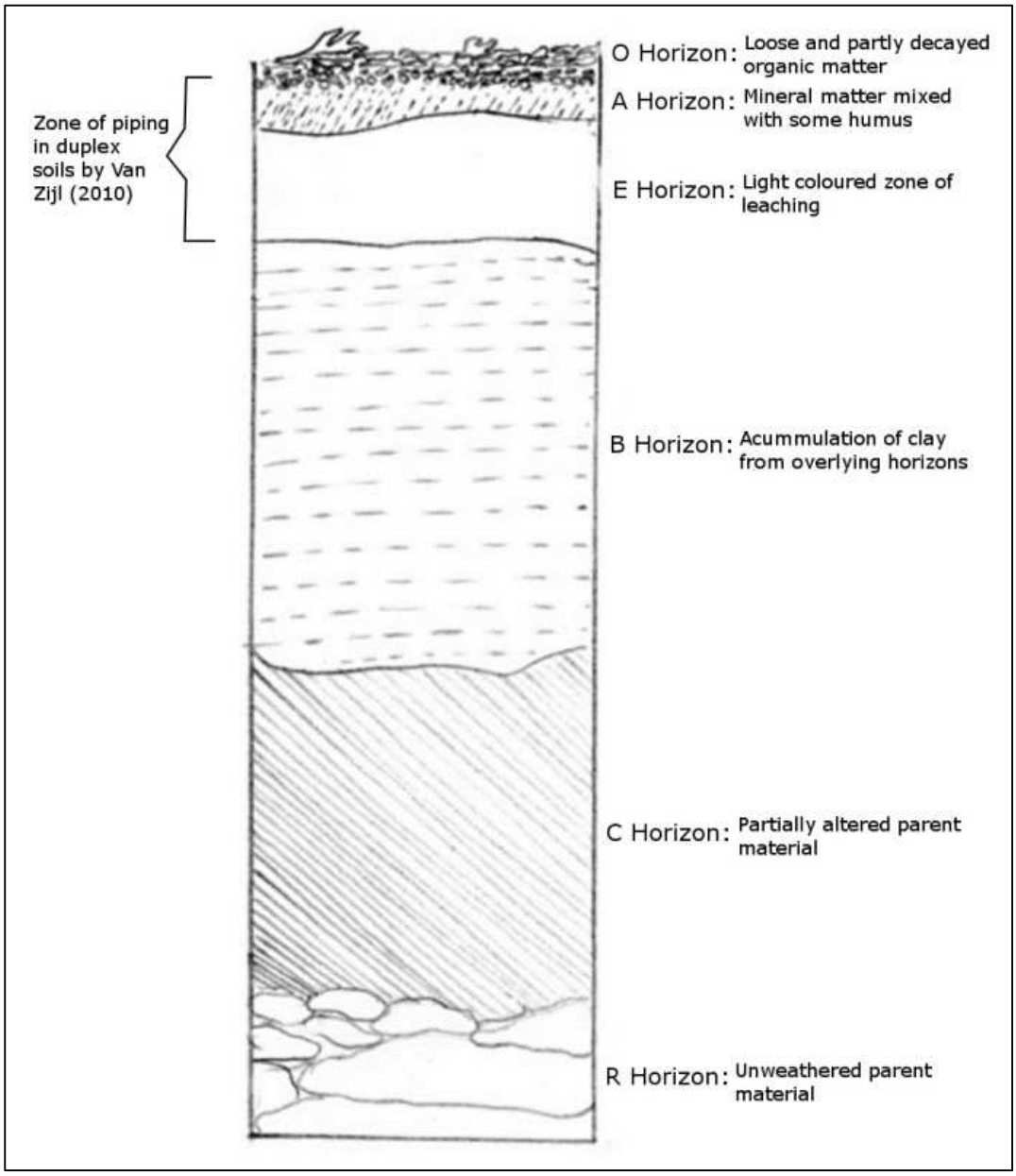

Figure 2.2 Gully erosion *via* piping caused by sub-surface flow

Furthermore, piping can also be initiated by plant root decay and animal activity (Hessel 2002). The small tunnels that result due to these activities are enlarged by subsurface water flow as it uses this as

a channel way. It may occur more frequently in soil that easily disperses in the presences of water which is governed by soil chemistry.

2.2.3 Working in unison

In some research areas both gully formation methods were observed during field work (Rienks *et al* 2000, Faulkner *et al* 2004, Samani *et al* 2009). This could indicate that gullying occur in multiple cycles transforming between piping and run-off as the dominant formation process (Jones 1994).

2.3 GULLY ENLARGEMENT

Section 2.2 is chiefly aimed at the gully formation processes and therefore its initiation. Both formation processes are however also involved in the enlargement of gullies. Concentrated overland flow causes gully head retreat due to splash erosion in the plunge pool as indicated in Figure 2.1 steps 4 and 5. This causes the gully channel to extend, becoming longer. Piping causes a sinkhole to form due to collapse once the pipes or tunnels become too large to bear the weight of the soil above it. This generally tends to take place at the pipe outlet on the open face of the gully head or wall causing an extension of the gully (Kirkby & Bracken 2009).

Other mechanisms are also involved in enlarging gullies. These can take the form of bank gullying, tension cracks and mass wasting (or land-sliding). These mechanisms play a large role in widening gullies by affecting the gully walls and have been shown to produce the majority of sediment from within gullies by Collison (1996). This has been confirmed by various authors that have estimated these processes to account for 50% and more of the sediment yield of gullies (Piest *et al* 1975, Blong *et al* 1982, Vandekerckhove *et al* 2000, Poesen *et al* 2002, Martıinez-Casasnovas *et al* 2003 in Martinez-Casanovas *et al* 2004).

Bank gullying occurs mainly when concentrated overland flow crosses the bank of a river or gully (Poesen 1993). Sub-surface flow however, can also result in bank gullying when a collapse occur near the pipe head in the wall. The resultant depression will be eroded further by overland flow (Poesen 1996) forming the bank gully.

Tension cracks can develop on the gully sidewall, but also at the gully head. Generally the development of this at the gully head is due to splash erosion in the plunge pool. This causes the gully head to become undercut exerting stress on the soil above the plunge hole due to gravity. Similarly, gully walls can become undercut due to channel flow leading to tension cracks (Oostwoud Wijdenes *et al* 2000, Poesen *et al* 2002). Furthermore, wet and dry cycles can also cause the development of tension cracks (Bradford & Piest 1985). Collison (2001) indicated that tension cracks reduce the stability of the exposed soil on the gully wall or head and upon a rain event water could infiltrate the

tension cracks which would then lead to failure with the soil collapsing. The collapsed soil is transported downstream in the gully channel to be deposited elsewhere.

Mass wasting or land-sliding happens on a larger scale in the sense that it produces more sediment per event as with tension cracks. The means involved in producing this are somewhat similar to those causing tension cracks. Martinez Casanovas (2004) indicated that mass wasting generally occurs when there is an undercut hollow caused by concentrated flow beneath the wall especially in high intensity or prolonged rain events. He also indicated that tension cracks that forms in this way, promote mass wasting events especially on steep gully walls. A further implication for steep gully walls near vertical are that it becomes structurally unstable when the soil becomes saturated, which also leads to mass wasting events (Collison 2001, Poesen *et al* 2002).

2.4 RESEARCH EFFORTS

"Historically research was focused on gullies formed by run-off but recently gullies formed by subsurface flow have received increasing attention" (Bryan & Jones 2000: 209). It is extremely important to study this type of gully formation in depth, as it is the most dominant form of gully formation in areas with a sodic or highly saline soil. As indicated in sections 2.2.2 and 2.2.3 piping can also work in unison with run-off. It is thus necessary to understand this process in order to see how the two formation systems interact.

"Gully erosion has long been neglected because it is difficult to study and to predict. More recently gully erosion has attracted a growing interest as reflected by recent international conferences as well as a yearly symposium on gully erosion. This can be explained by an increasing concern for off-site impacts that can only be tackled at the catchment scale" (Valentin 2005: 133). Van Zijl (2010) supported the idea of investigating gullies at the catchment level. Gullies follow a cyclical process of (1) Infill, (2) Comparative stability and (3) gully incision (Prosser *et al* 1994: 465; Carnicelli *et al* 2009: 541; Van Zijl 2010: 3). Van Zijl (2010) further found gullies to be localised phenomena with different gullies in the same catchment being at various stages of this cyclical process.

Oostwoud Wijdenes *et al* (2000) devised a set of criteria to identify in which stage of this cyclical process a gully was in. It was based on the geomorphological aspects of the headwall of a gully, thus strongly linked to its physical condition. The criterion, in Table 2.1 below, can be used to assess whether a gully head is very active, active, moderately active or stable, showcasing no activity, therefore not contributing to soil loss.

Table 2.1 Soil sample criteria comprising of gully activity

Active	**Not Active**
Sharp edges	Rounded edges
Plunge pool	No plunge pool
Undercut	Inclined gully head wall
Tension cracks	Vegetation on gully walls and bed
Recently deposited sediment	Extremely small contributing catchment area
Flow marks	
Piping	

Source: Oostwoud Wijdenes *et al* 2000

A gully head was classified as non-active when "characterised by rounded walls, partly overgrown with vegetation and with no overland flow marks" (Oostwoud Wijdenes *et al* 2000: 151). As opposed to this, very active gully heads had sharp edges, freshly exposed soil at its headwall and clearly distinguishable flow marks. Active gully heads were classified when its head comprised of sharp edges with little vegetation in addition to having flow lines and a plunge pool. A gully head was categorised as being moderately active when there were few flow marks, but had a headwall that was strongly undercut and had recently deposited sediment at the foot of the wall. If tension cracks were evident it was also deemed as a moderately active gully. Even though these criteria were developed for gully head classification, it could also be used, to a degree in the rest of the gully system. This is due to activity or non-activity along the channels and walls displaying similar physical characteristics to those developed by Oostwoud Wijdenes *et al* (2000).

Furthermore, "gully erosion is mostly a systemic threshold rather than a single factor threshold. This means that all the factors influencing gully erosion hold the system close to equilibrium. When this equilibrium is disturbed, a response which might be gullying, is induced which will operate until the system is in equilibrium again" (Van Zijl 2010: 10). Various factors can contribute to the system approaching equilibrium and even a seemingly insignificant change in the system can be responsible for the threshold to be crossed (Nordstrom 1988). Numerous factors are thus in play at any given time and the study of gully systems cannot rely on a singular factor. A multiple factor approach needs to be followed in order to understand the system at work. This research project will focus on the factors that have received most recent attention and seem to be the major control factors in initiating the gullying process. It will be discussed in the Section 2.5.

2.5 GULLY CONTROL FACTORS

The following is a short review on the factors that have received the majority of attention in recent literature.

2.5.1 Land use

One of the big questions of environmental science is the relative importance of climate and land use factors influencing erosion. An overwhelming amount of research has recently been done on this factor as it is seen as having the greatest impact on gully erosion (Poesen *et al* 2003; Martinez-Casanovas *et al* 2009). This is a human induced factor and therefore it is very diverse. Land use change can encapsulate a change in farming system intensification (Podwojewski *et al* 2002; Gomez *et al* 2003b), agricultural plantation change (e.g. Martinez-Casanovas *et al* 2009), road construction, tillage direction (Svoray & Markovitch 2009) and land abandonment (Lesschen *et al* 2007) to mention but a few.

Land use changes such as switching from wheat to maize, or to move cultivation onto steeper slopes can also have a dramatic erosional impact. Evidence from many parts of the world suggest that human impact in the form of clearance, cultivation and overgrazing significantly increases erosion rates (Cooke *et al* 2003; Boardman 2010). This is especially significant where natural deep root vegetation has been removed and replaced with agricultural plantations which in many cases have an insufficient root system that may destabilise the soil.

Research in RSA suggests that high erosion rates are often associated with cultivation and the abandonment of formerly cultivated land (Kakembo & Rowntree 2003; Sonneveld *et al* 2005).

“The main causes for gully initiation by land use change is an (1)increase in run-off that was caused due to removal of vegetation or building of roads and (2)reduction of the structural stability of the soil due to the depletion of the soil organic matter” (Valentin 2005: 140).

2.5.2 Slope

Gullies are common features of mountainous or hilly regions with steep slopes. Recent studies have been reported in various regions (Esteves *et al* 2005, Descroix 2008, Gomez *et al* 2003b, Zijl 2010). Steep slopes favour high run-off velocity and thus gully initiation. But under certain climatic conditions gentler slopes can create more run-off (Janeau *et al* 2003) “due to soil crusting decreasing the slope threshold for gully initiation” (Valentin *et al* 2005: 138).

Gullies are also found in low lying areas that is the valley floor. There are mainly two reasons for this: (1) Deep unstable soils tend to develop here (Laker 2004) due to sediment accumulation. “Add to this an accumulation of runoff water from upper slopes, bare soils left by cultivation and overgrazing and we have the ideal setting for gully erosion” (Van Zijl 2010: 18). (2) “When a perched water table

accumulates in the subsoil piping can occur" (Van Zijl 2010: 18) causing gullies to form via collapse when the tunnels reach a critical size.

2.5.3 Soil

Soil is the substance in which gully erosion occurs. Despite this, relatively few studies have focused on soil as being a major factor playing a role in gully formation with the knock on effect being that "little is known about the properties of soils and the associated processes that control its resistance to gully erosion" (Poesen *et al* 2003: 112). "The soil properties determine soil erosion in two ways namely by its influence on the run-off and its aggregate stability" (Van Zijl 2010: 6). A better understanding of the effect of soil properties on erosion is needed in order to effectively combat gully erosion. Focus should shift from a mere simple classification of soil to a more analytical approach when conducting gully research.

In studies that followed a more analytical approach the possibility that the intrinsic physical and chemical properties of a soil play a more significant role than human interference on gully erosion has been suggested (Cobban and Weaver 1993; Boucher and Powell 1994; Rienks *et al* 2000; Van Zijl 2010). An attempt to map out how physio-chemical properties affect gully erosion has been undertaken in recent studies (for example Rienks *et al* 2000; Rustomji 2006; Van Zijl 2010).

The intrinsic characteristics of a soil and its behaviour are most critically determined by a soil's clay fraction. This is due to its small particle diameter of less than 2 µm (Sparks 1995) causing it to "possesses the greatest specific surface area and is therefore most active in physiochemical processes" (Tanji 1990: 92). Clay platelets have a negative electrostatic surface charge thus having active exchange sites for cations. The cations are adsorbed and held in place as a result of this charge. The measure of the total amount of charge sites will vary with the clay fraction of the soil (increasing with an increase in clay) and this is known as the Cation Exchange Capacity (CEC). The CEC is important as this regulates aggregation processes in soils. From an environmental and agricultural point of view the basic alkaline cations to be attracted to these sites are of most interest and consist of the following: Calcium (Ca^{2+}), Potassium (K^{+}), Sodium (Na^{+}) and Magnesium (Mg^{2+}). These four cations are accepted to be the Effective Cation Exchange Capacity (ECEC) (Graaf van de & Patterson 2001).

These cations compete for places on the exchange sites. They are thus exchangeable and depend on their charge as well as hydrated radii. Cations with a larger charge and a smaller hydrated radius are more tightly held in these exchange sites. The order in which they will be adsorbed is: $Ca^{2+}>Mg^{2+}>K^{+}>Na^{+}$. Calcium is normally the dominant cation and cause clay platelets to bond in a process known as flocculation. When excessive amounts of sodium are present in the exchangeable sites clay aggregates become less stable and deflocculates in the presence of water. This is due to Na^{+} being mono-valent and incapable of effectively neutralising the charge on the clay platelets, therefore not being able to prevent swelling and dispersion (Brady 1990). A high presence of Mg^{+2} will

aggravate the deflocculation process further under certain conditions. “Thus, Na-Mg soils were found to have more clay dispersion and lower hydraulic activity than Na-Ca soils” (Mcneal *et al* 1968; Emerson & Smith 1970; Bakker & Emerson 1973 in Rengasamy *et al* 1986: 229) as it has an indirect influence on higher adsorption of Na^+ (Rahman & Rowell 1979).

Two different indices are often used to measure the potential of deflocculating occurrence in the presence of water which will determine its dispersibility. These are known as the Exchangeable Sodium Percentage (ESP) and the Sodium Absorption Ratio (SAR). Since there is a direct link between soil erosion by water, gully erosion, and water dispersible clay (Brubaker *et al* 1992; Igwe & Udegbunam 2008) it is important to incorporate these indices into the exploration criteria of gully development.

The ESP of a soil is the base saturation percentage of Na^+. This percentage would indicate the amount of exchange sites that Na^+ occupies in conjunction with other cations (Braday & Weil 1999) in the ECEC. ESP is an indication of the sodicity of a soil, being indicative of a soils structural stability as Na^+ favours dispersion in the presence of water. ESP is measured in millimoles per liter (mmol/l) and calculated using the below formula:

$$ESP = Exch\left[\frac{Na^+}{(Ca^{2+} + Mg^{2+} + K^+ + Na^+)}\right] * 100$$

Equation 2.1

SAR and ESP are closely related. Where ESP is the amount of Na^+ on the cation exchange complex of the clay fraction of a soil the SAR is the amount of Na^+ in the solution phase. SAR is measured in millimoles per liter and calculated using the below formula:

$$SAR = \frac{Na^+}{\left[\frac{1}{2} * (Ca^{2+} + Mg^{2+})\right]}$$

Equation 2.2

“Clay particles in a soil in contact with the water in soil will strive to be in chemical equilibrium with the water” (Graaff van de & Patterson 2001: 364). If the clay fraction of a soil consists over a high CEC the water surrounding the clay will also be densely populated by a high amount of cations. Also if a high amount of a specific cation like Na^+ are present in the water surrounding the clay particles a higher amount of Na^+ will be on the cation exchange complex of the soil (Graaff van de & Patterson 2001). This relationship can be expressed as:

$$\frac{ESP}{100 - ESP} = 0.015 * SAR$$

Equation 2.3

ESP and SAR portray soil structure and how dispersible the clay fraction is. They have been found to be a good indicator of soil dispersibility and have been closely linked to gully erosion (Rienks *et al* 2000; Faulkner *et al* 2004; Sonneveld *et al* 2005; Van Zijl 2010). Rienks *et al* (2000) also found SAR to have a good correlation to gully development. Even though a good correlation has been found with these two indicators, a soil's dispersibility cannot be solely judged on this. Electronic Conductivity (EC) as well as potential hydrogen (pH) needs to be used in conjunction to this to produce a more accurate picture (Mcbride 1994; Sparks 2003) as this has an influence on CEC and thus ESP and SAR.

EC is the "preferred index to assess soil salinity" (Sparks 2003: 223). It is based on the concept that an electrical current will be carried by the dissolved salts in solution and that the current will increase with an increased amount of dissolved salts (Mcbride 1994; Sparks 2003). The higher a soil's CEC the higher its EC would be as the cations on the exchange sites will enhance the current that is conducted. The universal unit in which EC is measured is desiSeimens per meter.

pH also influences the CEC. As pH increases CEC increases dramatically. This is due to the "dissociation of the H^+ cation from the functional groups of the Soil Organic Matter (SOM)" thus making new exchange sites available for the alkaline cations to be adsorbed.

The EC, ESP and pH values can be used to classify a soil as sodic or saline giving an indication of the structure, hence how easily it will disperse in the presence of water. Universally accepted threshold values are indicated in Table 2.2 below:

Table 2.2 Soil classification according to EC, ESP and pH.

	EC (dS/m)	**ESP (%)**	**pH**	**Soil Structure**
Saline	> 4	< 15	< 8.5	Good
Sodic	< 4	> 15	> 9.0	Poor
Saline-sodic	> 4	> 15	< 8.5	Fair

Source: Mcbride 1994

Even though the above is universally used, it was suggested by Beckedahl (1996) and Walker (2007) that the threshold values indicated in Table 2.1 are ill suited for RSA conditions. The critical values that classify a soil as sodic, thus having a poor structure and prone to disperse in the presence of water should be lowered when dealing with RSA conditions, especially if a high amount of exchangeable Mg^{2+} is present.

With regards to gully research, a strong correlation has been found between the dispersion of soils and the formation of gullies especially where piping is the dominant formation process (Rienks *et al* 2000, Van Zijl 2010). According to Rienks *et al* (2000) the soil does not have to be highly sodic (contain high levels of sodium) to disperse with an ESP value of 6% only. This is supported by Faulkner *et al* (2004) as well as Sonneveld *et al* (2005) finding that sub-surface dispersion can occur in materials that are only potentially dispersive, SAR < 3, and ESP values ranging from 0 - 19% respectively. Even though some studies use SAR, a better correlation exists between ESP values and soil dispersion (Rienks *et al* 2000; van Zijl 2010). Soil pH measurements are used in conjunction with ESP to determine the dispersion risk of soil. Where high pH values are measured lower ESP values are required for dispersion to take place (Sparks 2003).

2.5.4 Climate change

Little information exists on how gully systems may respond to climatic change. In areas where climates become drier vegetation will decay causing large areas to be unprotected. Runoff will increase promoting gully erosion (Valentin *et al* 2005). Global warming is expected to increase the frequency of freeze thaw cycles exacerbating the risk of gullying (Øygarden 2003).

2.6 A PLACE FOR NIR REFLECTANCE SPECTROSCOPY IN GULLY RESEARCH

The NIR region lies between the Visible and Mid Infrared (MIR) region of the electromagnetic spectrum. It occupies wavenumbers 12 500 – 4 000 cm^{-1} which correspond to wavelengths of 700 – 2500nm (Chang *et al* 2001; Siesler 2008). The region is indicated in Figure 2.3.

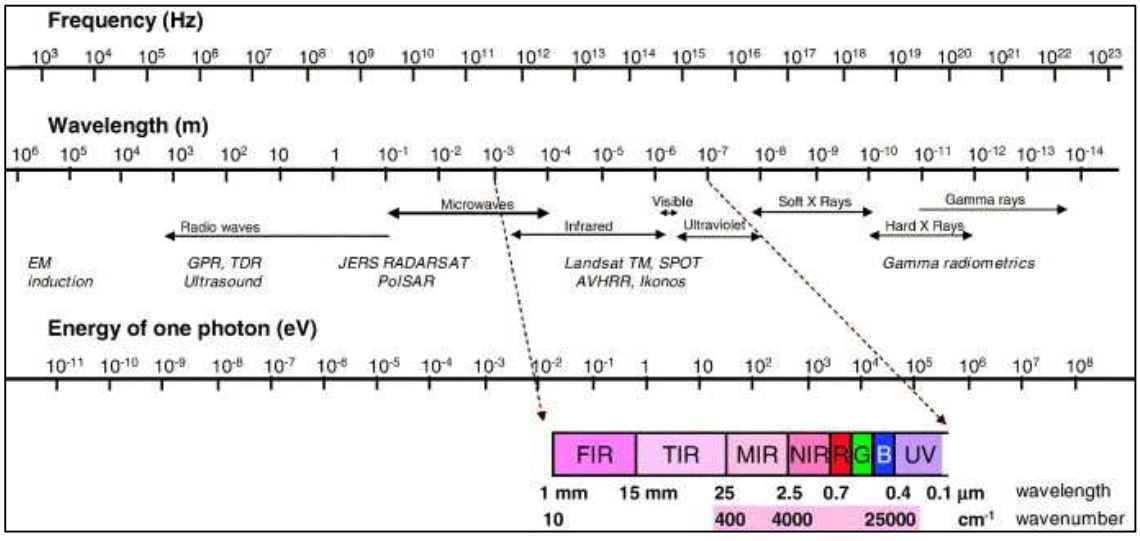

Source: Viscara Rossel *et al* 2008

Figure 2.3 NIR region

2.6.1 Background to NIR spectroscopy

When a sample is hit by NIR radiation several interactions can occur as indicated in Figure 2.4. Interactions c (absorption) and b (diffuse reflectance) has emerged as the interactions most used to enable quantification of sample properties in the agricultural sector (Newgard 2005).

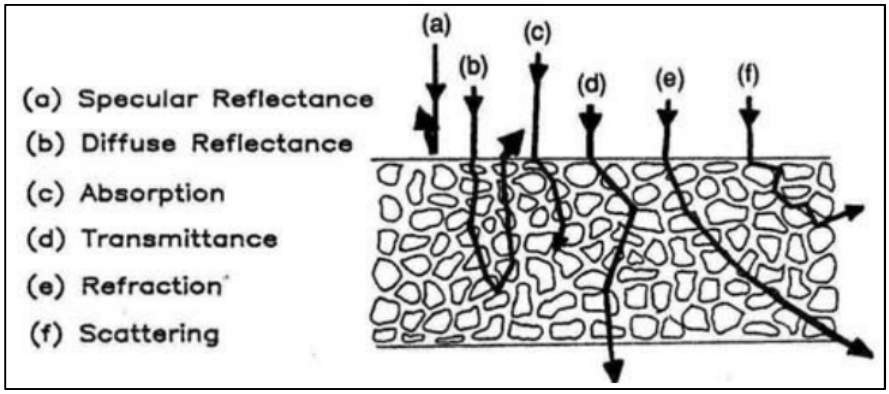

Source: Newgard 2005

Figure 2.4 Possible reactions of NIR radiation upon striking a soil sample

Reactions, as indicated in Figure 2.4 above, will correspond to the properties contained in a sample (Sternberg *et al* 2010). More specifically, the absorption and diffuse reflectance interactions can be used as ways to identify trends, thus creating a fingerprint for these properties. This is due to the NIR radiation causing the molecular bonds to vibrate by either stretching or bending (as indicated in Figure 2.5) and it is these motions that will dictate the absorbance and reflectance (Pasquini 2003; Newgard 2005; Siesler 2008). It is the degree of absorption and reflectance of the NIR radiation that can be used as a fingerprint to quantify the make-up of a sample as it is this that gives the spectra its unique shape (Miller 2001).

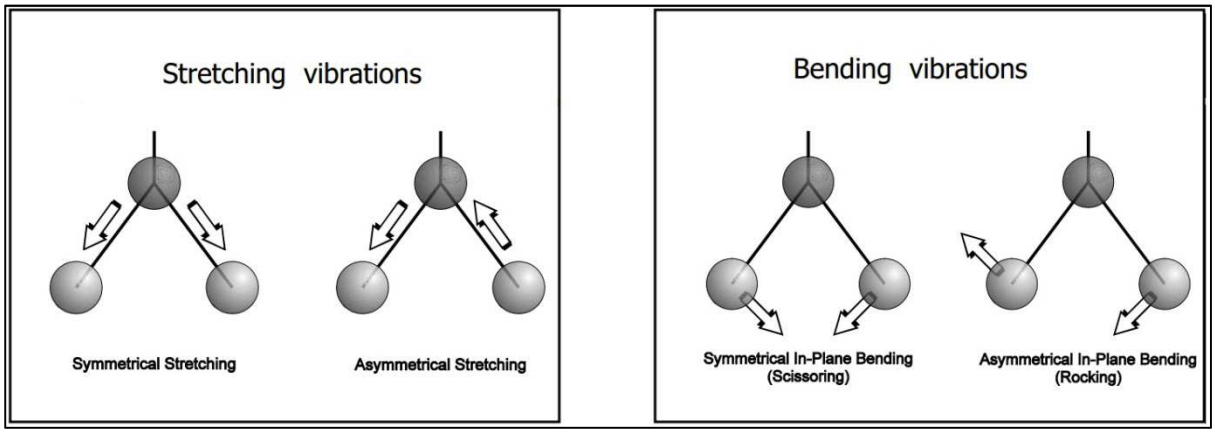

Source: Alander J 2004

Figure 2.5 Molecular bending and stretching

Upon NIR radiation interacting with a sample the vibrations as explained above are those of overtones and combinations of fundamental vibrations occurring in the MIR region (Sternberg 2010). "Molecular functional groups can absorb in the MIR, with a range of progressively weaker orders of overtones detected in both the MIR and NIR regions" (Sternberg *et al* 2010: 167), hence characterising the NIR region by weak superimposed vibrations resulting in broad absorption features. Furthermore, NIR spectroscopy requires both a dipole moment change and a large anharmonocity (Pasquini 2003). Both these phenomena exist where hydrogen bonds with another heavier element. The overtones and combination bands of the functional groups of O-H, S-H, N-H and C-H therefore dominates the NIR spectrum. The overtones and combinations that arise due to these functionalities occur approximately at ½ and ⅓ of the fundamental absorption wavelength (See Figure 2.6 for approximate locations) and the intensity decreases with an increase of overtone intensity (Sternberg *et al* 2010).

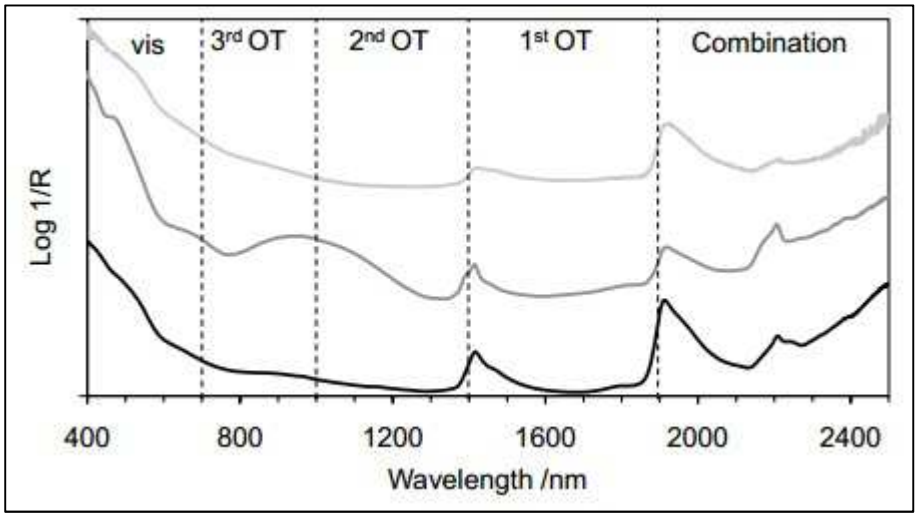

Source: Sternberg *et al* 2010

Figure 2.6 Locality of NIR combination and overtones

Upon using absorption or diffuse reflectance spectroscopy in the NIR region the spectra that is obtained in graph format is of direct consequence of the molecular vibrations. It consequently indicates the chemical compounds that exist in the sample. Due to broad and overlapping spectra obtained in the NIR region it makes it difficult to interpret. It necessitates the use of chemometric methods in order for it to be mathematically analysed to quantify sample make-up.

2.6.2 Application of NIR diffuse reflectance in soil science

NIR spectroscopy research initially focused on agricultural foodstuff in order to chemically characterise it by measuring the major properties of the material as well as some of the minor organic and inorganic properties (Batten 1998; Cozzolino & Morón 2003). This enabled a new way for establishing the nutrient content and thus quality control of food and forage. Due to the ease of use

and robust nature of NIR research, it also progressed to other fields beyond agriculture such as analysis of textiles (Ghosh & Rogers 2008), polymers (Kradjel & Lee 2008), wool (Hammersley & Townsend 2008), petroleum (Workman 1996; Buchanan 2008) and pharmaceuticals (Anderson *et al* 2008; Ciurczak 2008).

Recently, research with NIR has also been done on environmental work (Malley *et al* 1996). Soil plays an important role in this aspect. Soil serves as a water movement regulator in the landscape; it acts as an environmental filter for metals, nutrients and other contaminants; it is a biological habitat; and presently it has also been looked into as a possible answer for carbon sequestration (Stenberg *et al* 2010). In addition to the above, precision agriculture is also emerging. This is very data sensitive in it requires enormous amounts of data. It then becomes clear why NIR research in soil is steadily increasing.

Soil is a complex matrix that is formed of organic and inorganic matter, water and air. “The organic material of soil ranges from decomposed and stable humus to fresh particulate residues of various origins” (Sternberg *et al* 2010: 163). It is the different make-up of the organic materials as well as clays that influence the biological activity in soil, nutrient availability and dynamics, soil structure and aggregation as well as its water holding capacity (Skjemstad *et al* 1997).

The soil make-up is highly spatially variable and changes occur over short distances with variation even occurring in a single agricultural field. In order to manage this resource effectively a large amount of samples have to be collected and analysed due to this spatial variability. The soil science discipline has spent the past few decades to standardise analytical methods. Although these now conventional methods have become standard and are sound, they are very expensive. It is also a laborious exercise that produces hazardous chemical waste (Viscarra Rossel & McBratney 1998a & b; Volkan Bilgili *et al* 2010).

NIR diffuse reflectance spectroscopy is advantageous as it is a rapid process that allows for many samples to be analysed in a short time period; It is non-destructive which allows the basic integrity of the soil to be kept intact; It is less expensive than conventional methods and also does not require pre-treatment that often require chemicals, thus producing hazardous chemical waste as a final by-product (Viscarra Rossel *et al* 2006). Furthermore, a single soil spectrum obtained via NIR can be utilised to characterise various soil properties.

Due to these noticeable advantages Janik *et al* (1998) stated that NIR diffuse reflectance spectrometry should be considered a replacement of the conventional techniques or at the very least play a supportive role in order to enhance soil analyses. NIR will open the possibility to process large numbers of soil analyses making it possible to build up a soil database, giving concerted steps towards effective environmental management.

NIR spectroscopy has gained popularity over the past few decades due to success in determining constituents of a soil matrix despite soil being a complex matrix and its spectra being relatively monotonous. “The main focus has been on basic soil composition, particularly soil organic matter, texture, and clay mineralogy, but also nutrient availability and properties such as fertility, structure, and microbial activity” (Sternberg 2010: 166). Another keen research area that has gained popularity is the measurement of carbon in soil due to the possibility of using it as a pool for carbon sequestration (McCarty *et al* 2002; Reeves *et al* 2006).

The overarching aim of this research project is to understand the gully development in the Sandspriut Catchment with specific focus on the Malansdam gully system. Therefore, it is important to have information specifically involving the chemical make-up of a soil as mentioned in section 1.1 to establish how well it is structured, thus getting a dispersion index to see how easily it will deflocculate in the presence of water. The focus will therefore lie on eight variables. The first aim of this study is to explore the possibility of creating a NIR fingerprint for these eight variables namely the exchangeable cations Ca^{2+}, Na^{+}, Mg^{2+}, K^{+} as well as EC, pH, ESP, SAR and Magnesium Saturation Percentage (MS%). If this is possible it would generate a wealth of information with regards to soil dispersion with a singular scan, saving time but also making the process less expensive. Many samples can thus be done cost and time effectively making it possible to analyse a large amount of samples in a limited time window, be it for research purposes or agricultural.

Certain aspects of soil have well established NIR such as the mineralogy of clay which is spectrally active due to the metal-OH bend or moisture of a soil due to the O-H bond. (Clark 1999; Brown *et al* 2006; Sternberg *et al* 2010). Other soil constituents that are not spectrally active may be also be predicted successfully. This is thought to be due to correlations that exist with another constituent that is spectrally active (Ben-Dor and Banin 1995).

The exchangeable cations namely Ca^{2+}, Na^{+}, Mg^{2+} and K^{+} are not spectrally active in the NIR region therefore it cannot be measured through vibrations of the C-H, O-H or N-H bonds. Volkan Bilgili (2010) suggested that these cations can be measured and thus predicted due to their correlation with clay and Soil Organic Matter (SOM). The prediction of the four cations varies. Ca^{2+} and Mg^{2+} are usually predicted successfully (Chang *et al* 2001; Dunn *et al* 2002; Islam *et al* 2003; Malley *et al* 2004; Volkan Bilgilli *et al* 2010). This could be attributed to “correlations with carbonate content and factors influencing CEC, such as SOM content” (Malley *et al* 2004: 762). Na^{+} is sometimes well predicted (Dunn *et al* 2002; Malley & Yesmin 2002) possibly due to “chromophores related to the presence of salt, such as organic matter, or particle size distribution” (Malley *et al* 2004: 762) but poor results have also been widely reported (Chang *et al* 2001; Zornoza *et al* 2008; Volkan Bilgilli *et al* 2010). Predicted results for K^{+} generally deliver poor results (Chang *et al* 2001; Zornoza *et al* 2008).

ESP, SAR and the MS% are also not spectrally active. They are however closely related to the exchangeable cations. ESP and the MS% are both calculated with the exchangeable values of Ca^{2+}, Mg^{2+}, Na^{+} and K^{+}. ESP is calculated with equation 2.1 and the MS% is calculated with:

$$MS\% = Exch\ [Mg^{2+}/(Ca^{2+} + Mg^{2+} + K^{+} + Na^{+})] * 100$$

Equation 2.4

Due to the relationship that ESP and the MS% have with the exchangeable cations the possibility of successful prediction via NIR is thought to be possible. ESP has been predicted adequately (Dunn *et al* 2002) whilst the MS% has not yet received any research attention. SAR is another index that is dependable on the exchangeable cations. The reason for this is that the more there is of a specific cation on the exchange sites, more of that same cation will be attracted to be in solution surrounding those exchange sites (Sparks 2003). SAR is calculated by equation 2.2. Due to its dependency on the exchangeable cations it is expected to be relatively well predicted by NIR spectroscopy as was found by Seilsepour *et al* (2009).

Soil pH is not expected to be spectrally active as hydrogen ions are not primary absorbers of NIR radiation. Malley *et al* (2004) suggested that prediction of pH could well occur due to OH^{-} functional group or carbonate, whilst Chang *et al* (2001) suggested it to be due to covariation of SOM or clay which is spectrally active. The prediction of pH is partially successful (Reeves & McCarty 2001; Shibusawa *et al* 2001; Islam *et al* 2003). Optimum results are obtained when calibrations are done per field or agricultural unit as the covariation with the constituents that are spectrally active may differ from one unit to another (Reeves *et al* 1999; McCarthy & Reeves 2006; Sternberg *et al* 2010).

EC is also not spectrally active and its prediction is also based on soil constituents that have a primary response and thus active (Zornoza *et al* 2008). Predictions of EC are generally poor (Shibusawa *et al* 2001; Zornoza *et al* 2008; Volkan Bilgilli *et al* 2010).

2.7 CONCLUSION

Even though the control factors for gully erosion have been studied in isolation focusing mainly on anthropogenic factors rather than utilising a joint approach which would include control factors from both the anthropogenic and natural groups; gullies are well defined and their formation processes are also well understood.

It has been proved that gullies contribute significantly to total soil loss and it is therefore of paramount importance to determine the control factors driving gully erosion. This is something that has received minimal attention. Since gully erosion is systemic threshold phenomenon, a preventative plan to reduce gully erosion would require a focus on multiple factors. Such a plan will have to investigate

factors that include factors from both the anthropogenic and physical groups, as any combination of factors could initiate gully erosion.

NIR diffuse reflectance spectroscopy has emerged as a potential technology that could be utilised in not only environmental management but possibly gully erosion itself. Soil properties and indices that have been closely linked to gully erosion have been accurately predicted by various authors. Although it requires further investigation, NIR diffuse reflectance spectroscopy looks like a faster and more economical approach that could replace, or at the very least support, traditional wet chemistry techniques to obtain values for indicators of soil dispersion potential.

3 HYDROLOGIC RESPONSE TO LAND USE

3.1 GULLIES AND CONTOUR FARMING

As Meadows (2003) has indicated, the South Western Cape is vulnerable to high levels of soil erosion by water. To counteract this, farmers in this region employ a technique called contour ploughing to counteract soil loss and Meadows (2003) found that there is a total of 25 000km of contours in the Swartland region alone. As Steudel *et al* (*in press*) described it, a ploughed contour consists of earthen structures that are constructed on cultivated fields in a perpendicular manner to the slope experienced. It is suggested that this would reduce soil erosion as it reduces slope lengths and therefore flow velocity, by means of intercepting runoff (Wakindiki *et al* 2007) and channelling it into a stable waterway, natural depressions or grass areas as seen in Figure 3.1 (DERM 2004 in Steudel *et al* (*in press*).

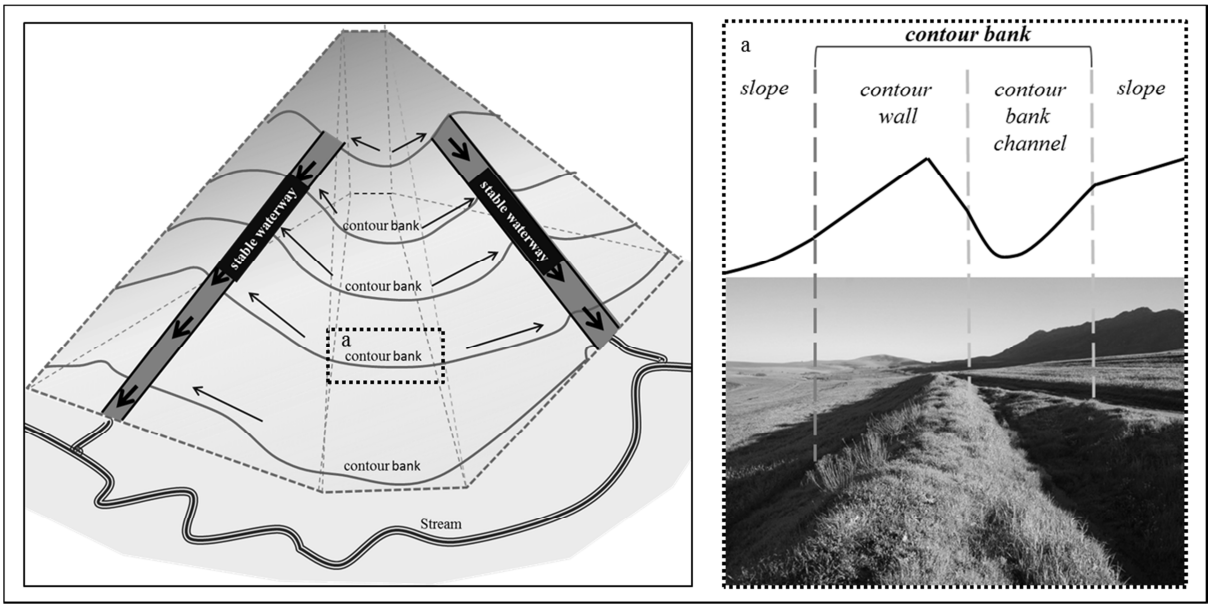

Source: Steudel *et al* (*in press*)

Figure 3.1 Influence of contour ploughing on landscape hydrology

If the stable waterway, as indicated in Figure 3.1, however is an active gully system such as at Malansdam, contour ploughing might have the opposite result as opposed to the intended result. Firstly, large amounts of water could be channelled into the gully system further upslope than would have occurred without ploughed contours. This would increase the water quantity as well as the flow velocity in an area where a steeper slope is experienced, with the net result being increase erosion capability. Secondly, the gully channels could grow into the cultivated field due to headward retreat of the gully as the ploughed contours would ensure a constant supply of water.

3.2 FIELD OBSERVATIONS

Field observations together with Google Earth imagery and high resolution GeoEye images were used to make decisions with regards to finalising test sites for this research project. Below is a brief discussion of a few of the observations made during fieldwork, starting from a holistic first impression and moving towards more localised phenomena.

3.2.1 Farming system: Ploughed contours

Figure 3.2 is a photo of the northern leg of the split gully system at Malansdam. It was orientated in a northerly direction and taken from the lower reaches of the gully.

Figure 3.2 Effect of contouring on the Malansdam gully system.

When looking at this photo it is evident that the contour farming system implemented, does have an effect on the gully as this can be seen by the natural vegetation stretching into the field units in a linear and methodical fashion. It is at these locations where the gully is growing and extending along the ploughed contours into the agricultural field units. The reason for this occurrence is that the contours are acting as channels, collecting water and redirecting the flow along it into the gully. It would seem that this is causing gully head retreat along the ploughed contour into the field. Due to the orientation of the photo, it appears to be more prominent in the eastern field unit, but the same phenomena also occurs in the western field unit. Furthermore, as the gully spreads into the natural vegetation numerous gully scars can be witnessed.

3.2.2 Badland Development

The upper slopes of Malansdam gully system is in a state of intense gully development. This is evident from the numerous gully channels existing in close proximity from another. Figure 3.3 depicts this and was taken in a southerly orientation from one of the gully walls in the northern leg. The numerous channels with the bare walls are indicative of the soil being dispersive and could result in badland development.

Figure 3.3 Badland development in the upper reaches of the Malansdam gully system

In addition to this, it can be observed that the main gully channel runs along the field boundary fence, which splits the two cultivated field units. However, it is progressing into the field units behind the ploughed contours lending further support to the observation and assumption made from Figure 3.2. Furthermore, as the gully moves south towards the top of the picture it veers into the field unit breaking which was once a singular unit into two. Expenses may increase due to fuel costs, longer labour hours and wear on machinery, as the farmer will struggle to gain access to the cultivated areas, because the gullies cannot be crossed.

3.2.3 Gully processes in action

After a long wet spell, it was thought a good idea to go to the field to try and investigate a few of the gully developing processes in action. Figure 3.4a and b is a small compilation of the processes observed.

Figure 3.4 Gully processes in action at Malansdam: *a) Contours collecting and channelling water; b) This water collected are fed into the gully causing headward erosion*

Figure 3.4a shows the water collecting capability of ploughed contours. This serves as confirmation of the observation made in Figures 3.2 and 3.3. As the water is fed into the gully, the water increases in speed and velocity and thus the erosive force as it falls over the edge of the gully head into the splash zone as seen in Figure 3.4b.

3.3 MATERIALS AND METHODS

A GeoEye DEM, with a vertical accuracy of 0.7m and a spatial resolution of 1.5m x 1.5m, was attained from Mashimbye (2013). This DEM was hydrologically corrected where upon a hypothetical natural drainage pattern was generated by making use of the hydrology toolbox in the Spatial Analyst extension of ArcMap 10. This represented the natural drainage pattern, if there was no agricultural activity in the catchment. This was used in unison with the digitised gully system to establish water entry points into the gully. Polygons were constructed to establish the surface area for each entry point in an effort to determine the net runoff into the gully system under the hypothetical condition.

Thereafter, the ploughed contours were digitised. This was done with the aim of producing a conceptual model of how the hydrological system would interact with the current agricultural activity. Since the contours channel runoff towards the gully, the points where the contours meet the gully were digitised as the water entry points. Subsequently contour lines were closed according to relief (watershed boundary) in order to calculate the area which would produce runoff for each entry point.

The volume of water entering the gully under circumstances for both the hypothetical approach as well as the actual agriculture induced drainage was determined by Equation 3.1

$$Runoff = 0.001m \times area\ (m^2)$$

Equation 3.1

Due its purpose only being illustrative of the difference the agricultural activity has had on the landscape hydrology, runoff was calculated to be 100% rain dependent thus having no infiltration. 1mm of rainfall was used to compute the total run-off for comparative purposes.

3.4 RESULTS

Drainage patterns were determined for both a hypothetical normal flow directly from the DEM as well as a drainage pattern induced onto the landscape due to ploughed contours. Refer to Figure 3.5 and 3.6 respectively

.

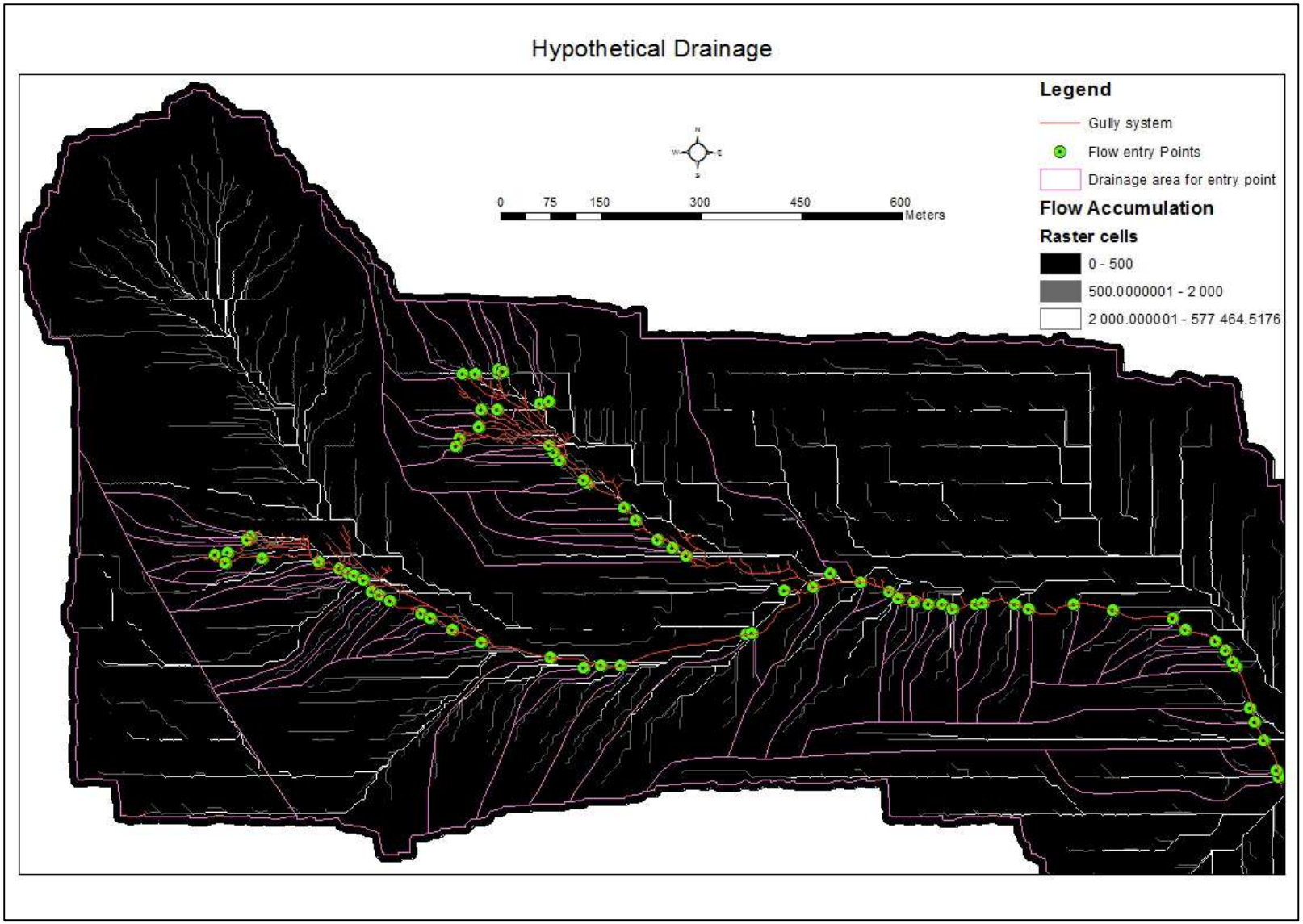

Figure 3.5 Hypothetical (Normal) drainage of Malansdam sub-catchment

The hypothetical drainage system as shown in Figure 3.5 had numerous small pathways into the gully system on the southern side of both the northern and southern legs. Water flow entry points into the gully in this area are spaced irregularly and close together. The area of these drainage pathways ranged from 274.71m^2 to 12 380m^2. A large drainage pathway runs between the two legs along the southern gully leg only to enter the gully system where the two legs join. This is also the largest drainage area pathway amounting to 349 809m^2.

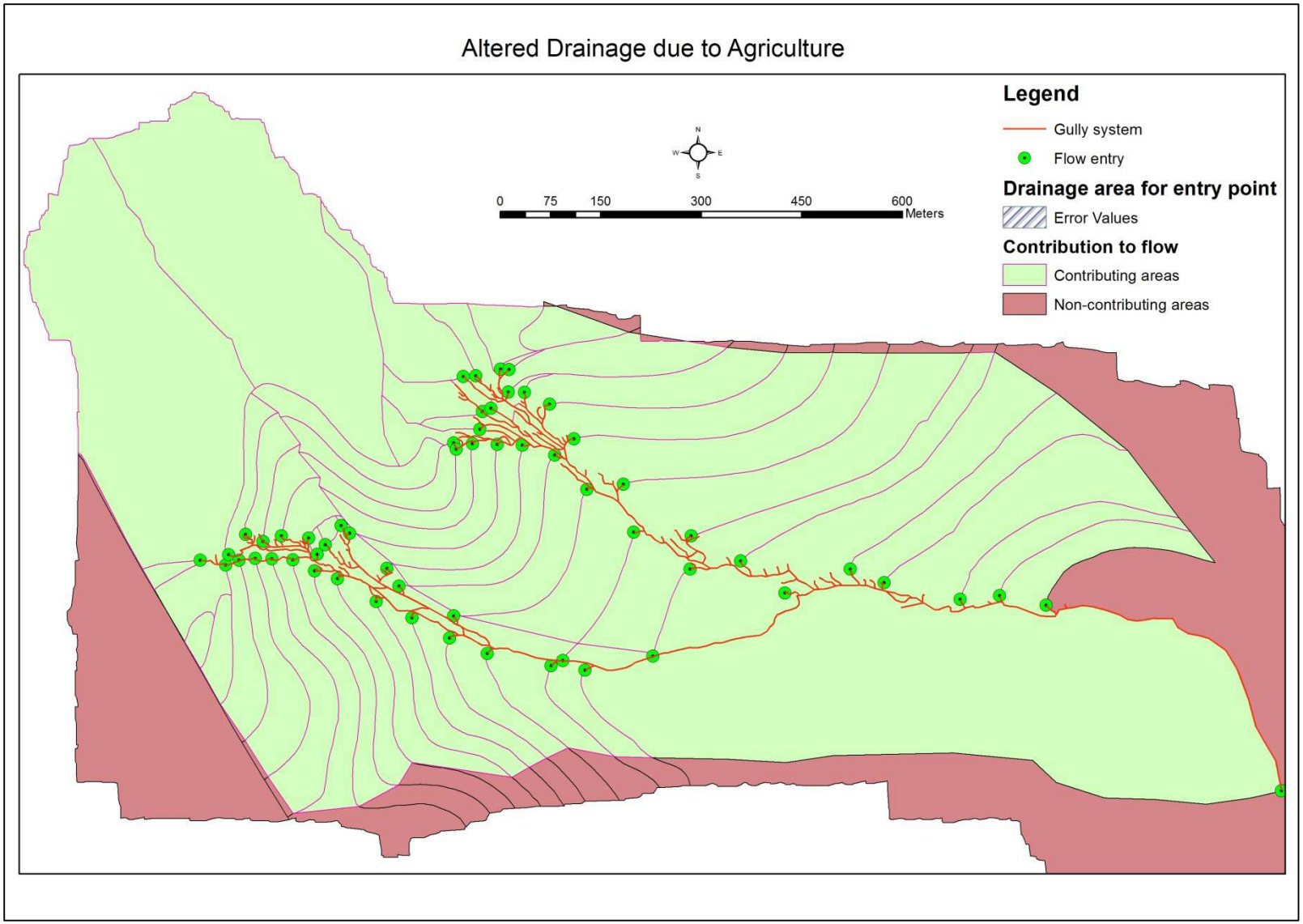

Figure 3.6 Current drainage as affected by agricultural activities with the employed ploughed contours at Malansdam

The drainage pattern produced by the ploughed contours in Figure 3.6 lends a structural nature to the landscape hydrology. Entry points of flow along the contours are less erratic and more evenly spaced. There is however, still a wide range of sizes per drainage area with the largest area of 216 528.76m^2, this being significantly smaller than the hypothetical drainage pattern. Areas contributing to flow have been indicated in green whilst areas not contributing to flow have been indicated by red.

The volume of water flowing into the gully system at each point was scaled and presented as maps in Figure 3.7and 3.8 respectively. In each map a small insert map has been placed to indicate the various entry points for each scenario. Furthermore, the entry points were colour coded. Red entry points show a point where at least 10mm or more water would enter the gully system with the light blue being less than 10mm. Due to the scaling effect, the entry points with very little water entering the system are barely visible with the larger entry points overlaying some entry positions in other areas.

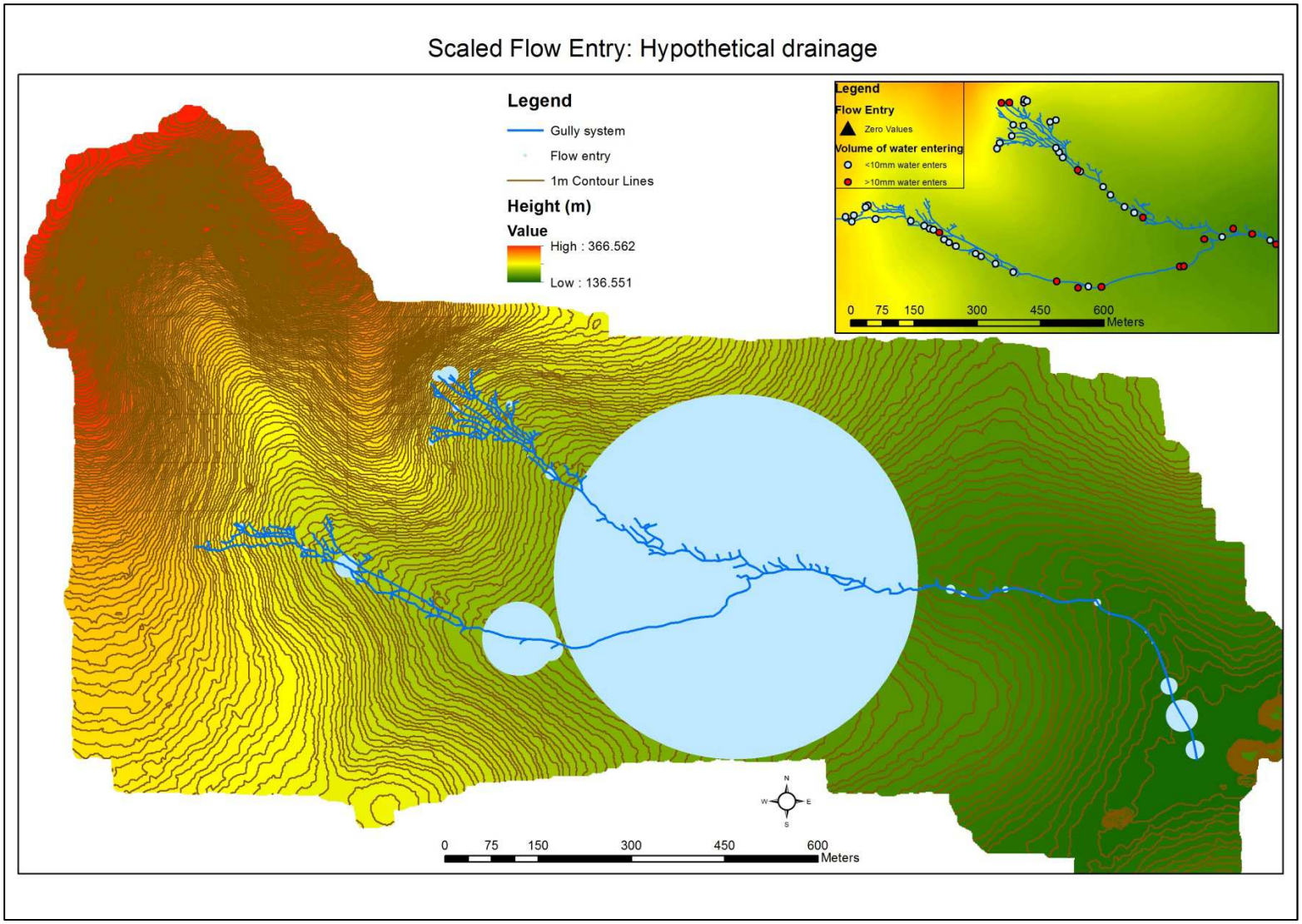

Figure 3.7 Scaled flow entry under hypothetical (normal) circumstances at Malansdam

Due to the calculation procedure the amount of flow entering the gully system is heavily dependent on surface area. As seen in Figure 3.7 a large number of entry points are south of the northern and southern legs. They are however densely grouped with small catchment areas, consequently having little effect on the volume of water entering the gully system in the upper reaches where the steeper slopes are experienced. The largest amount of water, calculated at 349.81m^3, enters the gully where the two legs join. Prior to this large inlet into the gully, only ten entry positions have a flow of 10mm or more into the gully system. This is indicated by the red symbols in the insert map of Figure 3.7. Of this only three entry points occur in an area of a steep slope. Two are located at the gully origin of the northern leg and one is located in the southern leg.

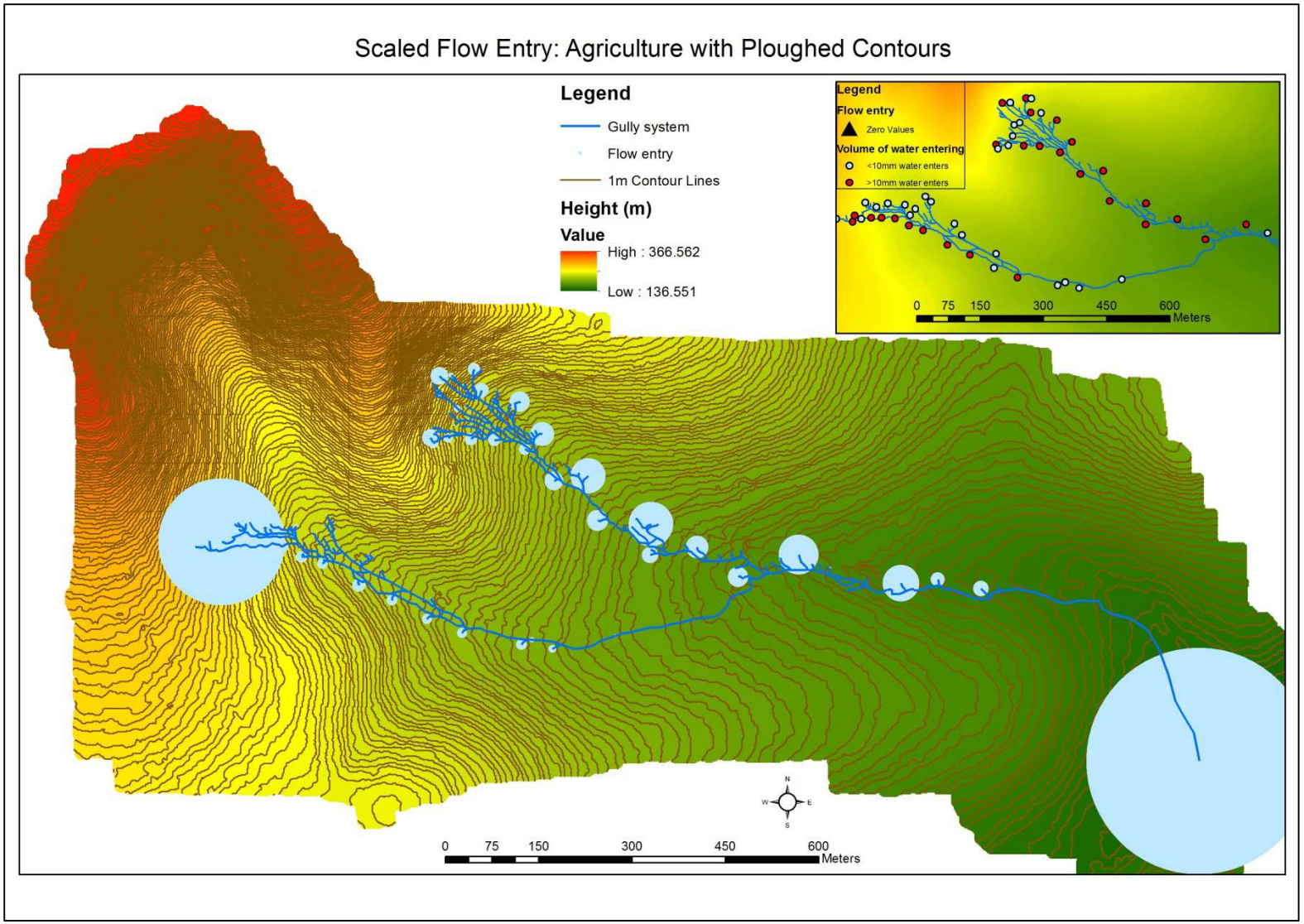

Figure 3.8 Scaled flow entry under current agricultural conditions (with ploughed contours) at Malansdam

Figure 3.8 illustrates the volume of water flowing into the gully along the ploughed contours. It is evident that the cultivation techniques applied has given a structural response to the landscape hydrology. Also noticeable due to the scaled symbols, is that more water enters the gully system in the higher reaches where a steeper slope is still experienced. More than 20 entry points produce a flow of more than 10mm into the gully system in the upper reaches, with a large volume of water (121.28m3) entering the southern leg of the gully system at its origin. The entry points exceeding 10mm of flow into the gully have been indicated by red symbols in the insert map, whilst the 121.28m^3 of water flow is shown by the large circular scaled blue symbol at the gully origin of the southern leg.

In order to establish a clearer comparison between the hypothetical flow and that incurred due to agricultural activity a series of points were selected at 100m intervals on both the southern and northern legs of the gully system (Refer to Figure 3.9). After the southern and northern legs joined the intervals were increased to 200m between points. At each of these points the cumulative volume of water flow coursing through the gully were calculated for both circumstances. This was calculated by adding the values of water flow volume at each entry point above the particular point together. This procedure was followed for both hypothetical and current agricultural conditions. See Figure 3.9 for results achieved for flow accumulation at all the points.

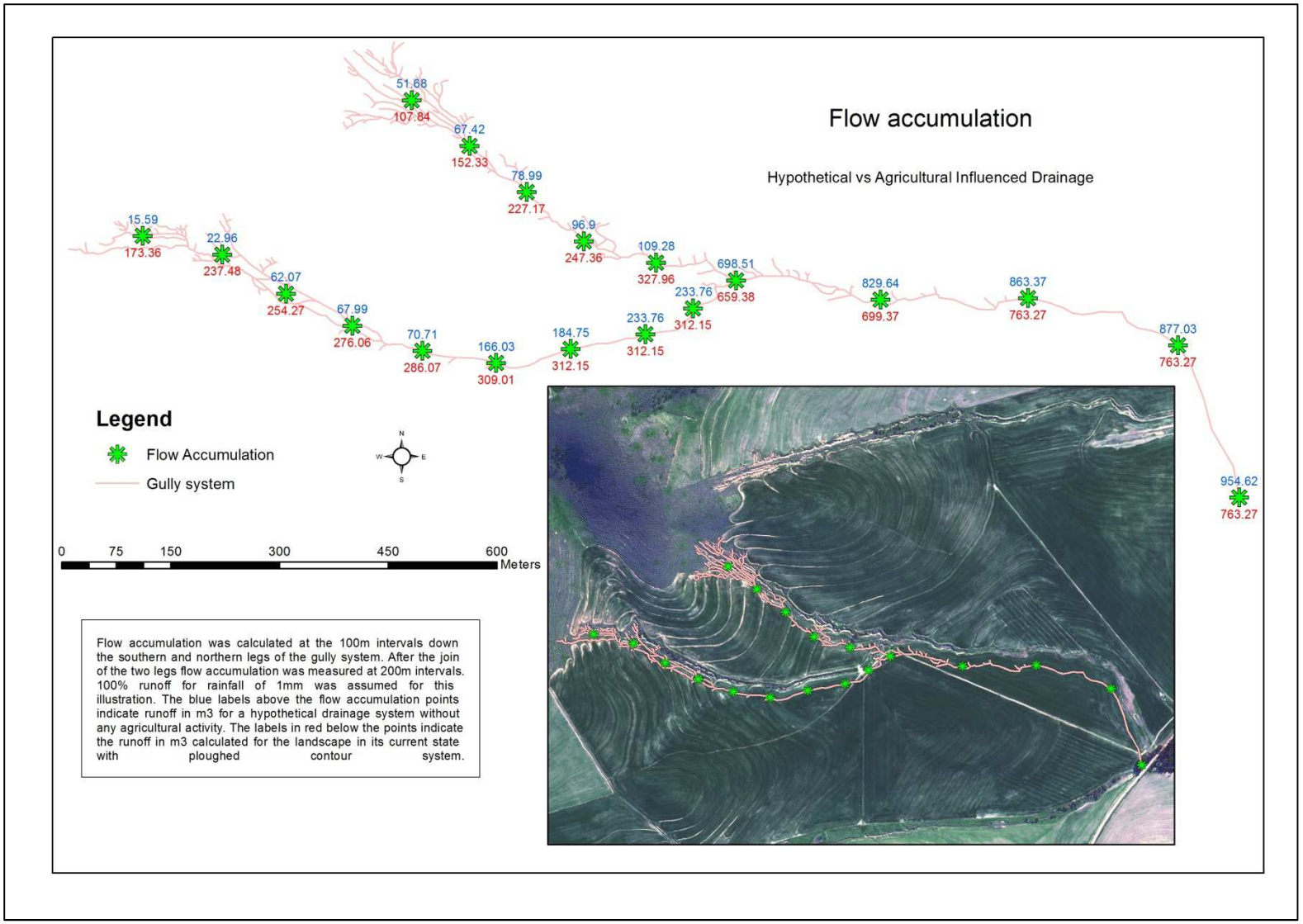

Figure 3.9 Volume of flow at selected points, at Malansdam, moving through the gully system: Hypothetical (Normal) vs Agriculutal Influenced Drainage

The volume of water flow is indicated by blue and red text along the gully channel in Figure 3.9 and has a measurement unit of m^3. The text (water volumes) corresponds to the green point symbol. These are the positions that were selected to calculate cumulative water flow. The cumulative flow occurring under hypothetical drainage is given by the blue text. The red text indicates accumulated flow under current agricultural conditions where ploughed contours have been used on the landscape in order to try and reduce erosion.

At the origin of both the southern and northern legs, the current agricultural scenario starts with a much larger volume of water than that of the hypothetical flow. Upon further scrutinizing the two values a pattern emerges. This is that under current conditions, extra water is systematically added to the gully system resulting in large volumes of water coursing through the gully in the upper reaches with a steeper slope. The flow entry under the hypothetical conditions has no structure and is fully dependant on the relief. Due to this little water, when compared to the current conditions, are flowing in the gully system in the upper reaches, with a singular large entry only occurring upon the two legs joining.

For a better visual representation and therefore an appreciation of the difference in accumulation for the two approaches, refer to Figures 3.10 and 3.11. Scaled symbols were used for the same points where accumulation was calculated as in the above Figure 3.9. With the help of this visual aid, the trend indicating the larger accumulation of water higher up in the gully under current agricultural conditions when compared to the hypothetical approach becomes clearer.

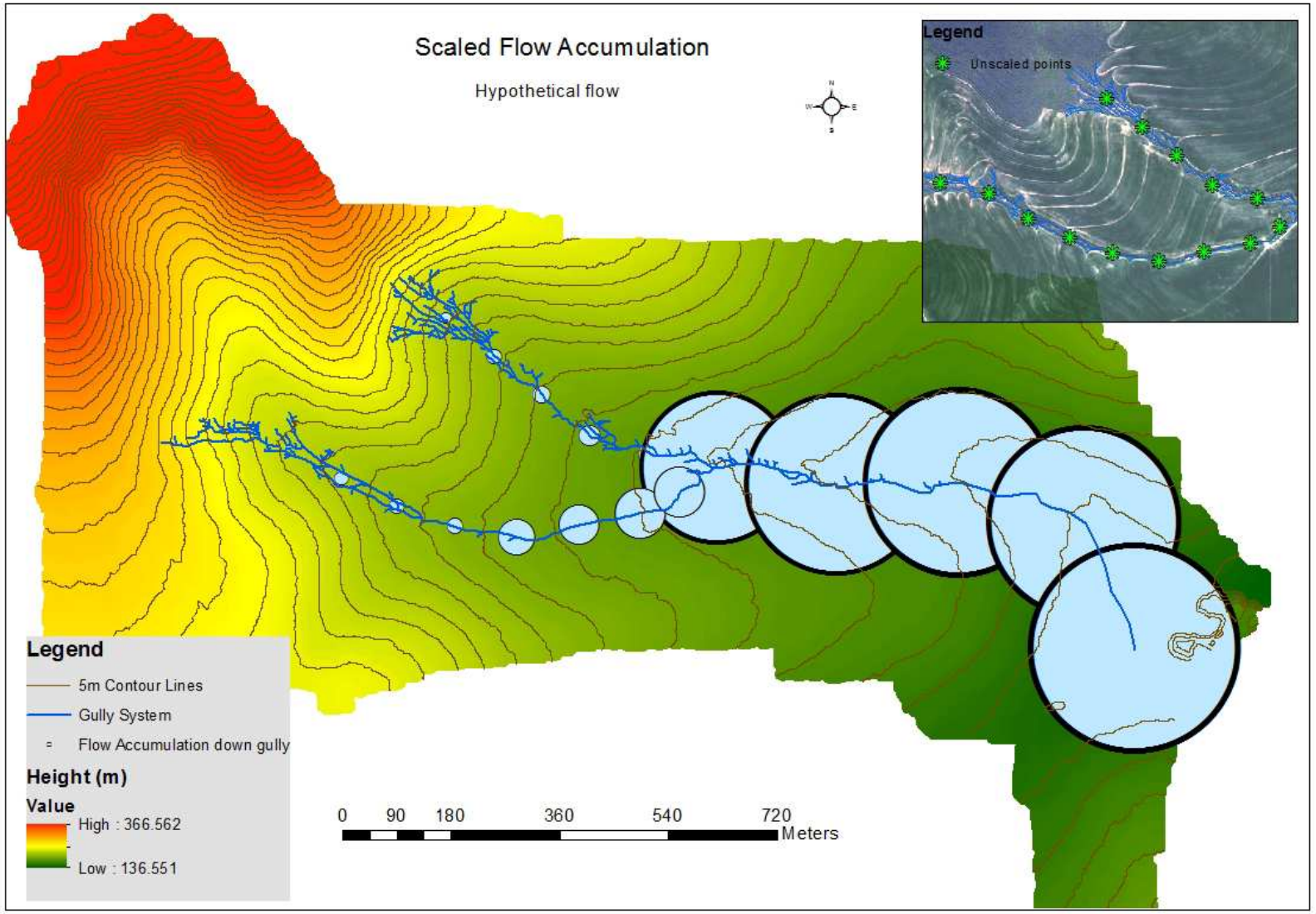

Figure 3.10 Scaled accumulative flow in the Malansdam gully system under hypothetical conditions

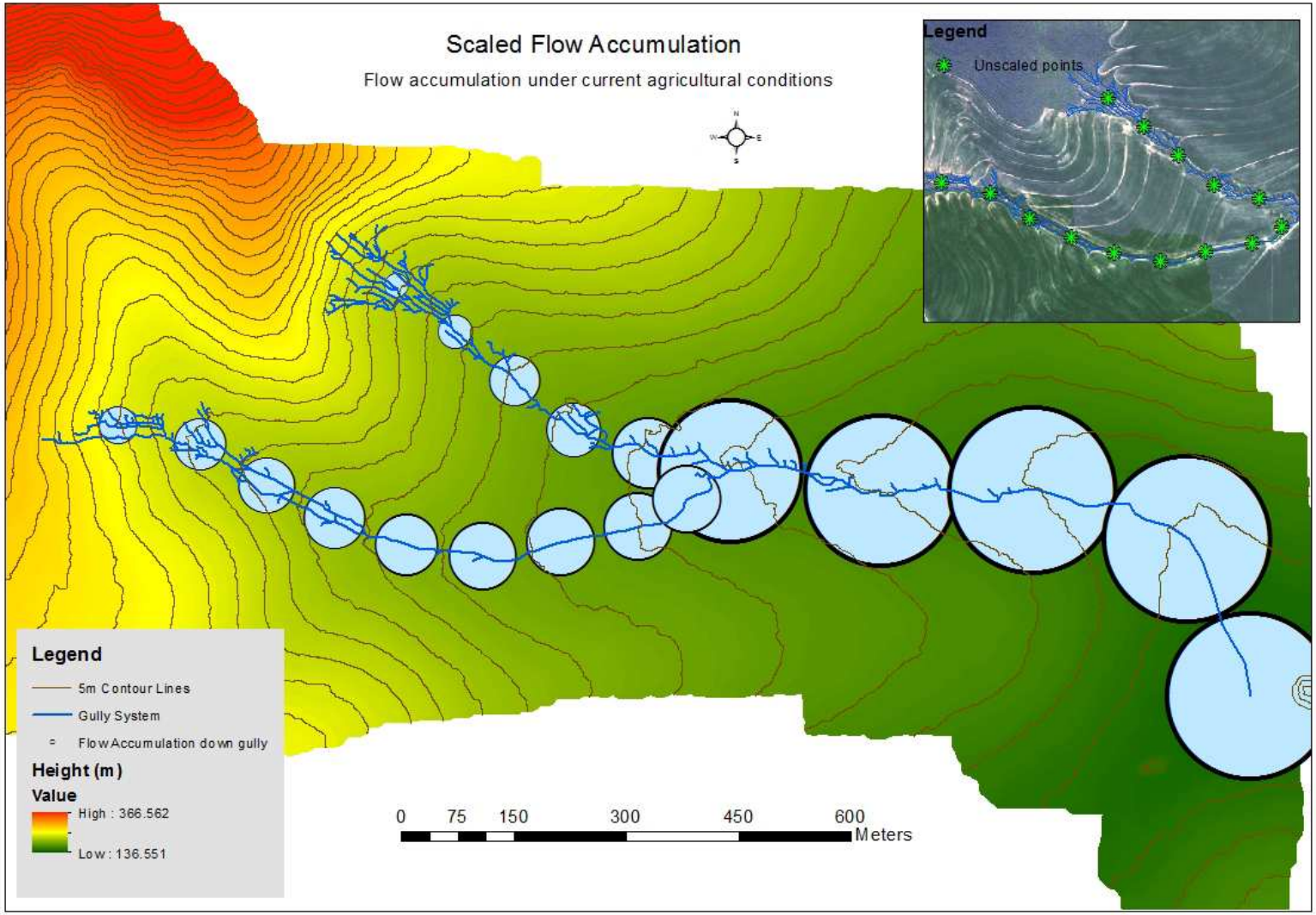

Figure 3.11 Accumulative flow in the Malansdam gully system under agricultural activities

The scaled symbols in Figures 3.10 and 3.11 accentuate the evidence produced by Figure 3.9. The hypothetical scenario produces little flow in the northern and southern legs, especially in the areas with a steep slope. Only once the legs merge does large accumulation of water flow occur. The slope in this area is gentle, thus reducing the erosive power of the water. Under current agricultural conditions, with the ploughed contours, water systematically accumulates. This results in much more water being in the gully system when compared to the hypothetical conditions at the same measurement points. Also, this is where steeper slopes are experienced meaning that water has a higher erosive potential.

Due to the curvature of the ploughed contours significantly less water enters the entire gully system. The total cumulative volume of water flowing through the gully system under the hypothetical approach amounts to 964.62m^3 whilst under current conditions it is only 763.27m^3. However, when volumes in the higher gradient upper reaches of the gully are compared, the quantity under current conditions is much higher than the hypothetical approach for both the southern and northern legs.

3.5 DISCUSSION

If the above can be seen as a measure of how well the contours channel the water and deliver it to the gully two further problems crop up.

Firstly, according to Poesen *et al* (2003) and Valentin *et al* (2005) the drainage area required for gully initiation plays an important role; it can only develop when a certain catchment threshold is reached with this threshold becoming smaller with a steeper slope. Vanwallaghem *et al* (2005) concurred with this especially in the case of large classical gullies like the Malansdam gully system. This would explain the formation of first order gully channels developing behind the ploughed contours as it creates a larger drainage area than would have occurred if no cultivation came about on the landscape. Oostwoud Wijdenes *et al* (2000) took the drainage area: gully relationship further by finding that this also contributes to its activity. When the drainage area decreases due to headward retreat there will come a point where it has shrunk too far causing the gully to become inactive as the water supply would become depleted to such an extent that it no longer warrants the velocity and quantity to cause erosion. When conducting an investigation into this on the test site this result seems to be accurate. This produces a worrying scenario for the landowner. As explained above ploughed contours instigated first order gully formation due to the large drainage area it creates with the outlet being into the larger gully channel. Due to ploughing of the cultivated fields headward retreat of these gullies will be stopped as the receding head will be filled with soil upon ploughing. The gully will thus return to its original starting position every year. This will however mean that the gullies will retain the same drainage area every year suggesting it will have access to the same velocity and quantity of water. The

rest of the gully system at Malansdam will thus grow deeper with the main channels growing wider due to it becoming undercut, invading the farm roads and cultivated fields. Larger soil losses from the cultivated fields into the first order gully channels will further amplify soil loss per annum.

Secondly, the ploughed contours causes the quantity of water that is channelled into the gully system in the upper reaches to be higher when compared to if no contours existed. This is demonstrated in Figures 3.9, 3.10 and 3.11. In Figure 3.9 specifically, the quantity of water entering the Malansdam gully system is shown under both hypothetical conditions without any farming activity but also under current conditions with the ploughed contours. This illustrates that the amount of water entering the gully overall has been decreased most likely due to the curvature of the contours that in certain areas causes a hindering of water flow. This is especially noticeable in the southern part of the map, indicated by red, in Figure 3.6. However the ploughed contour system causes the quantity of water to enter the gully in the upper reaches to be much greater than it would have been under normal conditions. This is also where a steeper gradient occurs and the erosive force would thus be enhanced.

3.6 CONCLUSION

Famers in the Sandspruit Catchment engage in a technique known as contour ploughing in order to curb soil erosion by water. The ploughed contours act as a partition reducing slope length and diverting water into a waterway which, in the case of Malansdam, is an active gully system. Due to this it seems as if the ploughed contours are counterproductive. Instead of limiting soil loss it is partly driving the growth of the gully system in two ways.

Firstly, it diverts water into the upper reaches of the gully system where a steeper slope is experienced. This amount is larger than it would have been if no ploughed contours were in place. Once this increased amount of water enters the gully it can flow without obstruction thus having an increased velocity which in turn results in an increase in soil erosion potential. Soil loss would therefore occur on the gully floor when the velocity of incipient motion is overtaken. It could further increase soil erosion of gully walls upon following the bends undercutting the gully's walls. This would result in soil loss from the walls but also enlarge the width of the gully when the wall collapse due gravity when the wall becomes undercut.

Secondly, the gully could expand into the cultivated field behind the contours due to headward retreat. Evidence of this can already be seen in Figures 3.2 and 3.3 and is further supported by the photos in Figure 3.4. The ploughed contours act as a constant supply of water after rainfall events. Due to the retreat valuable soil is lost but it also makes cultivating the fields harder as farmers will have to travel around each gully as it proceeds into the field.

4 PHYSICAL CHARACTERISATION OF THE DISCONTINOUS MALANSDAM GULLY SYSTEM

4.1 INTRODUCTION

Gullies have been identified by various studies (Watson 2000; Sonneveld *et al* 2005; Keay-Bright & Boardman 2007; Kakembo *et al* 2009) to be "very effective sediment sources in Southern Africa" (Sidorchuk *et al* 2003: 508). However, these studies have tended to focus on Kwazulu-Natal, the Karoo area and RSA's home lands, Lesotho and Swaziland. Meadows (2003) have pointed out that the Western Cape of RSA with its Mediterranean climate has the ideal setting for gully erosion occurrences. Thus far, few studies have investigated this specific area even though gully erosion is of immense concern in semi-arid Mediterranean climates such as France, Italy, Portugal, Spain and Greece (Kosmas *et al* 1997; Oostwoud Wijdenes *et al* 2000; Vanderkerckhove *et al* 2000; Poesen 2003). Land use has been attributed as one of the main drivers behind gully erosion in these environments (Kosmas *et al* 1997, Poesen 2003 *et al*, Valentin 2005 *et al*, Martinez-Casanovas 2009).

The ArcMap desktop study relating to the landscape hydrology suggested a positive correlation with land use with regards to gully development. This is evident by the spatial distribution of the gully channels. The relationship between the formation of the gully channels and contours ploughed by the farmers in the Malansdam area is apparent. However, before such a conclusion can be made the gully system needs to be physically investigated in order to see whether evidence obtained in this way supports this notion.

4.2 FIELD OBSERVATIONS

Field observations were used in unison with Google Earth imagery, as well as purchased high resolution GeoEye images to make decisions with regards to finalising test sites for this research project. Below is a brief discussion on some of the observations made during fieldwork.

4.2.1 Gully formation systems present

Both gully formation systems, as presented in Section 2.2, were identified in the Malansdam gully system and shown in Figure 4.1a and b respectively.

Figure 4.1 Gully formation systems at Malansdam: *a) Sub-surface flow identified as gully formation system by visibility of pipes in the gully wall and the collapsed soil; b) Gully formation by concentrated overland flow which is recognised by active plunge pool and sharp gully edges*

Piping was identifiable by pipes or tunnels that formed and were visible in the gully wall as indicated by the arrow in Figure 4.1a. In some cases the pipe reached a critical size causing a collapse of its roof resulting in a small sinkhole identified as a hollow on the surface (encircled in Figure 4.1a).The occurrence of piping in the area suggests soil as a driving factor contributing to soil erosion by way of gullying (Rooyani 1985; Van Zijl 2010). Rienks *et al* (2000), Sonneveld *et al* (2005) and Van Zijl (2010) found soil to be a determining factor in gully erosion.

The more dominant gully formation process observed was caused by concentrated overland flow. These gullies were identifiable as having a near vertical gully head with an active plunge pool below. This is indicated in Figure 4.1b. Further indicators of this type of erosion was sharp edges at the top of the gully head, the gully head being undercut due to splash erosion in the plunge pool and fresh deposited sediment. All these indicators are visible in Figure 4.1b, although a gully was deemed active when having a combination of any two of the aforementioned indicators for the purpose of this study. Dormant or inactive gullies were also observed, usually having a rounded gully head without a plunge pool and plentiful vegetation.

4.2.2 Gully size variation

A large variation of gully sizes were seen in both depth and width dimensions. The gully sizes ranged from the threshold value employed by Hague (1977) to differentiate between rills and gullies. When it was deemed necessary to distinguish between ephemeral and classical gullies the definition developed by Foster (1986) was used. Transitions between ephemeral and classical gullies were observed (Figure 4.2a) as well as large classical gullies (Figure 4.26b) of up to 4m in depth.

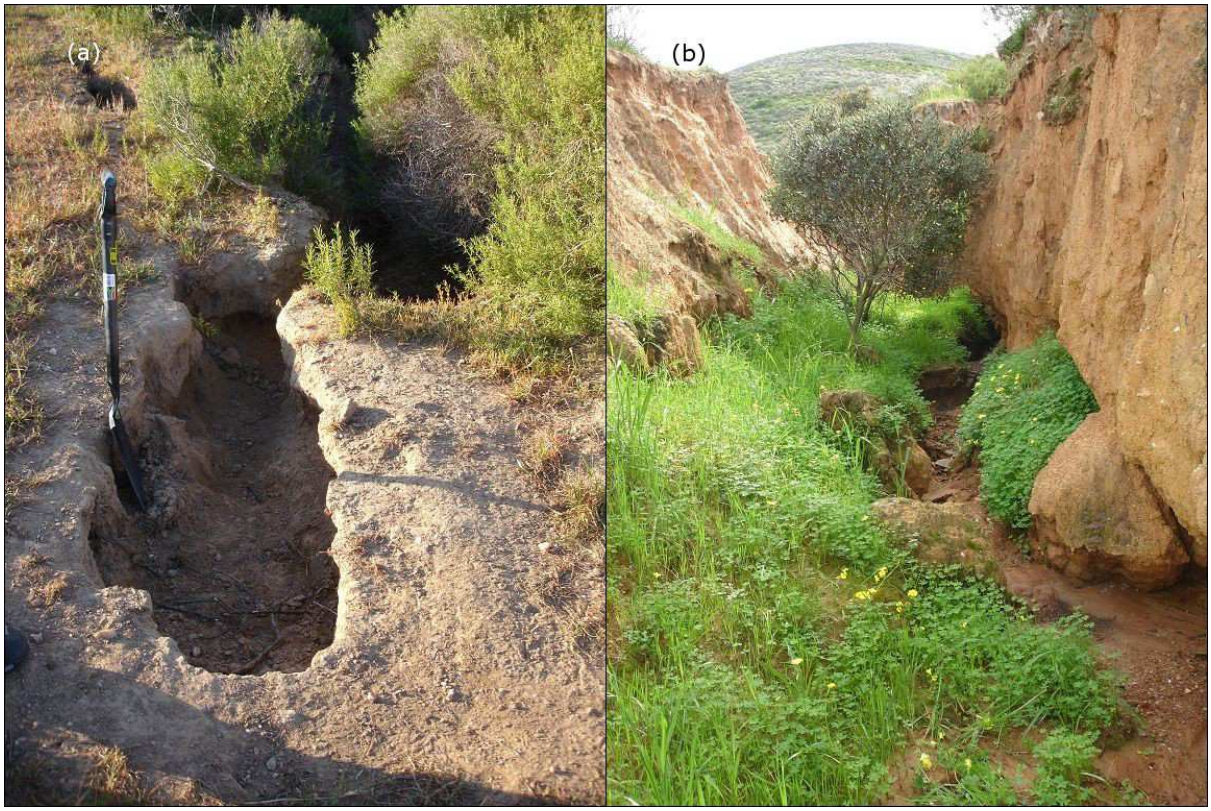

Figure 4.2 Gully size variations found at Malansdam: *a) A small gully channel leading into a larger and more mature one; b) Larger and older, yet still active, classical gully channel*

4.2.3 Gully sidewall processes

Three processes were identified that were causing gully width to increase. Figure 4.3a is indicative of gully wall collapse through mass wasting. This occurred when water flow within the gully caused the wall to become undercut. As the depth of the hollow increased, a critical stage was reached where the gully wall could not support its weight any longer. This caused the gully wall to collapse. A large part of gully wall, which was originally at the starting point of the arrow, collapsed in its entirety against the opposite gully wall (arrow head). Furthermore, the rectangle indicates an area that was still damp while the topsoil was already completely dried out. This could be indicative that the near vertical gully wall became unstable upon saturation, possibly due to subsurface flow. An additional process, namely bank gullying in Figure 4.3b, was also identified that causes gully widening. The process inflicts widening, when water slowly flows over a very gentle slope and then increases suddenly as it falls over the bank of a river or wall of a primary gully. Hence, hydraulic energy cause incision into the bank or gully wall as seen in Figure 4.3b.

Figure 4.3 Gully widening processes in the Sandpruit catchment: *a) Sidewall collapse occurring due to the gully wall becoming undercut; b) Bank gully formation due to water flowing over the gully sidewalls*

As indicated in Section 2.3 tension cracks also cause the widening of gullies. Figure 4.4a shows tension crack development on the gully wall. During a rain event, water can infiltrate the tension cracks which could lead to failure with the soil collapsing. Figure 4.4b indicates two areas on the gully wall where this has taken place. The darker soil being the newly exposed soil with the sediment produced from the failure already transported downstream. This process also leads to the widening of gullies, but on a smaller scale than those processes observed in Figure 4.3.

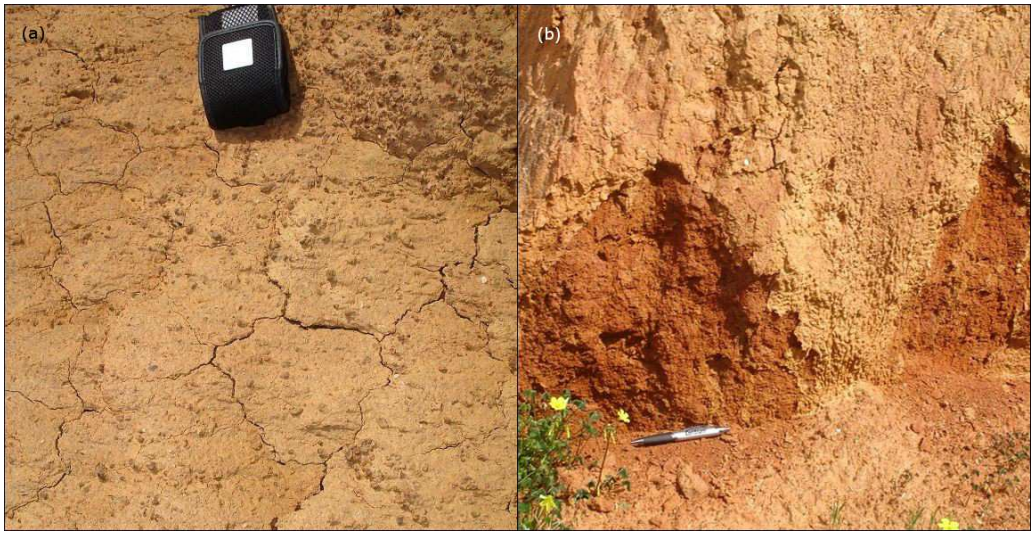

Figure 4.4 Tension cracks causing gully widening at Malansdam: *a) Visible tension cracks on the gully sidewall; b) Soil loss occurring due to collapse as a result of the tension cracks*

Other aspects with regards to the gully walls were also observed. These are indicated in Figure 4.5.

Figure 4.5 Gully wall processes found in the Sandspruit catchment: *a) An extreme case of bank gullying exhibiting the different hardness levels of the soil horizon on the gully sidewall on the right hand side; b) Salt precipitation on gully walls*

Figure 4.5a indicates the various hardness levels of soil horizons. It was noticed due to bank gullying and it is more visible on the gully wall on the right as a steeper surface slope is experienced here. Bank gullying would thus be more pronounce on the gully wall on the right when compared to the left where the surface slope leading to the gully wall is only between 0 and 1°. The harder horizons protrude from the gully wall whilst the softer horizons are eroded more easily resulting in the interesting shape observed in Figure 4.5a. Salt precipitation was observed on the walls of certain gullies as in Figure 4.5b. This is indicative of a soil with a high level of salinity. The origin of the salt may be from water used for irrigation. As the water infiltrates it will move sub-surfacely along the

gradient towards the gully. Upon reaching the gully the water will leach out of the gully wall whilst precipitating salt (zoomed in circle in Figure 4.5b).

4.2.4 Gully floor sediment production

Additionally to the above observations made on the gully walls, especially with regards to the widening, it was interesting to see the existing Malansdam gully system deepening by smaller gullies forming within it as seen in Figure 4.6a and b. Figure 4.6a is a photo taken from above, clearly indicating the new "freshly" eroded gully channel in the older more established channel. Figure 4.6b is a photo taken from within the new gully. The new gully is highly erosive. This is evident by the newly exposed soil on the gully walls as well as the lack of vegetation on it. Freshly deposited sediment can also be seen, which is further indicative hereof. The red notebook can be seen as a scale throughout both images showing that it is already dramatic in size.

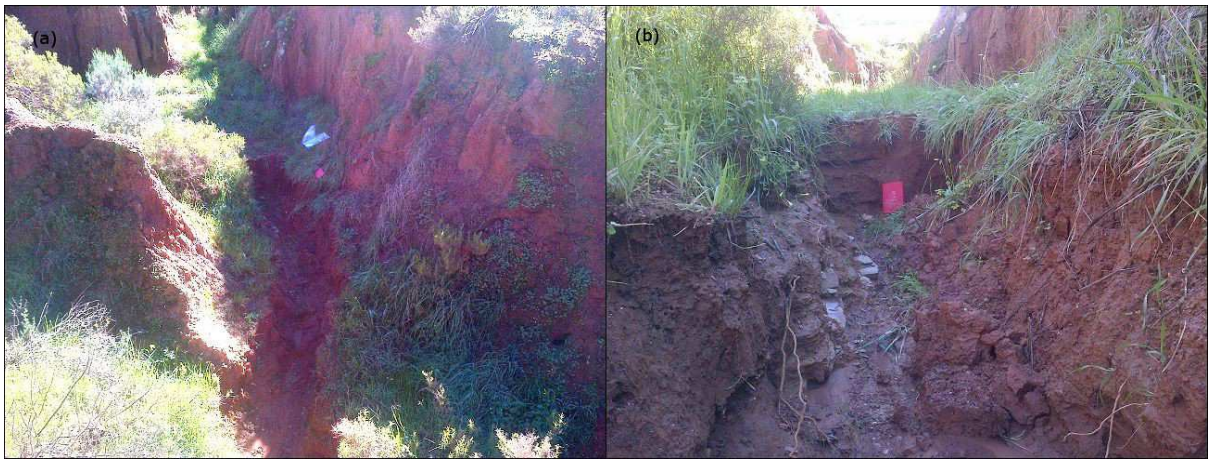

Figure 4.6 Gully within a gully phenomenon found in the Malansdam gully system: *a)Top view of the gully within a gully phenomenon; b) Photo taken within the gully-within-a-gully indicating its high degree of activity*

Also in Figure 4.6a two channels can be seen merging just before the new gully head. The hypothesis for the formation of this is velocity increase as well as turmoil, which is caused by the water flow when the two channels join. This results in the development of a depression in the soil, with a new gully as the end result. The Malansdam gully system is riddled with this "gully within a gully" phenomenon at points where gully channels join another and would therefore seem that within the global Malansdam gully system there are many smaller local gully systems. This was however confined to the upper reaches where a steeper slope was found. This phenomenon would make gully modelling in terms of sediment loss and production very problematic due to miniature gully systems having their own incision and deposition cycles.

4.2.5 Seasonal change: Winter vs Summer

As the winter season progressed vegetation especially grass started growing in the gully channels to the extent that the totality of some of the gully floors were covered (Figure 4.7a), making it difficult to negotiate as well as finding the installed sediment traps as shown in Figure 4.7b.

Figure 4.7 Vegetative growth within the Malansdam gully channels: *a) Gully channel completely covered in a grass layer; b) Sediment traps hardly visible below the grass coverage*

Vegetation has been shown to play an important role in curbing erosion (Morgan *et al* 1997, Cerdà 1999). Rey (2003) found the same trend occurring within gully channels where low vegetated cover existed to such an extent, that gullies would become inactive if a vegetation cover of 50% is exceeded. With regards to the Malansdam gully system, this percentage value determined by Rey (2003), was exceeded as shown by the photos in Figure 4.8a (summer) and 4.8b (winter).

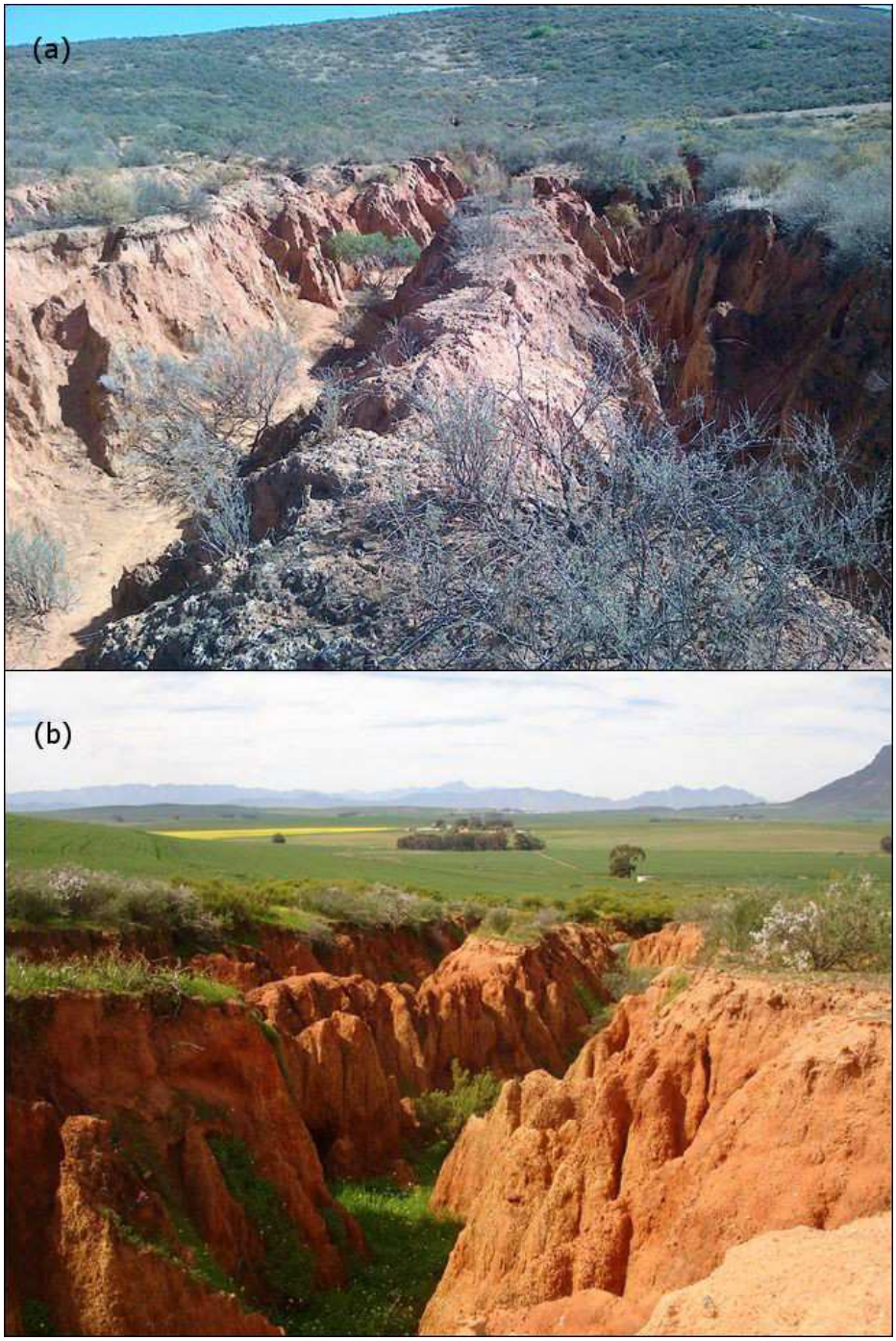

Figure 4.8 Vegetation growth within the Malansdam gully channels: Summer vs Winter: *(a) Depicts the bare channels after summer; (b) depicts vegetated channels after winter*

The founding by Rey (2003) may also be accurate for Malansdam. The hypothesis being: In the initial stages of winter, indicated in Figure 4.8a, the rains would meet bare soils which would result in minimal infiltration and therefore a higher amount of concentrated overland flow that would not have had much resistance. This would be the optimum time for erosion to occur. As the winter season progress, vegetation will start to grow, as shown in Figure 4.7a and b until whole gully floors previously bare are covered in grass as shown in Figure 4.8a - b. With the increase of vegetation

cover, a decrease will be experienced in erosion and sediment yield. The grass coverage will act as a trap for the sediment that has been transported from the cultivated fields along the contours as well as sediment from the gully itself causing it to be deposited in this area. It would further lower the erosive force of the water. This process can lead to the extent where an active gully becomes temporarily inactive. Therefore, the start of winter season may be the critical stage at which gully prevention and control methods need to be implemented.

4.2.6 Sediment movement

The farmers at Malansdam built a makeshift bridge across the southern leg of the gully system as seen in Figure 4.9. This altered normal erosion and deposition processes; therefore the section layout differs from the other gully channels occurring in the southern leg and also the northern leg of the system (which did not have any modifications made to it). In the photo above the bridge a large amount of sediment has been deposited due to the bridge acting as a wall. The deposited sediment is almost level with the bridge. This is a clear indication of the large amount of sediment that is transported in the gully system and motivates why it should be researched. The origin of the sediment is not only from the gully itself but also from the cultivated field units. In terms of the gully, the sediment results as it expands in terms of the widening processes observed in Figure 4.3 and 4.4, headward retreat of gullies (as explained in section 2.2.1), and depth increase through water transport in the gully channel as well as the “gully within a gully” observation (Figure 4.6). With regards to the cultivated fields, the sediment results from concentrated overland flow transporting sediment. As observed in Figure 3.2, 3.3 and 3.4 this usually occurs along the ploughed channels into the gully from where it will be transported within the gully. The yearlong grass cover that is found and seen in the photo at the position where the sediment has been deposited may further indicate valuable fertile soil that has been eroded away and now lies inert in the gully where it is inaccessible to be cultivated.

Figure 4.9 Human modification on the Malansdam gully: A bridge was built across the gully channel which is causing sediment build-up

Furthermore, as the gully channel level grows higher and closer to becoming level with the bridge this could pose a potential problem in the future. When this does eventually become level, water flow can occur over the bridge and start the erosion thereof; especially since it is a makeshift bridge that was not made of sturdy material. Evidence of preventing this from happening is already present. The photos (Figure 4.9) illustrate rocks and a corrugated zinc sheet on the side of the bridge in an effort to reduce erosion and structural stability.

4.2.7 Farm road assisting gully development

Upon driving along the veld roads next to the Malansdam gully system, ephemeral gully formation was noticed on the veld roads as seen in Figure 4.10. This is due to the compacted road gravel not allowing water to infiltrate causing an increase in concentrated surface flow.

Figure 4.10 Gully development along veld roads next to the Malansdam gully system

From Figure 4.10 the path of a rill is visible proceeding from behind the bakkie moving along the road until an incision point developed more to the forefront of the photo where the transition from a rill to an ephemeral gully starts. This ephemeral gully thus fulfils the criteria proposed by Hauge (1977) and later employed by various authors (Poesen *et al* 1996, Vandaele *et al* 1996, Svoray & Markovitch 2009). A similar observation was made with regards to the second ephemeral gully that extends horizontally on the photo with a rill path moving from the field onto the road, where the incision point occurs and the ephemeral gully starts. An interesting manifestation is that this ephemeral gully showcases the same processes as much larger classical gullies: definite incision point indicating the gully head; gully head retreating headward along the rill flow path; undercutting of the gully walls causing the collapse thereof. The classical gully is also growing in the direction of the ephemeral gully probably due to the water velocity increase that is experienced as the water falls from the ephemeral gully into the classical gully. This expansion might render this road unusable after a few more rain episodes as the classical gully could grow much further than where it is situated in Figure 4.10. The above Figure 4.10 might also be indicative that a buffer zone of natural vegetation is required between the gully and the cultivated area in an effort to stop the growth of the classical gully into the road and later into the field itself as the natural vegetation should break the energy of the water.

4.3 MATERIALS AND METHODS

Two approaches were deemed necessary to physically classify the Malansdam split gully system. These consisted of remotely sensed data utilised in a GIS platform and secondly, by means of physical in-situ field measurements.

4.3.1 GIS as a classification tool

A demarcated catchment boundary of the Sandspruit was obtained from the Soil Science Department at the University of Stellenbosch. Thereafter Google Earth was used in unison with aerial photos obtained from the Centre of Geographical Analysis (CGA) to identify gully systems in the catchment. The discontinuous split gully system at Malansdam was selected within the catchment to serve as the active study site. In order to constitute an order to the complex, bordering chaotic gully system, a modification of the Horton method (1945) namely the Strahler method (1964) was used assigning stream order values to the various gully channel branches.

The Strahler (1964) stream order (SSO) allocations process with regards to the Malansdam gully system worked as follows: The incision point at the gully head which indicates the start of the gully was given order 1. Where two order 1 gully channels joined an order 2 channel was the result. Where two order 2 channels joined an order 3 channel started, *etcetera*. If two different order channels joined the lower ordered channel would not have an effect on the resultant order number and it would therefore remain as the highest order. If for example an order 2 channel joined an order 3 channel the resulting channel would remain an order 3. Refer to Figure 4.11 below as a visual representation of the stream order process followed.

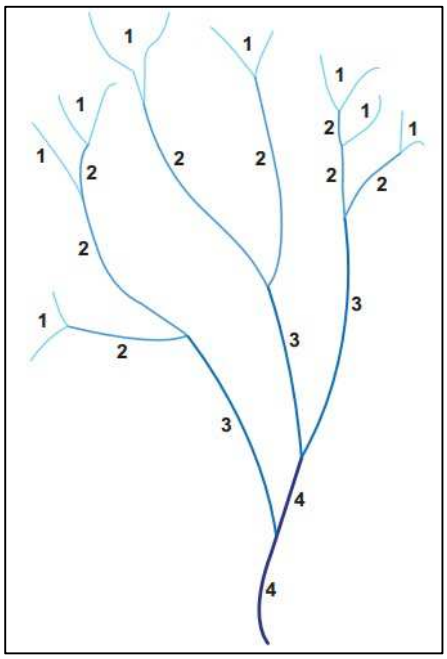

Source: Pierson *et al* 2008

Figure 4.11 Stream order classification according to the Strahler method (1964)

The Malansdam gully system is very complex and split channels occur in both the northern and southern legs. In an attempt to avoid increasing the total stream order value of the Malansdam gully system artificially a technique was adopted that was used by Pierson *et al* (2008). This stated that where a split channel occurred the "main" channel was kept at the same order number, but the split channel was decreased by 1. To use Figure 4.12 as an example: When a gully channel with a stream order of 4 split into two channels the "main" channel remained as an order 4 channel whilst the diverted "minor" channel was downscaled by one order to become an order 3 channel as indicated. When the two channels joined again the outcome would still be an order 4 gully channel.

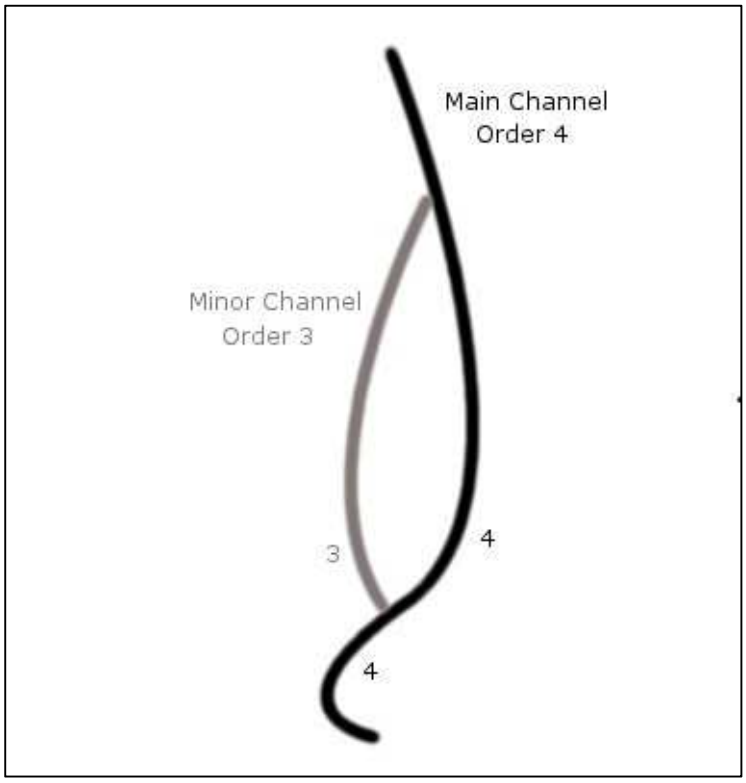

Figure 4.12 Strahler order allocation with incidences of split channels

The above SSO allocation with the addition of the Pierson *et al* (2008) method was employed in ArcMAP 10. This was done by importing high resolution GeoEye stereo images acquired in July 2011 into ESRI ArcMap 10 where after a string network was constructed manually. In order to highlight the gully channels, a string network consisting of polylines were drawn as close to the middle of the channel as possible. Fieldwork was used to clarify areas of uncertainty. After the completion of the string network, it was edited in ArcMap 10, to deconstruct the total network into a system made up of separate polylines lines with each polyline representing a SSO gully channel. This facilitated in easier calculations and analysis for the different gully channel orders.

Once the above-mentioned was completed, the gully system underwent a further classification procedure. This was done according to global slope. Upon combining the GeoEye stereo images and a

cross section along the gully channels from the hydrologically corrected DEM attained from Mashimbye (2013), three distinct phases were apparent. The gully system was divided into the following three parts accordingly: active gullying in the upper slope, transition phase and deposition phase where the slope was minimal.

4.3.2 Physical measurements

The data returned from the stream ordering and the slope classification was used in conjunction with each other to identify a position for physical field measurements. This position consisted of an area of approximately 0.24km^2 and had a variety of different stream order allocations. It was located in the upper slope classification. Perforated sediment traps with a diameter of 110mm were inserted into the gully channel floor in the flow path with the uppermost part of the sediment trap being level with the gully floor. The sediment traps conformed with results from Gardner (1980) who found that cylindrical sediment traps with a height to width ratio between two and three yielded best results. The sediment traps implanted into the gully channel at Malansdam had a height of 300mm and a width of 110mm resulting in a suitable ratio of 2.7. The constructed and installed sediment trap can be seen in Figure 4.13a – d.

Figure 4.13 Sediment trap: *(a) Depicts a side view with the length being 300mm; (b) top view with a diameter of 110mm; (c) indicates the perforated bottom of the sediment trap to allow water drainage; (d) installed sediment trap, at Malansdam, in line with the water flow in the channel and level with the surface*

These sediment traps were placed at the end of each gully channel order or before a new gully order channel entered the measured channel. Erosion pins were placed at 300mm intervals along the gully wall approximately 500mm back from the sediment trap towards the gully head if order 1 or towards the lowest order if not an order 1 gully channel. A typical measurement position would look like Figure 4.14. The location of these measurement points were captured by a GPS and imported into ArcMap 10. The field work for this research project was conducted during the winter season of 2012. The winter was chosen as the Western Cape has a Mediterranean climate with a winter rainfall regime caused by frontal depressions.

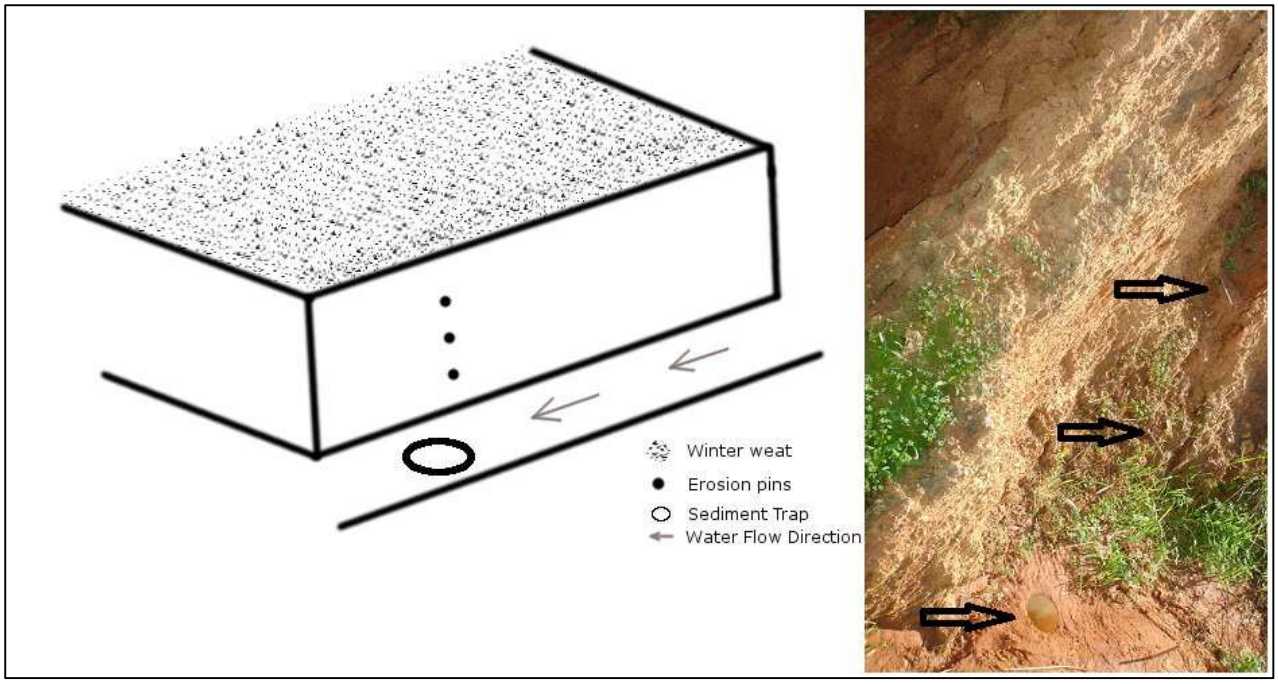

Figure 4.14 Physical measurement methods employed at Malansdam

The sediment traps were emptied once a month. The soil collected was dried in a heated room and sieved with a 2mm as well as a 0.05mm sieve in order to divide the sediment into gravel, sand and a combined clay and silt fraction. In order to establish the minimum flow velocity required for incipient motion of the captured sediment, a modification of the Hjülstrom curve (Hjülstrom 1935, Refer to Appendix A) namely the Sundborg diagram (Sundborg 1956) in Figure 4.15 was used in conjunction with the largest captured grain size.

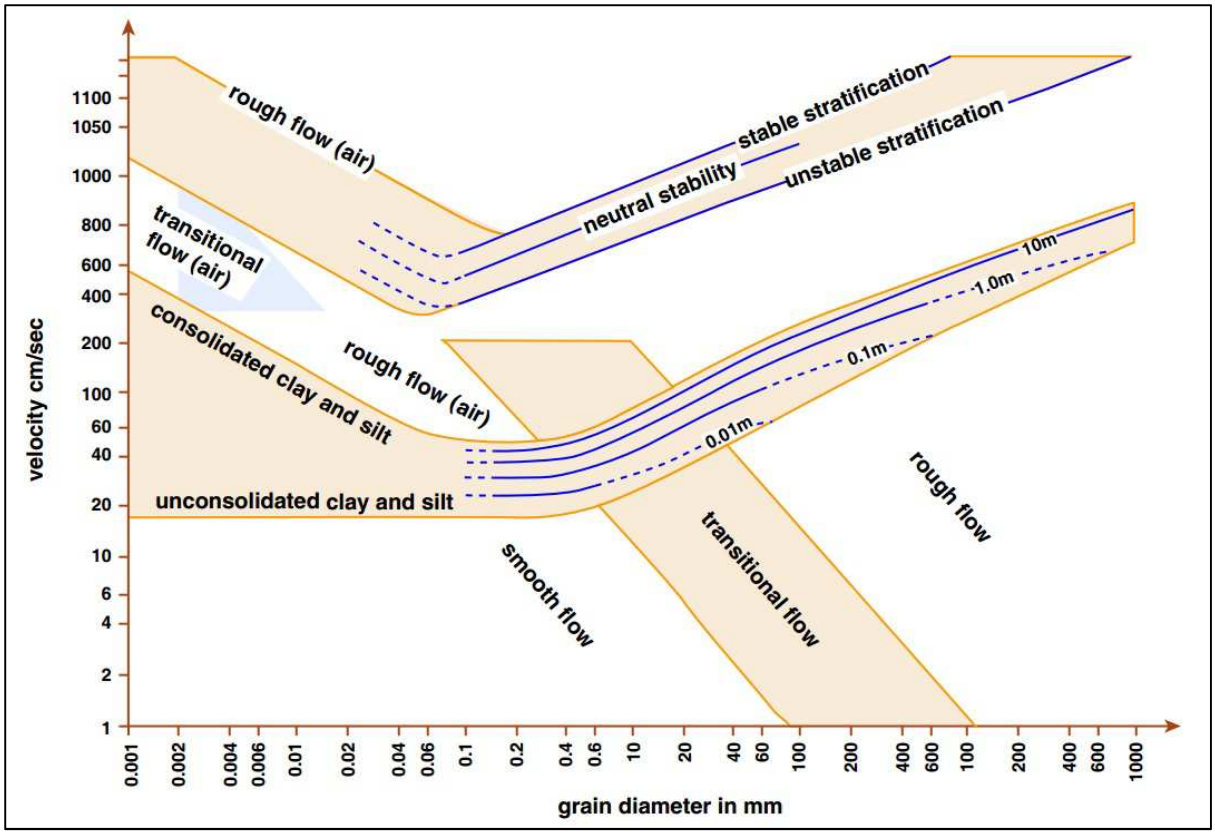

Source: Southard 2006

Figure 4.15 Sundborg diagram (1956) consisting of various curves indicating particle movement thresholds at different water depths

Furthermore, a Trimble FX 3D scanner was used to scan the area under investigation in order to specifically look at erosion taking place on the gully walls. This was deemed a better alternative as the measurements obtained by the "erosion-pin" method, because the erosion pins produce information that is too local and therefore not a good representation of what was occurring on the gully walls. The Trimble FX 3D scanner has a large 360° x 270° field of view with a range of up to 80m and is able to capture 216 000 data points per second on average, delivering an accuracy of 1mm resulting in fast and precise data. An added advantage is that multiple scans can be seamlessly joined resulting in a total picture of the study area.

4.4 RESULTS

The results attained for the methods applied for both the GIS investigation and the physical measurements are presented below.

4.4.1 Structural classification

Upon completion of the string network, each gully channel was assigned with a SSO number with the Pierson *et al* (2008) adaptation. This method was systematically continued downstream until each

gully channel was awarded with a SSO number. The Malansdam gully has been classified as a Strahler (1947) order 5 gully system (Refer to Appendix B).

To further classify the gully channel, the slope of the terrain on which it occurs was taken into account. It was initially eyeballed using Google Earth imagery where after a cross section for both the northern and southern legs of the Malansdam gully system was created in ArcMap 10. Figure 4.16 showcases this with the Google Earth imagery divided into 4 windows. Windows 1, 2 and 3 indicates three different zones of activity whilst window 4 indicates the 3D Scene view. Window 1 indicates an area of intense activity while Window 2 shows an area of the gully system that has a moderate level of activity. The zone in Window 3 is inactive and thus an area of deposition.

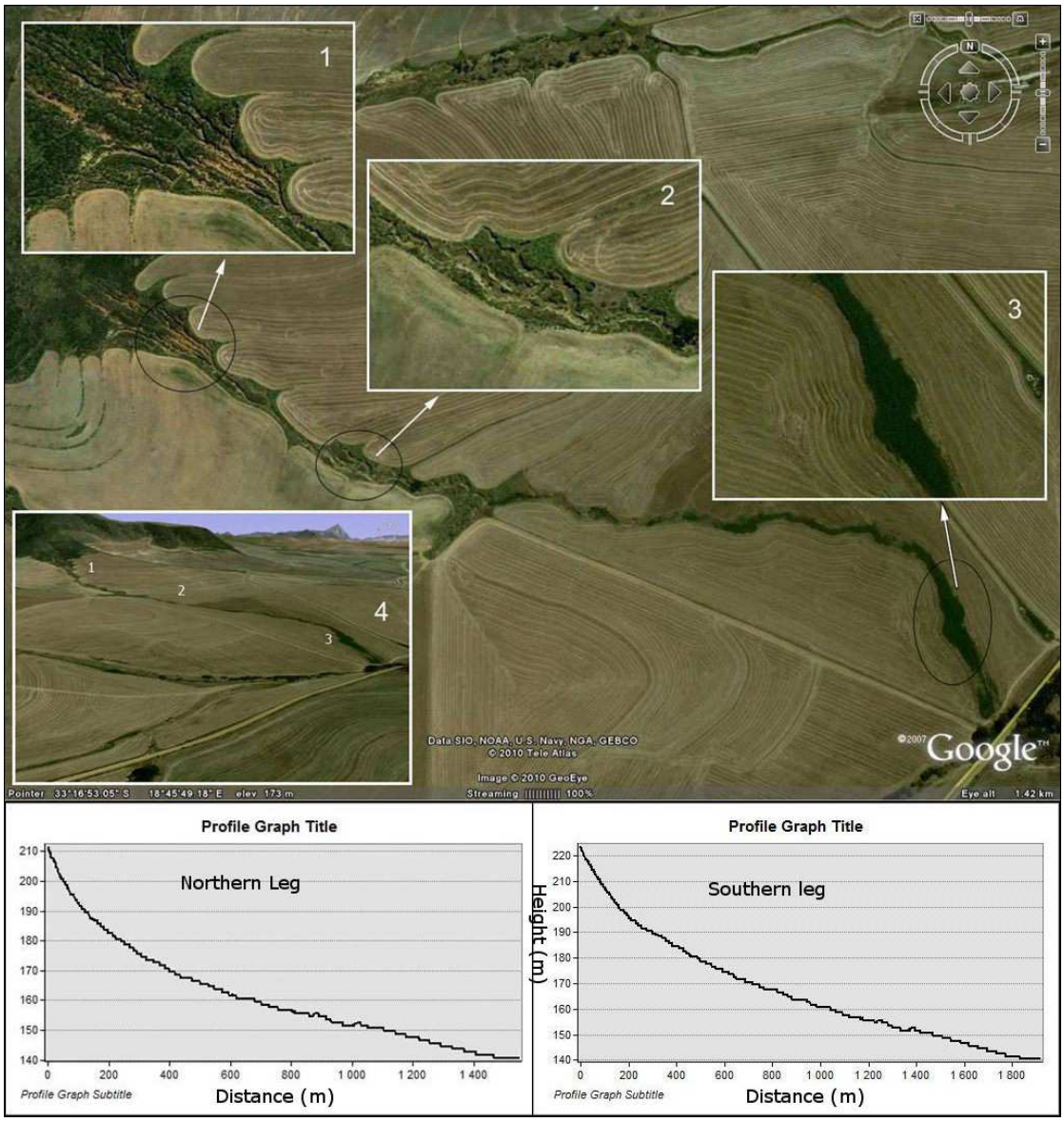

Figure 4.16 Slope classification according to activity at Malansdam: *(1) Very active upper reaches; (2) Moderate activity; (3) Deposition zone; (4) 3D view of the Malansdam gully system with cross sections of the southern and northern leg*

Also in Figure 4.16 immediately below the Google Earth Imagery are two cross sections which were drawn in ArcMap 10 to support the 3D scene obtained from Google Earth. The first cross section is of the southern leg whilst the second one is for the northern leg. Both legs have a similar cross sectional sequence and aided in remotely identifying the three zones of activity: It starts with a very steep slope (area of intense activity in Window 1) where after the slope becomes moderate (Window 2 where moderate levels of activity are found) and eventually flattens out to produce a deposition zone for the gully system (Window 3).

4.4.2 Physical measurements

The two above classifications namely stream order and global slope were used to identify a test site to conduct further research with regards to erosion rate experienced in the Malansdam gully system. Sediment traps and erosion pins were installed at the test site in positions indicated in Figure 4.17.

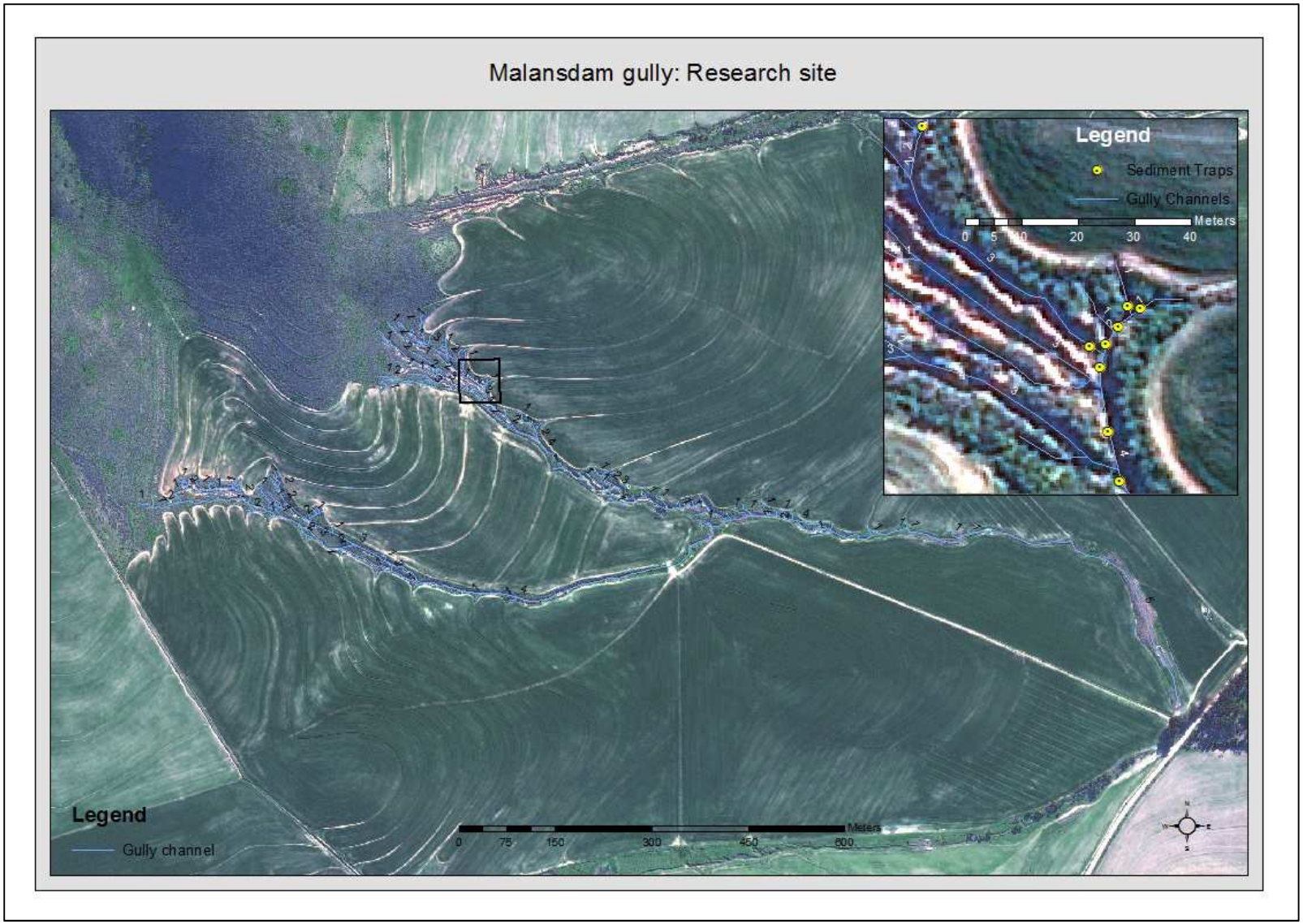

Figure 4.17 Test site with installed sediment traps at Malansdam

The sediment traps were installed on 13 April 2012 and emptied during the winter period on 16 June, 16 July, 16 August and 24 September 2012. Data with regards to soil deposition or erosion surrounding erosion pins were also measured on these dates. Unfortunately data collected through the "erosion-pin" method was found to be negligible. The pins were found to be too localised with the resulting data deemed unsuitable for use. Refer to Table 4.1 for the characteristics of the soil collected from the sediment traps.

Table 4.1 Soil characteristics from soil collected from sediment traps.

Sed Trap no.	**Stream order**	**Activity and Length (m)***	**Total soil weight (g)**	**Gravel >2mm (%)**	**Sand 0.05 – 2mm (%)**	**Silt an clay <0.05mm (%)**	**Largest particle size (mm)**
13 April – 16 June							
1	1	A, 9.27	119.2	5.54	87.42	7.05	5
2	1	N, 9.89	91.2	13.82	82.13	4.06	3.5
3	2	A, 23.4	1 883.8	4.16	93.74	2.10	5.5
4	2	A, 34.37	1 423.7	11.55	86.09	2.35	8.5
5	3	A, 130.96	1 624.7	6.83	89.73	3.44	5.5
6	3	A, 170.53	252.4	17.00	78.76	4.24	4.8
7	4	A, 720.6	563	1.72	88.72	9.56	3.5
8	4	A, 1 468.37	5 272.9	34.37	63.13	2.50	17.5
9	1	A, 30.12	887.2	14.59	80.04	5.38	6.5
17 June – 16 July 2012							
1	1	A, 9.27	69.6	7.18	85.06	7.76	4.5
2	1	N, 9.89	8.6	4.65	75.58	19.77	2.2
3	2	A, 23.4	514.5	6.26	93.41	0.33	5.5
4	2	A, 34.37	0	0.00	0.00	0.00	0
5**	3	A, 130.96	2 045.7	12.62	86.02	1.35	10.5
6	3	A, 170.53	29.6	1.35	37.50	61.15	2.2
7	4	A, 720.6	588.2	1.34	93.59	5.07	5
8	4	A, 1 468.37	4 283.4	35.11	63.06	1.83	10
9	1	A, 30.12	712.2	7.78	90.09	2.13	10.5
17 July – 16 August 2012							
1	1	A, 9.27	161	4.41	88.51	7.08	4
2	1	N, 9.89	0	0.00	0.00	0.00	0
3	2	A, 23.4	752.1	3.67	93.03	3.30	5

Sed Trap no.	Stream order	Activity and Length (m)*	Total soil weight (g)	Gravel >2mm (%)	Sand 0.05 – 2mm (%)	Silt an clay <0.05mm (%)	Largest particle size (mm)
4	2	A, 34.37	177.9	7.64	85.83	6.52	4.7
5	3	A, 130.96	1 493.9	11.89	84.95	3.16	12.5
6	3	A, 170.53	196.6	15.31	72.79	11.90	4.5
7***	4	A, 720.6	*No data*	*No data*	*No data*	*No data*	*No data*
8	4	A, 1 468.37	2 512.9	37.18	60.80	2.02	16
9	1	A, 30.12	512.4	12.16	80.33	7.51	5
17 August – 24 September 2012							
1	1	A, 9.27	105.6	7.10	83.43	9.47	4.5
2	1	N, 9.89	0	0.00	0.00	0.00	0
3	2	A, 23.4	96.3	6.75	81.83	11.42	4.5
4	2	A, 34.37	145.3	2.68	85.41	11.91	3.3
5	3	A, 130.96	125.3	12.13	80.53	7.34	4
6	3	A, 170.53	53	0.38	78.87	20.75	3
7	4	A, 720.6	138.7	7.93	79.74	12.33	4
8****	4	A, 1 468.37	*No data*	*No data*	*No data*	*No data*	*No data*
9	1	A, 30.12	349.2	16.92	77.23	5.84	5

** Activity measured according to section 2.2.1 Figures 2.6 and 2.7. A is active an N not active.*

*** Mass movement activity from the wall of sediment trap. Not all sediment in the trap would have occurred via water flow.*

**** Sample contaminated with decomposing mouse.*

***** Sediment trap were damaged irreparably.*

The sediment traps were installed in 9 different gully channels. Three of these were SSO 1 channels, whilst the remaining six channels consisted of two channels each in the SSO 2, 3 and 4 classifications.

The three SSO 1 channels had a combined length of 49.28m. Sediment Trap (ST) 9 was installed in the longest SSO 1channel which measured in at 30.12m whilst ST 1 and 2 were of similar lengths: 9.27m and 9.89m respectively. The channels in which ST 1 and 9 were installed were deemed active whereas the channel where ST 2 was installed was not active according the specifications given in Section 2.4, also tabulated in Table 2.1.

Two SSO 2 channels were incorporated into the test site and ST 3 and 4 were installed. The combined length of the gully channels upstream were used to calculate the length of SSO 2 and above. This resulted in lengths of 23.4m and 34.37m for ST 3 and 4 respectively. ST 4 was installed 4.24m down the channel. Both SSO 2 channels were found to be active.

ST 5 and 6 were installed in two different SSO 3 channels with lengths of 130.96m and 170.53m totalling 301.49m of gully channel length. Both channels had evidence of activity.

Lastly, two SSO 4 channels were also investigated. ST 7 and 8 were installed in these SSO 4 channels. ST 8 was installed downstream of ST 7. Furthermore ST 8 was also installed 1.9m downstream of an active inter-gully plunge hole. The gully channel length of ST 7 amounted to 720.6m and ST 8 to 1 468.37m. Both channels were active. Although the Malansdam gully system was found to be a SSO 5 system no ST was installed in this specific channel, as the soil was too shallow for ST installation.

More soil, in dry weight as presented in Table 4.1, was collected in ST 9 than ST 1 and 2 for all four collection sessions with regards to SSO 1 channels. This correlates well with the length difference. The channel where ST 9 was installed was approximately three times the length. The least amount of soil was collected in ST 2 which was deemed inactive according to the criteria based on research done by Oostwoud Wijdenes *et al* (2000). In all three cases the sand fraction was dominant with values ranging between 77.23% - 90.9% of the samples collected excluding the zero values obtained from the inactive channel where ST 2 was installed in August and September.

A reversal occurred with the trapped soil from the two SSO 2 channels with ST 3 and 4 installed. More soil was collected in the shorter channel in ST 3 than in 4. This phenomenon might be explained by the installation procedure. ST 4 was installed 4.24m down the channel thus giving the opportunity to ST3 to trap soil before it reached ST 4. Sand was the dominant fraction collected with values from 81.83% to 93.41% when values exceeded 0g of soil.

With regards to the soil collected in ST 5 and 6 in the two SSO 3 channels, more soil was collected in the shorter channel where ST 5 was installed. It has to be kept in mind that the channels leading to ST 5 was uninterrupted, as opposed to the channels leading up to ST 6 that had installed sediment traps. This could have influenced to total weight collected. The sand fraction was dominant with percentage values of 70% plus.

ST7 and ST8 were installed in SSO 4 channels. A large amount of sediment was collected from ST8 throughout the collection time period. This is due to it being installed 1.9m down channel from a very active inter-gully plunge hole. Freshly scoured and eroded soil would have found its way into ST 8 without any obstruction. Far less soil was collected in ST 7, but this could again be due to the channels leading up to it being heavily sampled by other ST's. The sand fraction in ST 7 was similarly dominant but the gravel fraction was much higher in ST 8 than any other sample. Values ranged from 34.37% to 37.18%. This may be the scouring effect of the water which would have occurred at the plunge hole, causing larger particles to be eroded and therefore deposited into nearby ST 8.

4.4.3 Indirect determination

A minimum stream velocity was determined for each channel where sediment traps were located. This was done in an indirect method correlating the largest particle size for each sediment trap indicated in Table 4.1 with the Sundborg diagram (1956) for the depth of 0.1m in Figure 4.15. The minimum stream velocity incurred at each point is given in Table 4.2 measured in centimetres per second. The velocity values were closely correlated with each other with values ranging from 36.5cm/s – 39.8cm/s, with the exception of all velocity data for ST 8, the 16 July data for ST 5 and 9 as well as the velocity in ST 5 for the collection date of 16 August. The velocity data given for ST8 could be an over estimation due to it being installed close to an active plunge pool. The larger sediment sizes collected could therefore be a result of the turmoil caused at the plunge hole, instead of a higher flow velocity experienced in the channel. Similarly, the higher velocity indicated for ST 5 in 16 July and 16 August could be an overestimation as this could be the result of the mass movement activities from the gully wall that took place in that specific period. Collapsed soil from the gully wall could have entered the sediment trap. The high flow velocity of 47.3cm/s for ST 9 on 16 July is unexplained.

Table 4.2 Minimum stream velocity experienced in gully channels

Sediment Trap	13 April - 16 June (m/s)	17 June - 16 July (m/s)	17 July - 16 August (m/s)	17 August - 24 September (m/s)
1	39	38.8	38.5	38.8
2	38.3	37.6	0	0
3	39.3	39.3	39	38.8
4	40.8	0	38.9	36.7
5	39.3	47.3	48.3	38.5
6	38.9	37.6	38.8	36.5
7	38.3	39	*No data*	38.5
8	50.6	42	50	*No data*
9	39.8	47.3	39	39

4.4.4 3D scan

The erosion pins installed against the gully walls did not yield any positive results. It was too localised and did not produce an accurate picture of the actual erosion processes transpiring on the gully walls. A 3D scan was thought to give a better understanding of the entirety of the processes affecting the walls but also the channels. Refer to Figure 4.18 for the resultant image from the 3D scan taken on 29 September 2012..

Figure 4.18 The 3D scan taken of the study area in the Malansdam gully system on 29 September 2012

Four scans were joined to create the image in Figure 4.16.

4.4.5 Rainfall

Hourly rainfall data was obtained for the area from the field station at Langewens farm. This enabled gathering data with regards to the cumulative amount of rain received in addition to intensity. Figure 4.19 indicates rainfall data from the date of sediment trap installation on 13 April 2012 to the first collection date on 16 June 2012. A total of 94.8mm fell over this period at a daily average of 1.46mm. The hourly and daily lows were both 0mm. 30 April produced the highest hourly rainfall as well as the highest daily rainfall for the time period of 5.8mm and 16.2mm respectively.

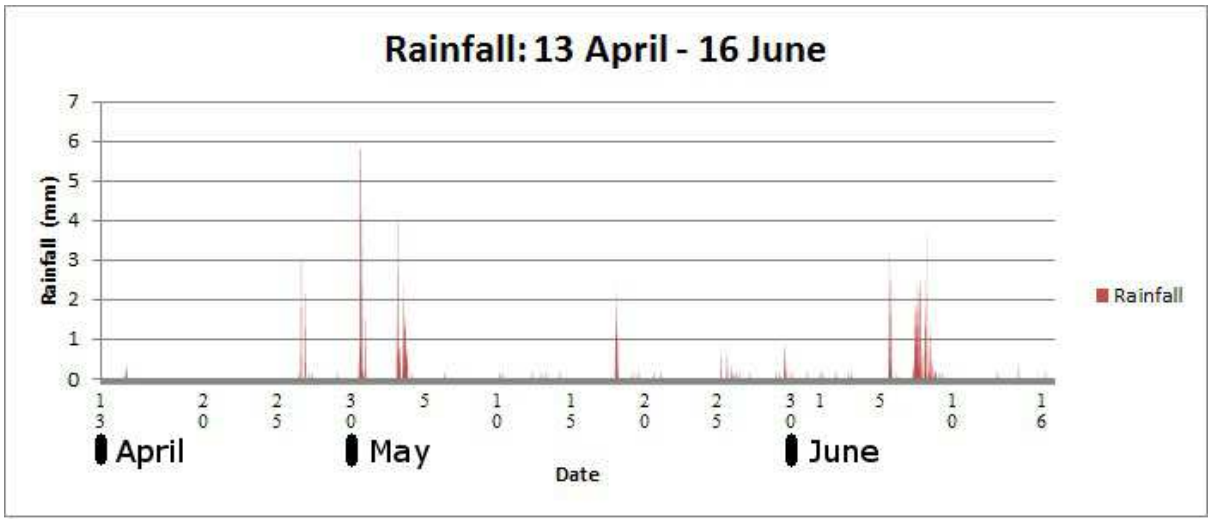

Figure 4.19 Hourly rainfall data for 13 April – 16 June obtained from Langewens weather station

Hourly rainfall data from 17 June 2012 to 16 July 2012 is shown in Figure 4.20. During this 30 day span the average daily rainfall was 1.92mm totalling 57.6mm. The highest rainfall recorded per hour was measured at 8.4 and fell on 4 July. 10.8mm was the highest recorded daily rainfall and occurred on 24 June 2012.

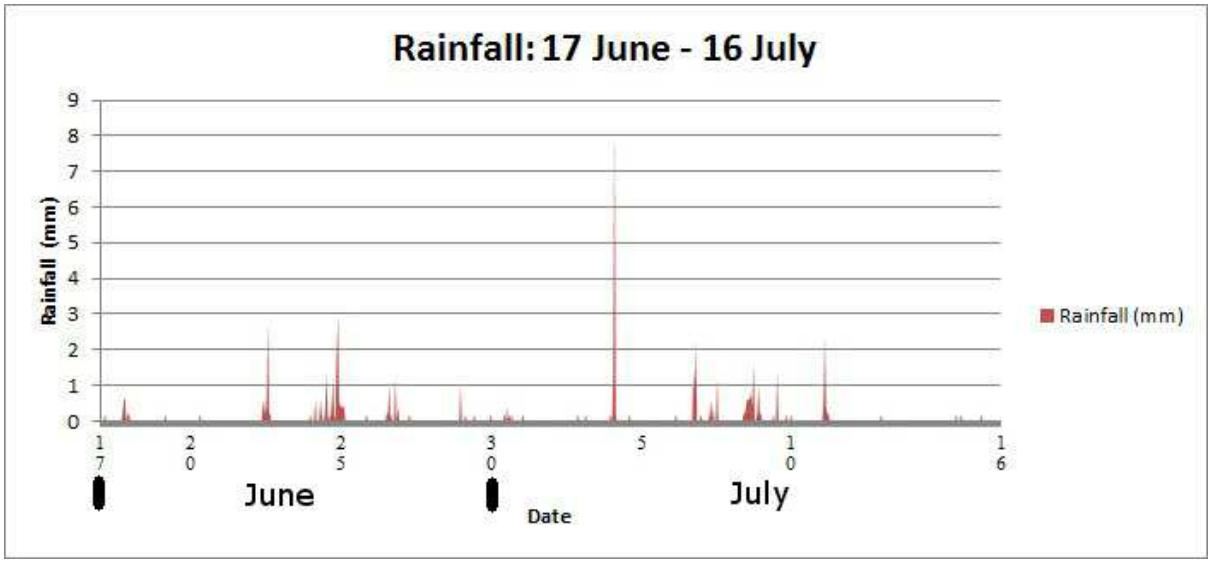

Figure 4.20 Hourly rainfall data for 17 June – 16 July obtained from Langewens weather station

Figure 4.21 displays the hourly rainfall data from 17 July 2012 to 16 August 2012. These 30 days were wetter when compared to the previous collection period indicated in Figure 4.19 with a total rainfall of 79.4mm. The majority of rainfall is coupled around four rain events as indicated in Figure 4.21. A daily average was calculated for the month and amounted to 2.65mm per day. The most amount of rainfall measured for both per hour and per day took place on 6 August 2012. The hourly high was 7mm whilst the daily high was 10.6mm.

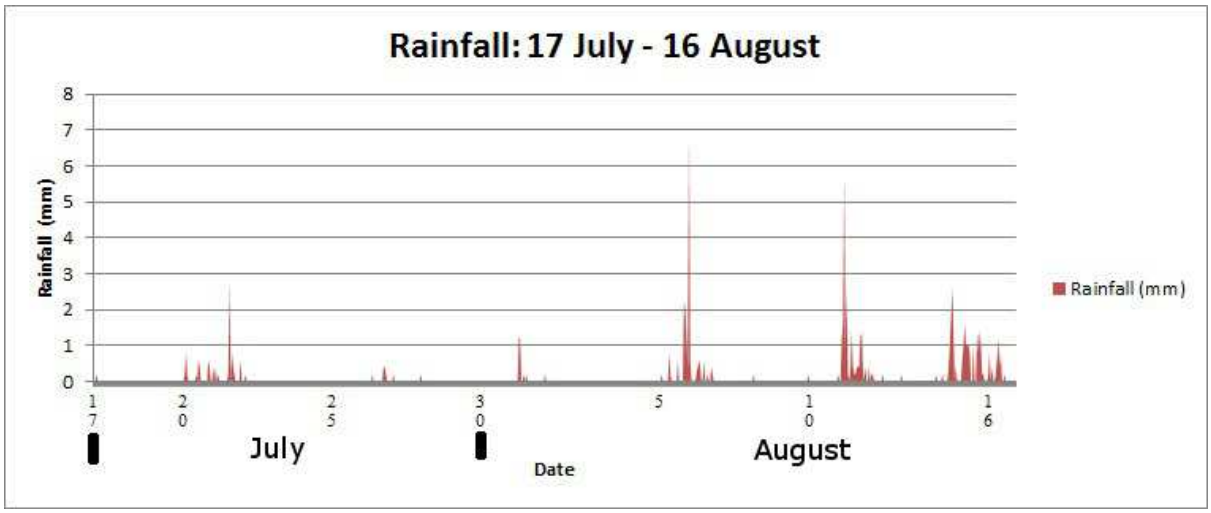

Figure 4.21 Hourly rainfall data for 17 July – 16 August obtained from Langewens weather station

The last collection period stretching from 17 August 2012 to 24 September 2012 was the driest receiving a total of 50mm of rain. Rainfall was evenly scattered throughout this time period. This can be seen in Figure 4.22. The most rain that fell in an hour was recorded during the morning of 21

September totalling to 4.8mm. This was also the wettest day during the collection period with rain amounting to 12.2mm for the day.

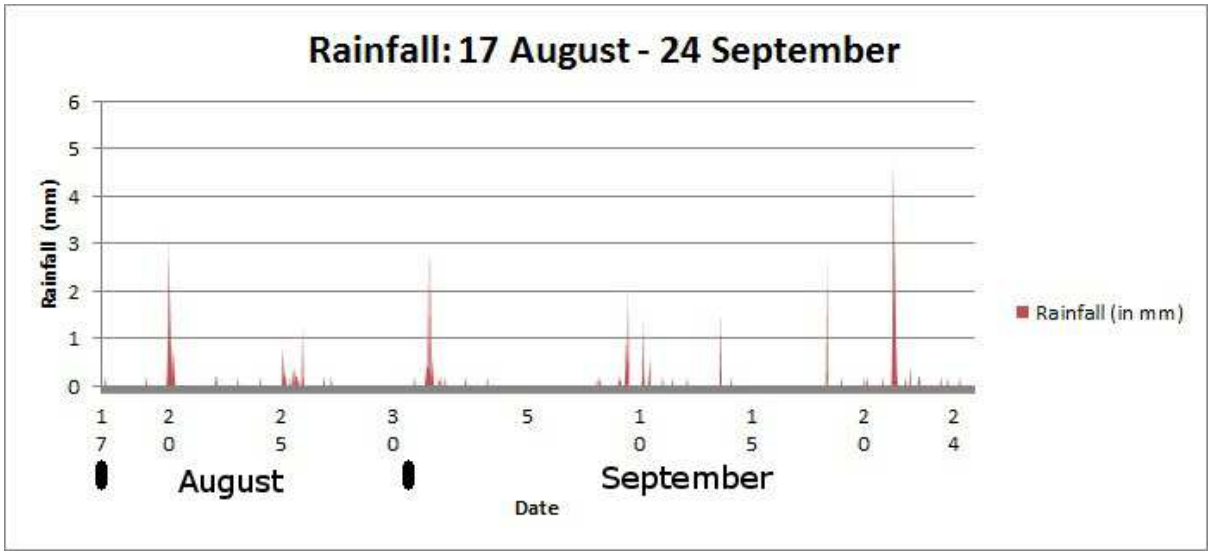

Figure 4.22 Hourly rainfall data for 17 August – 24 September obtained from Langewens weather station

In order to derive a comparison between the four collection periods, important statistics regarding the rainfall data was tabulated below in Table 4.3.

Table 4.3 Rainfall data per sediment collection period

	Collection period	Duration	Total Rainfall (in mm)	Highest daily rainfall (in mm)	Highest hourly rainfall (in mm)
1	13 April-15 June	64 days	94.8	16.2	5.8
2	17 June-16 July	29 days	57	10.8	8.4
3	17 July-16 August	30 days	79.4	10.6	7
4	17 August-24 September	38 days	50	12.2	4.8

The most amount of rain fell during the first collection period although it was also approximately twice the time span than the other collection periods. The highest amount of rain that occurred during one day was also in this period. Event wise the second collection period had the largest intensity event while the third collection period was the second wettest of the four collection periods. During the spring (fourth) collection period the least amount of rain occurred although it had the second highest amount of daily rain measured.

4.5 DISCUSSION

Due to the innovative nature in which the Malansdam gully system was classified and investigated, certain results are not comparable to other work since no authors have produced work of a similar nature. The discussion that follows will compare results with other published work where applicable; however where comparisons cannot be drawn, sensible discussion of deductions will follow.

4.5.1 Structural classification

From the high resolution Geo-eye images it was apparent that the Malansdam gully was a discontinuous gully system. It has its incision point on the steep valley upper reaches and has a deposition zone on the lower valley floor without deposition occurring in a stream or river. It is a complex system that is dendritic in design and has been classed a SSO 5 gully system. Although the Malansdam gully system is not as extensive in length and depth as a gully system in Duagava Valley in Latvia (Soms 2006) it has a larger SSO classification when compared to it. It is therefore, the highest SSO thus far recorded for a gully system.

SSO 1 channels dominate the gully system down the valley with 115 channels which is especially dense in the uppermost part of the gully. The SSO 1 channels were calculated to have a total length of 2 019m. The longest channel was in the fynbos in the upper reaches and stretched to a length of 76.17m with the shortest channel being much shorter at 2.63m. There was a large drop in the amount of SSO2 order channels when compared to SSO 1 with 33 channels amounting to 954.95m. Three of these channels were minor split channels from SSO3 channels with the remainder being “proper” SSO2 channels. SSO3 and 4 channels had total length of 962.67m and 1 053.28m. After the southern and northern legs with SSO values of 4 joined, the SSO5 channel ran a length of 901.19m before the discontinuous gully came to an end.

4.5.2 Physical measurements

The Malansdam gully system was investigated but for physical measurements a smaller test site was identified. This identification was done according to two classification measures. Firstly, the SSO classification was used. The test site chosen needed to consist of the bulk of the SSO classification scale of 1 to 5. Secondly, global slope was used. The area considered for testing had to show evidence of activity. This occurred more readily in the upper reaches where a steep slope was experienced.

Observations made it apparent that the gully system was more active in the upper reaches due to the spreading network of multiple bare channels. This is also where a steeper slope is experienced with a slope of up to 14.5° in the uppermost part of the gully system where multiple channels extend into the fynbos. This is concurrent with findings from Poesen *et al* (2003) and Valentin *et al* (2005) which indicated that with a steeper slope, the drainage area required to initiate gully formation decreases; therefore the Malansdam gully has been able to generate multiple channels in close proximity of each other, with this area bordering badland formation.

Using these two classification systems a test site on the Northern leg of the Malansdam gully system was decided upon. The test site was selected in a region which consisted of SSO classifications of 1 through to 4 and had a gradient of 5° which can be classified as strongly sloping (USDA 2003). This corresponds to findings of Kakembo *et al* (2009) who found the area between 5° and 9° as a "markedly preferential topographic zone" (Kakembo *et al* 2009:192) for gully formation.

As expected there is an increasing trend with regards to SSO classification and length of the gully channels. Refer to scatter plot in Figure 4.23. The exception to this rule is a 30.12m long order 1 channel where sediment trap 9 was inserted.

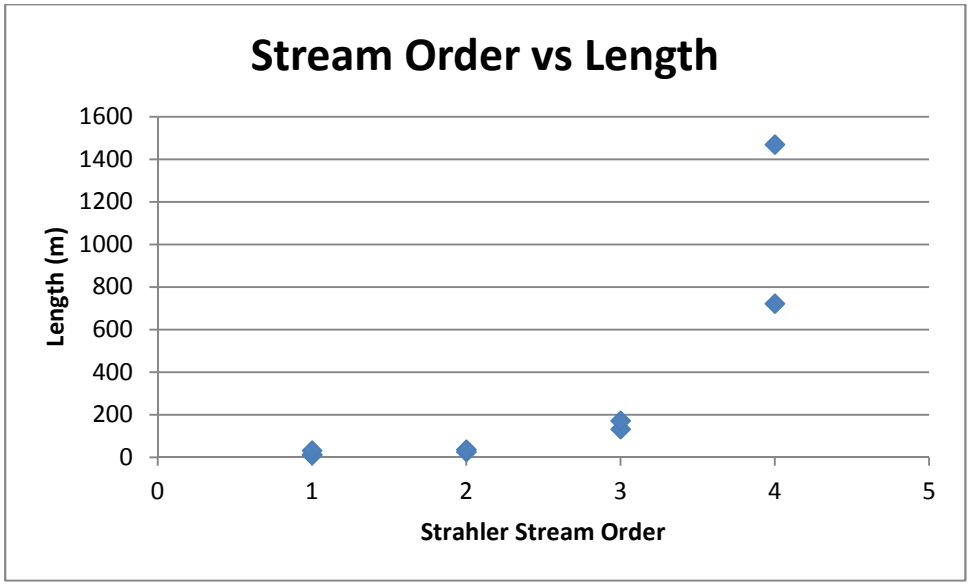

Figure 4.23 SSO and gully channel length relationship at the Malansdam gully system

The amount of soil captured per stream order shows an increasing trend as indicated in Figure 4.24. However, three anomalies did occur. Two sediment traps, one in a SSO3 channel and another in a SSO4 channel (encircled in black in Figure 4.24) captured much less sediment than its counterparts in the same SSO channel which also had a similar length. This could be due to the shape of the gully. The sediment traps were installed almost exclusively in V shaped channels. This allowed easier installation of the sediment trap in the flow path due to the narrow channel floor. The two encircled data points for sediment traps in SSO3 and 4 were placed in broad U shaped channels. Two reasons can thus be imparted for the low amount of sediment captured. Firstly, the installation might not have occurred in the exact flow path; secondly the concentrated flow through the narrow V shape channels would diverge as it reached the U shaped channel. The sediment trap only has a width of 110mm and would not have been able to cover the whole floor area. Both these situations would have caused an underestimation of the actual amount of sediment moving through that channel causing the collected sediment to be much less when compared to the V shape channels. A third grey circle was drawn around sediment trap 3 installed in a SSO1 channel. In comparison to the other SSO1 channels it

captured a large amount of sediment in a similar range of the SSO2 channels. This may be due to the length playing a determinate role in the mount of sediment produced which corresponds to Holy & Cowan (1982) whom considered this to be the most important factor of sediment production in gully systems.

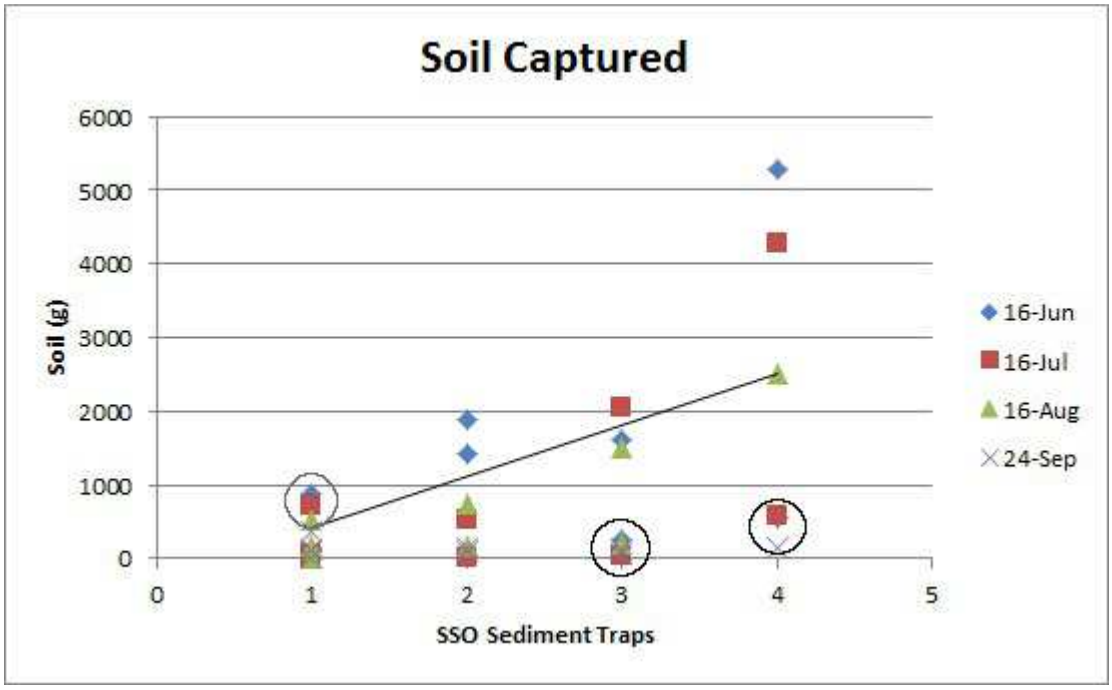

Figure 4.24 Soil captured in SSO sediment traps at the Malansdam gully system

Sub-processes were identified within the gully system. New miniature gully heads (drop and plunge zones) were seen on the main gully floor. This phenomenon was observed on numerous occasions and could complicate the task of estimating soil loss from gully erosion. The most amount of soil that was captured in a sediment trap at the Malansdam test site was installed in a SSO4 channel a few meters down channel from an active plunge hole of a “gully within a gully” channel. This was also observed by Soms (2006) where new V shaped gullies were cut into previously inactive broad U shaped channels.

Upon comparing the rainfall data and the sediment data the third collection date was expected to produce the second largest amount of sediment. The second and the last collection periods received similar amounts of total rain for the period with similar daily highs. It was expected to have similar sediment yields. However, the pattern of sediment yield following the rainfall occurrence did not emerge. Instead there was a steady decrease in sediment yield throughout the four collection periods. This decrease is indicated Figure 4.25 where it has been divided into their respective SSO categories.

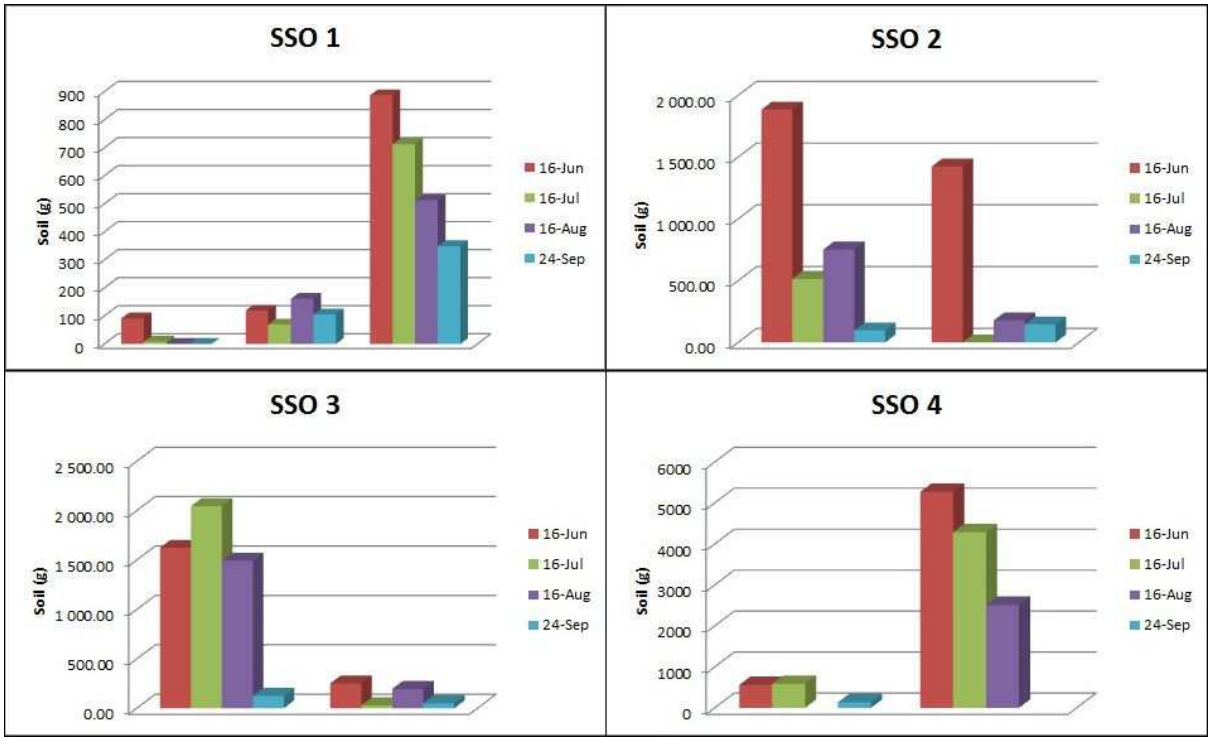

Figure 4.25 Soil captured per sediment trap and SSO channel at the Malansdam gully system

The pattern does become more apparent when the total sediment yield per collection date is put on a graph as in Figure 4.26. This trend is in line with findings from Rey (2003) who found that when vegetation within a gully exceeds 50%, the gully can become inactive in terms of sediment production. During the winter vegetation within the Malansdam gully increased dramatically from bare soils to grass cover as in Figure 3.12 as well as wheat from the cultivated fields and fynbos from the upper channels. With this increase of vegetation, sediment production fell by 91.6% from the first collection date of 16 June to the last collection date of 24 September. The results not only concurs with the findings of Rey (2003) and Mian *et al* (2009) but also supports findings from Gyssels & Poesen (2003) who found that grass and wheat, the same vegetation found in the Malansdam gully, resulted in an exponential decrease in erosion rates.

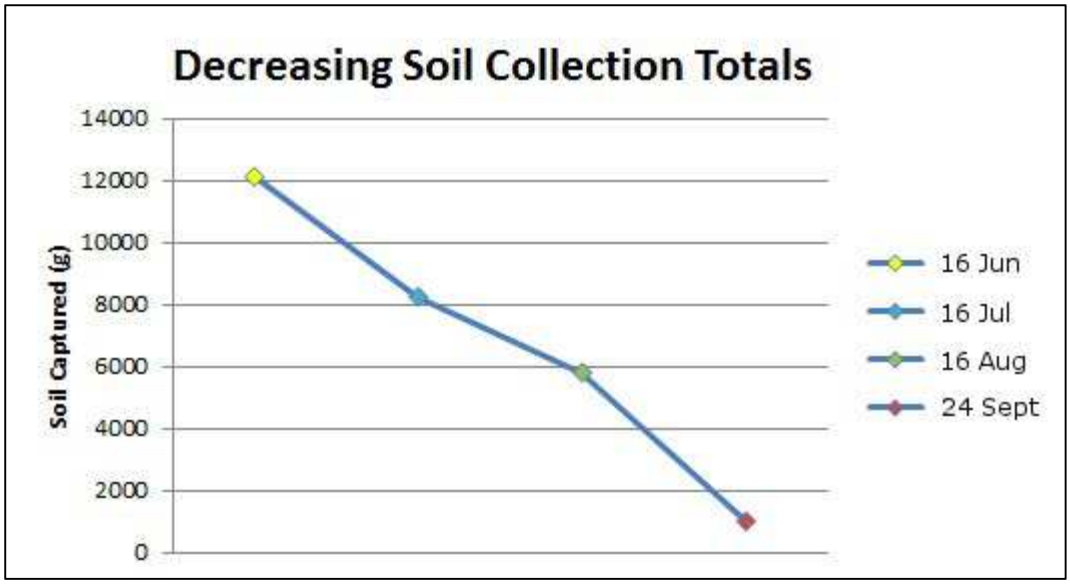

Figure 4.26 Total soil captured throughout collection time frame at Malansdam

An investigation into the soil fraction made it apparent that the sand fraction was the dominant soil fraction captured. As the winter wore on the sand fraction remained dominant, but there was a reversal in the clay and gravel fraction captured. This can be seen in Figure 4.27 where the first and last collection dates are compared with each other.

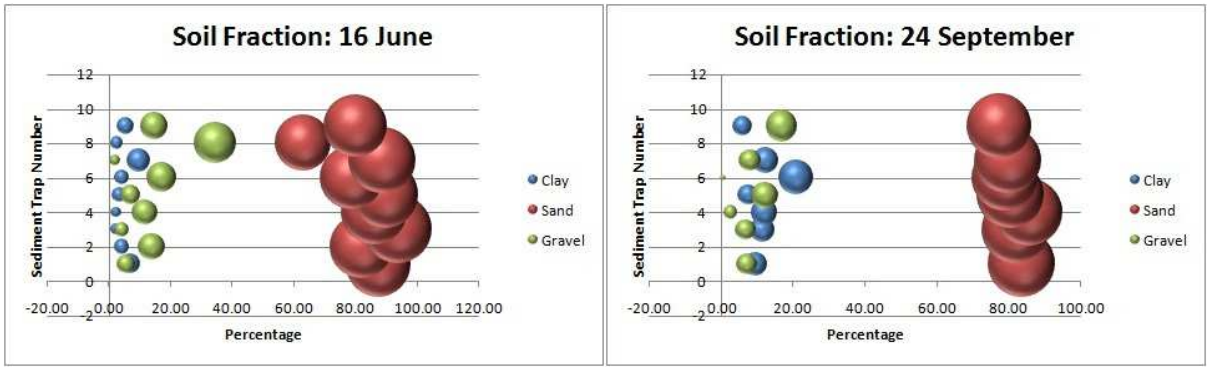

Figure 4.27 Temporal variation of soil fractions recovered from installed sediment traps at Malansdam

The symbols in Figure 4.27 are scaled according to the percentage of each fraction captured with regards to the combined total sediment yield. The sand fraction remained relatively stable. The reversal of the clay (finest particles) and gravel (largest particles) fractions may have occurred due to the increase in vegetation in the gully channel. Firstly, this would have made the gully floor less prone to erosion. Secondly, it may have limited the movement of the larger grains. It would therefore require a higher flow velocity in order to move the same grain size in September than in June. Therefore, less gravel were put in motion and thus captured in the ST's as the flow velocities obtained from the Sundborg diagram (1956) remained approximately the same for all four collection periods.

4.5.3 Indirect determination

The minimum velocity measured in the gully system was gauged by making use of the logarithmic Sunborg diagram (1956), which is a derivative from Hjülstrom's graph (1935). The minimum average velocity measured was therefore done according to largest sediment size and was measured at 37.6 to 40.2cm/s with the exception of only a few (the reasons for this is given in the Results section which is 3.9). This is the minimum velocity required to have flowed to move the sediment as it was measured from the bottom of the movement zone on the graph. This can further be considered a conservative approach since "vegetation not only reduce flow but also constitutes a lining that protects the bed from erosion" (Nogueras *et al* 2000: 207). Therefore it could be argued that the velocity, specifically for the last collection date of 24 September had to be greater than for the first collection date of 16 June to have moved a similar size grain. The speed of the flow within this gully system could be indicative of the channelling power of the ploughed contours and also how the gully system has improved the hydrology function to such an extent that water drains rapidly leaving the catchment too quickly. This could have a detrimental effect on produce, thus the economic viability of farming.

4.5.4 3D scan

Even though the image created by the 3D scan in Figure 4.18 has an accuracy of 1mm, grass coverage in the gully channels and other vegetation would make it difficult to determine sediment loss. Analyses on sediment loss making use of 3D scan would therefore be limited to the bare areas on the gully walls, when used on a seasonal basis or after specific rain events.

Alternatively, it could be used as an annual scan during the summer months when little to no vegetation occurs within the gully. In this way erosion can be monitored by overlaying the images created from successive scans. Upon doing this a simple subtraction and area calculation can be used to instantly quantify soil loss on an annual basis. Valuable data can thus still be retrieved with regards to erosion prone areas, which could help the land owner or manager to put suitable measures in place to inhibit soil erosion as well as identify areas for rehabilitation.

4.6 CONCLUSION

A physical characterisation and classification process was undertaken to establish the relationship between landscape hydrology and geomorphologic gully development. This process involved scrutinizing gully formation processes and exploration of sediment yield within the gully system.

The Malansdam gully system was found to be a discontinuous gully system with a SSO of 5. Numerous channels were densely grouped in the vicinity of the border between the edge of the ploughed contours in the cropland and natural vegetation which is indicative of an area of intense gullying. This was also in the upper reaches where a steeper slope was also experienced.

During the physical investigation a test site was decided upon in this densely populated area which consisted of the majority amount of SSO classifications. Sediment was collected on a monthly basis. The sediment data showed that the gully was still active, as all but one channel provided regular sediment gains. The channel that was not active concurred with criteria from Oostwoud Wijdenes *et al* (2000) in Section 2.4. Furthermore, this gully channel had its head adjacent to the crop land and not next to the ploughed contour, which according to the ArcMap hydrology desktop study would mean that it would no longer receive much water flow. See Figure 4.28 below.

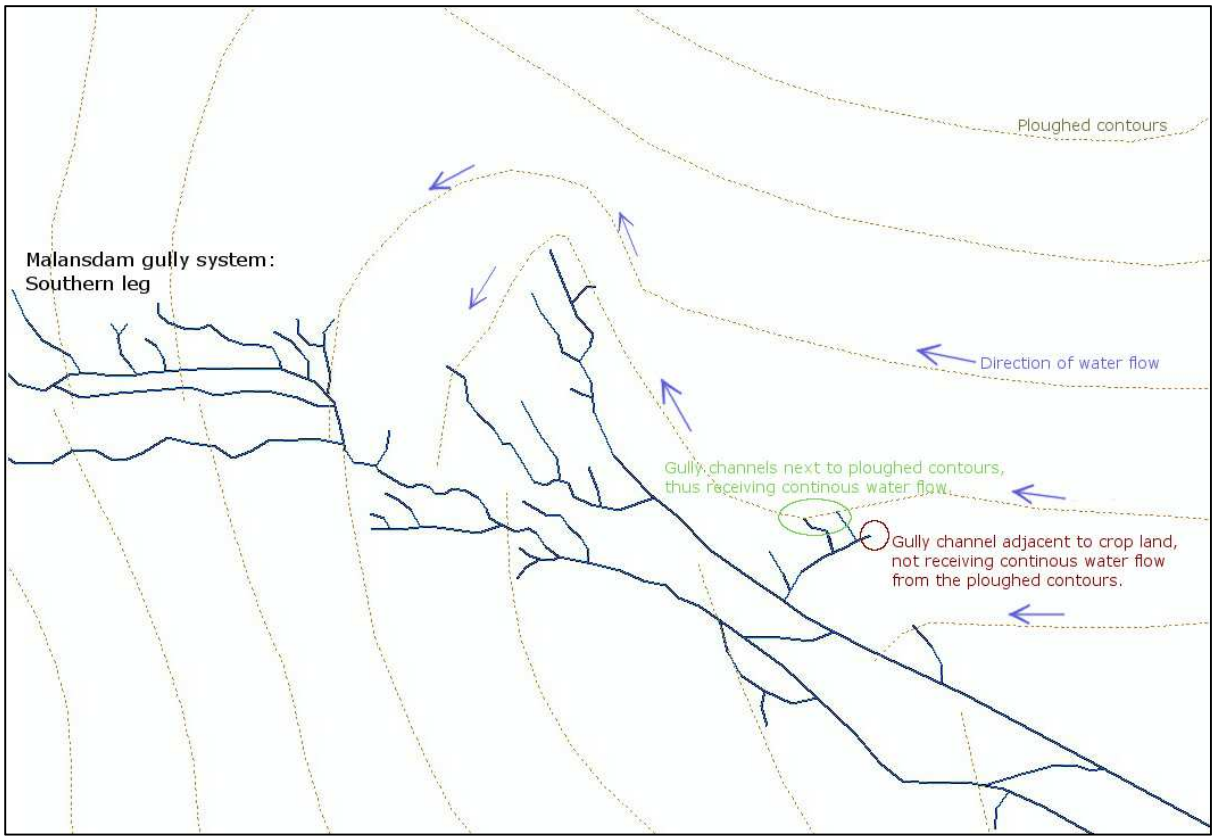

Figure 4.28 Inactive gully channel not receiving water flow due to its position not being adjacent to the ploughed contour (at Malansdam)

The sediment data provided clues as to the water velocities in the gully channel. This was done according to the Sundborg diagram. High flow velocities were deducted lending further support to the desktop study as this would indicate water being constantly channelled towards it upon rainfall. This lends worrying support to the concept that the ploughed contours aid in gully formation. Also, it would seem as if this would lead to an improved drainage, to such an extent that water leaves the catchment too quickly before infiltration and thus water storage occurs.

The physical characterisation process provided support to the theory reached in Chapter 3, which is land use has an impact on gully erosion in the Malansdam area. In this case, it is the ploughed contours that the farmers use to prevent soil erosion by water that is causing severe gully erosion and

the formation of numerous channels resulting in loss of valuable soil. Even though this concluded that land use had an impact on gully formation there was enough evidence to suggest that soil, either in terms of chemistry or structure, was also a role player in gully formation. This was evident due to the piping observations made upon field work in the area. To further the exploration of gully erosion and identifying the causes of it, the next step was to include soil as a variable and examine its contributing affect.

In addition to the above, field observations and results obtained from sediment data it would seem as grass would be a good preventative measure to put in place in order to try and curb or reduce gully erosion. Sediment yield in the gully channels reduced heavily when the channels had a large amount of vegetative growth. Since the Sandspruit catchment is situated in the Western Cape, which has a Mediterranean climate, it would be advisable for it to be in place with the commencement of winter when the rainfall season starts.

5 IMPACT OF SOIL CHEMISTRY ON GULLY DEVELOPMENT

5.1 INTRODUCTION

Much of the work done in RSA on factors controlling gullies have focussed on the human impact (Hoffman 1999b; Kakembo 2001; Boardman *et al* 2003). It focuses on land use changes upon European colonisation. Thus far, land use has also been shown to be of importance in the Malansdam area; not in terms of their crop type for example wheat, vineyard and olive groves but rather due their land management practises in terms of ploughing contours. However, during fieldwork it was observed that gullies were also forming due to piping. This formation process was identified by pipes or tunnels in the gully wall sometimes also linked with collapsed soil as shown in Figure 4.1. Piping normally goes hand in hand with a poor soil structure and a chemical imbalance. It was thus of pertinent importance to include this physical factor and investigate this as a further possible driving factor behind gully formation.

In studies that explored the intrinsic physical and chemical nature of soil and its contribution to soil erosion, it was found to play a significant role in gully erosion (Cobban and Weaver 1993; Boucher and Powell 1994; Rienks *et al* 2000; Rustomji 2006; Van Zijl 2010). They found that the inherited chemistry of the soil would affect its dispersive nature and that this might play a more significant role in gully erosion than any human elements such as land use patterns.

Various indices exist that could be utilised in identifying a soil's dispersion potential. ESP and SAR have been proved to be good indicators of this and have also been closely linked to gully erosion (Rienks *et al* 2000; Faulkner *et al* 2004; Sonneveld *et al* 2005). In order to calculate these indices (Equation 2.1 and 2.2) the cations present in the soil have to be determined. This information can also be readily used to examine dispersive potential of a soil as high amounts of Na^{+} and Mg^{2+} present would cause deflocculation in the presence of water (Mcneal *et al* 1968; Emerson & Smith 1970; Bakker & Emerson 1973, Beckedahl 1996). EC can be used to complete the investigation as this is the "preferred index to assess soil salinity" (Sparks 2003: 223).

Critique was presented in Chapter 1 and 2 about neglecting suitable investigation into soil as being a driving factor in gully erosion studies. Since gullying is a systemic threshold (Van Zijl 2010) phenomenon, thus potentially having multiple factors driving it at any given time, soil will be investigated even though land use has already been identified as having a discernible impact on gully erosion.

5.2 MATERIALS AND METHODS

Investigating the soil factor in a more advanced level required field work to be coupled with laboratory work.

5.2.1 Soil sampling

Top- and subsoil samples were taken in the Sandspruit catchment at two gully systems consisting of a continuous gully system under Kasteelberg and a discontinuous gully system at Malansdam respectively. Surface samples consisted of sampling taking place from 0 – 15cm of the surface and subsurface samples were taken in intervals of 15 – 30cm, 30 – 45cm and 45 – 60cm. This range of the sampling was taken twice per gully head. The first set was taken one meter away from the gully head in the direction of gully head retreat. Another set was taken from the walls of the gully head. The sample collection design was random but did have two prerequisites. The first of these being that the gully channel had to be an order one gully channel. The majority of these were found behind the ploughed contours in the agricultural field. The second was that the gully head and channel had to show evidence of being active. The degree of activity was based on work done by Oostwoud Wijdenes *et al* (2000). The criteria used in order to assess and thus classify a gully head as active or non-active is given in Table 5.1 and Figures 5.1 and 5.2.

Table 5.1 Soil sample criteria comprising of gully activity

Active	**Not Active**
Sharp edges	Rounded edges
Plunge pool	No plunge pool
Undercut	Inclined gully head wall
Tension cracks	Vegetation on gully walls and bed
Recently deposited sediment	Extremely small contributing catchment area
Flow marks	
Piping	

Source: Oostwoud Wijdenes *et al* 2000

For the purpose of this study Oostwoud Wijdenes *et al* (2000) gully headwall classification was adapted to distinguish between active and non-active only.

For a gully head to qualify as being active it had to have a minimum of two of the active criteria in Table 5.1 (see also Figure 5.1). Any combination would suffice and therefore be regarded as evidence of activity as each criterion given, except for piping is interlinked. Gully head activity and gully head retreat can be explained according to the following criteria: A gully head with sharp edges and little vegetation is normally coupled with a plunge pool that is created due to the hydraulic energy of falling water. The energy of the water would scour the gully channel below the head in all directions causing the headwall to become undercut. Once this has happened, there is no more soil beneath the top part of the gully headwall to bear the weight of it. Due to gravitational force, tension cracks will start to develop on the upper parts of the gully headwall. When the cracks reach a critical size the headwall will slump with the end result being fresh sediment being deposited close to the headwall; where after

the process will start again. Further evidence of activity would be flow marks above the head, towards it and also below it in the gully channel. Piping is the one criterion that is not set in motion or interlinked to the other criteria as it is caused by subsurface water flow, although it could lead to fresh deposited sediment due to collapse when the pipes become too large.

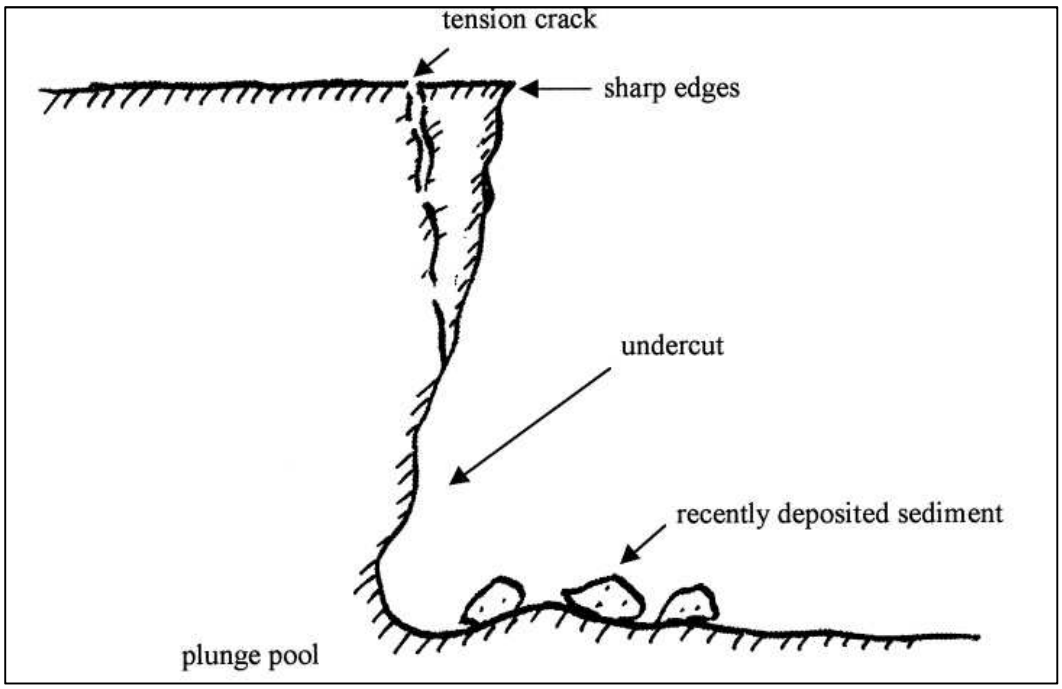

Source: Oostwoud Wijdenes *et al* (2000)

Figure 5.1 Active gully

The manner in which the sampling occurred was as follows: Sampling only occurred at active gully heads with the above criteria. A Geographical Positioning System (GPS) with a positional accuracy of 0.5m was used to log the location of the sample measurement points. This would allow for the points to be imported into a Geographical Information System (GIS) and successfully mapped. Eight soil samples were taken from each gully. Four samples were taken 2m from the gully head by making use of a manual core drill at 0 – 15cm, 15 – 30cm, 30 – 45cm and 45 – 60cm intervals. Another four samples were taken at the same intervals from the exposed soil of the gully wall. The majority of active gullies that were sampled at Kasteelberg and Malansdam developed behind contours ploughed by farmers. The most common criteria combination thus consisted of flow marks leading up to the gully head along the ploughed contour and an active plunge pool that caused the headwall to become undercut. Fewer gullies had a combination of tension cracks with recently deposited sediment. One gully had the combination of piping and recently deposited sediment.

A gully head was classified as not active when it had all or a combination of two or more of the non-active criteria in Table 5.1 and Figure 5.2 as this is deemed as evidence of stabilisation. The gully head with rounded edges void the possibility of the development of a plunge pool. The absence of

flow marks and the abundance of vegetation are further indicative of inactivity. A small contributing catchment indicates a small source of water to enable erosion and this would thus also limit erosion activity.

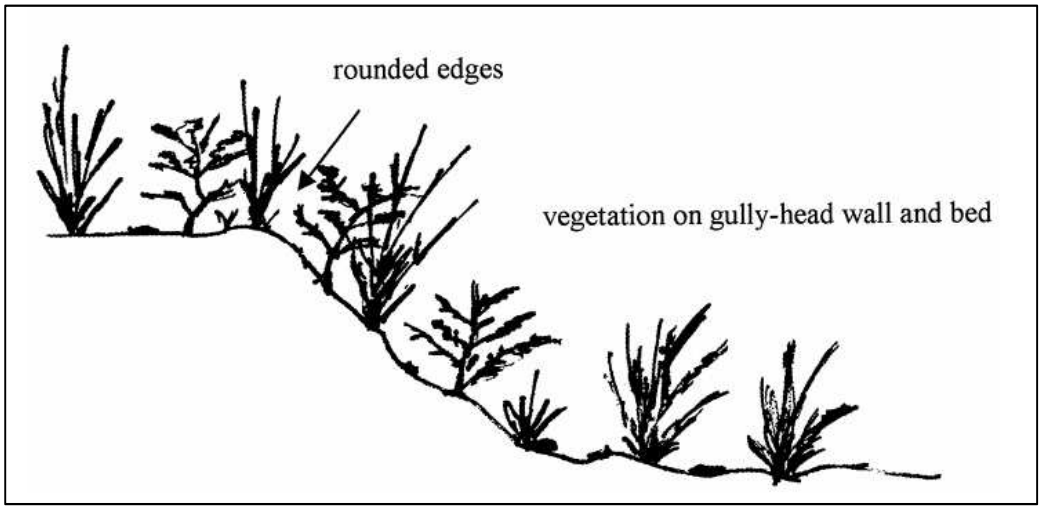

Source: Oostwoud Wijdenes *et al* (2000)

Figure 5.2 Inactive stabilised gully

Inactivity at Kasteelberg and Malansdam was dominated by a combination of rounded edges without a plunge pool and an abundance of fynbos. These gullies were not sampled.

5.2.2 Laboratory analysis

The soil samples collected from Kasteelberg and Malansdam were pre-treated prior to wet chemical analysis. They were air dried in a heated room. Thereafter, each sample was crushed by using a mortar-and-pestle. The crushed sample was sieved with a 2mm sieve to rid it of excess plant, other organic material and rock fragments. After the completion of pre-treatment the samples were ready to be subject to wet chemical analysis.

The following analysis method was used in order to establish pH, EC and SAR. For this a 1:5 ratio of soil: Milli-Q water (White 1969) was made by bottling ten grams of pre-treated soil and adding fifty millilitres of Milli-Q water. This was done for each sample that was collected in the field. The wet bottled samples were shaken at a hundred and fifty revolutions per minute (RPM) for one hour and left to stand overnight. The pH was measured with the soil colloids still in suspension (White 1969). After completion of the pH measurement, the EC of the sample was measured also with the soil colloids still in suspension (Rayment & Higgonson 1992). Once these two measurements were completed, the samples were prepared for SAR analysis. They were centrifuged for one hour at an approximate angle of 45° at 30000 RPM to remove suspended material. Thereafter, it was also filtered using 300 grade filter paper in order to remove any remaining organic material and colloids that were

still in suspension. The resultant clear liquid of each sample was sent to the Central Analytical Facility (CAF) laboratory for a CEC analyses by way of an atomic absorption spectromoter. Equation 2.2 was used to calculate the SAR for each sample, using the cations in millimoles per liter established from the CEC analysis.

Another wet chemical analysis method was used to measure the exchangeable cations occupying exchange sites and also to determine the ESP with equation 2.1 as well as the MS% with equation 2.9. The decision on which method to follow was based on two aspects. Firstly, the majority of research has been conducted using the 1 Molar (*M*) ammonium acetate (CH_3COONH_4) buffered at pH 7 method and this would allow this work to be comparable to other published research. Secondly, the soil pH results obtained indicated that the soil did have a high acidity level. Therefore the 1*M* ammonia acetate buffered at pH 7 method was suitable (Ross 1995). This was done according to the RSA Soil Classification standards (Macvicar & De Villiers 1991)

The 1*M* ammonium acetate was made using ammonium acetate crystals. It has a molar mass of 77,08g/mol and thus 77g of CH_3COONH_4 crystals were mixed with one litre of Milli-Q water. Thereafter, it was buffered to a pH of seven with the use of 25% aqueous ammonia and acetic acid (Knudsen *et al* 1982). A 1:5 ratio was created by bottling 10g of the pre-treated soil where after 50ml of the buffered ammonium acetate solution was added. The bottled sample was shaken at 175 RPM for one hour and left to stand overnight. The solution was transferred into centrifuge bottles and centrifuged at an approximate angle of 45° at 30000 RPM in order to remove any suspended material such as soil colloids and organic material. After this procedure, the solution still had some very fine soil colloids and organic material in suspension and this was removed by pouring the solution through 300 grade filter paper. The clear fluid was then sent to the CAF laboratory for a CEC analyses via an atomic absorption spectrometer. From the data received ESP was calculated using equation 2.1 and the MS% was calculated using equation 2.9.

5.3 RESULTS

The results returned from the traditional wet chemical soil analyses with regards to SAR are given in Figure 5.3 and 5.4. Figure 5.4 was inserted to clarify the values as sample M3B yielded high values dwarfing the values from the other samples. Excluding sample M3B, SAR values obtained were low ranging from a low of 0.66 measured for sample M2A 30 – 45cm to a high of 2.03 for sample 2A 0 – 15cm.

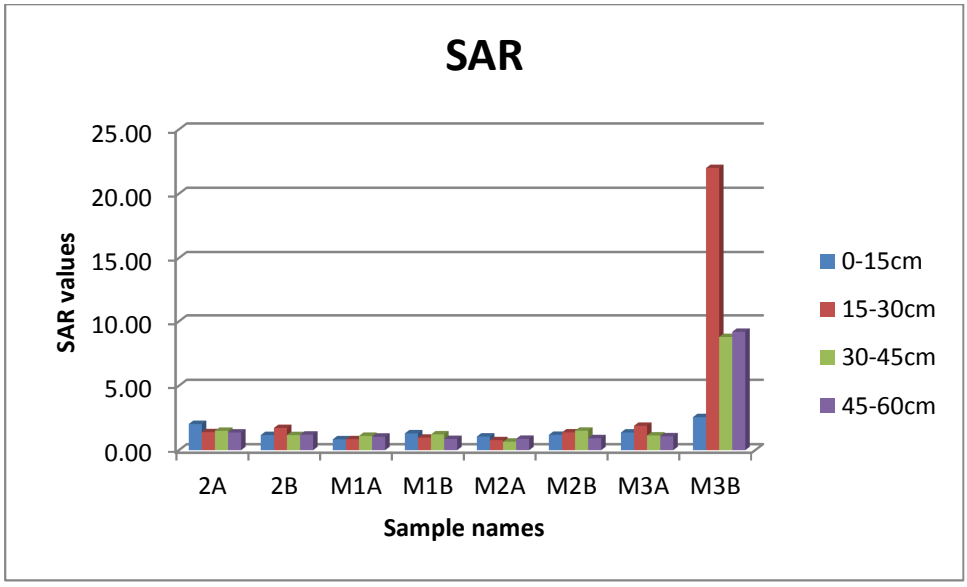

Figure 5.3 SAR values obtained for all samples from the Sandspruit catchment

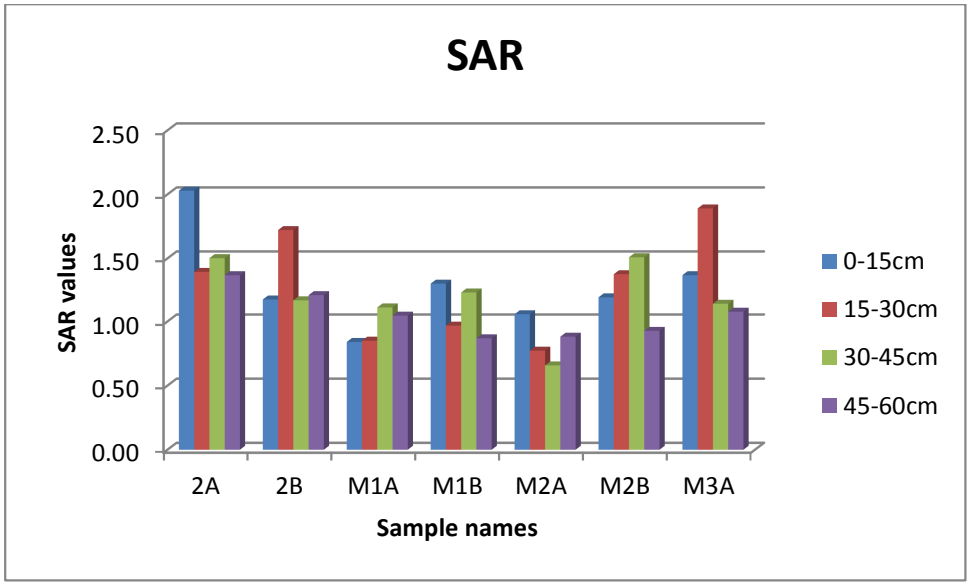

Figure 5.4 SAR values for samples from the Sandspruit catchment excluding M3B

The EC data returned, also from the wet chemical analysis, is given in Figures 5.5 and 5.6. In Figure 3.18 sample M3B was removed in order to establish a clearer image of results for the other samples. All samples except for M1B showed an increasing trend with regards to EC as there is moved from the upper soil interval, 0 – 15cm, towards the intervals deeper into the subsoil.

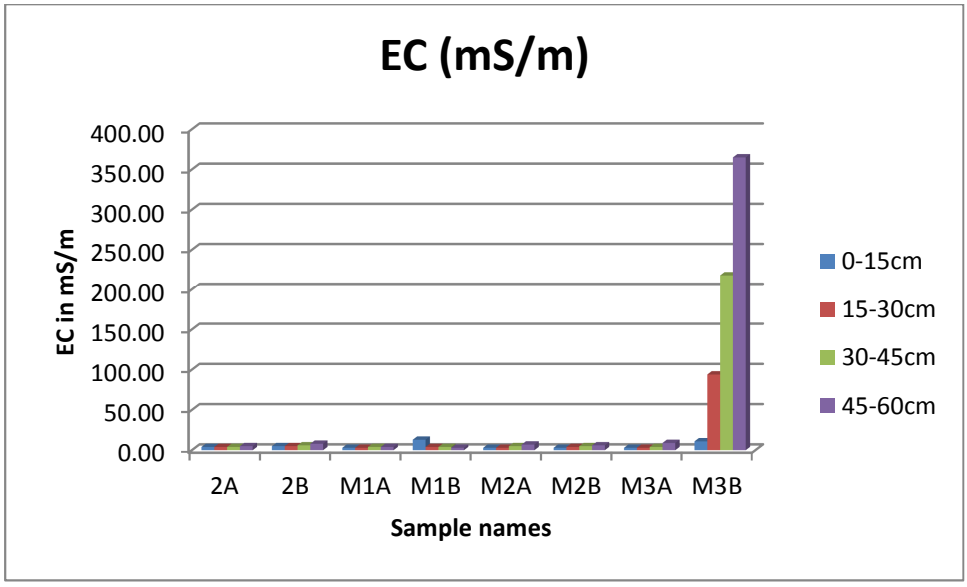

Figure 5.5 EC values for all samples from the Sandspruit catchment

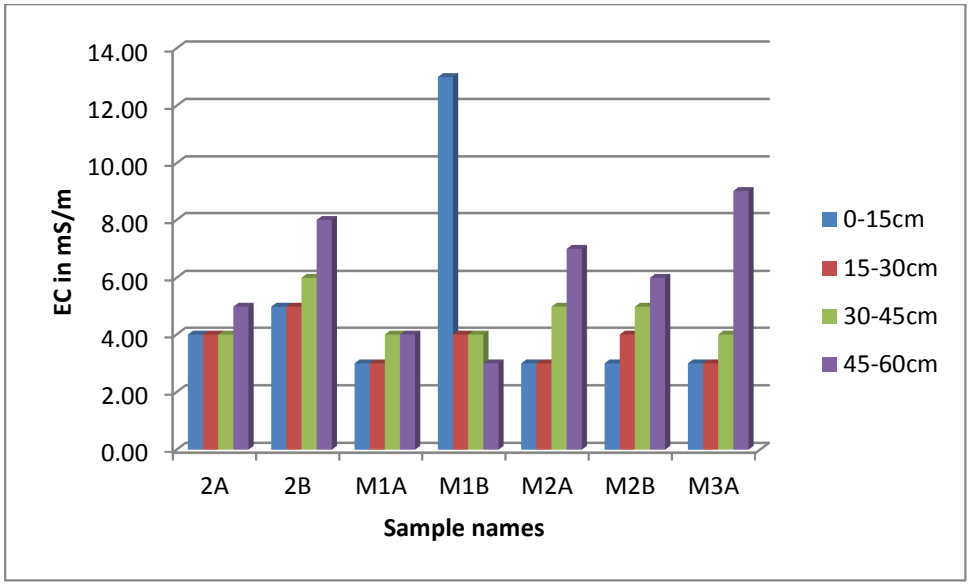

Figure 5.6 EC values for all samples from the Sandspruit catchment excluding M3B

Due to the small amount of samples sent in for wet chemical analysis, samples from a gully system with a similar soil profile at Kasteelberg were combined with those of the Malansdam samples. The results of these analyses are given in Table 5.2.

Table 5.2 Wet chemical analysis data from surface and subsurface soil samples

Sample Name	pH	Ca^{2+}	K^{+}	Na^{+}	Mg^{2+}	ESP	MS%
1A 30-45	7.1	3.66	1.34	0.87	5.17	8.89	52.54
1B 0-15	6.6	2.92	0.37	0.45	2.92	6.8	43.85
2B 15-30	7.5	3.21	0.45	1.19	5.88	11.1	54.76
K1A 0-15	7.3	3.33	0.51	1.73	7.36	13.38	56.91
K1A 30-45	8.3	1.21	0.58	0.6	3.58	10	60.07
K1A 45-60	8.7	0.86	0.49	0.1	0.45	5.48	23.74
K2A 0-15	6.7	1.39	0.62	0.2	1.39	5.69	38.75
K2B 15-30	6.4	1.39	0.47	0.33	2.66	6.73	54.83
M1A 30-45	3.4	4.8	3.27	15.09	8.83	47.15	27.59
M1B 30-45	6.5	0.98	0.12	0.16	0.61	8.63	32.64
M2A 45-60	6.5	2.43	0.26	0.54	0.76	13.53	18.99
M3A 0-15	5.9	1.16	0.22	0.26	0.23	13.79	12.16

The exchangeable Na^{+} values were lower than expected with the values at the Malansdam site being the highest with values between 0.45 – 1.73 (if sample M1A30-45 was to be excluded). Due to the low values the ESP index for soil dispersion was affected and thus fell below international proposed thresholds. The exchangeable Mg^{2+} however, were high with values ranging between 0.23 – 8.83. The high percentage can be seen as calculated by the MS%, with a high of 60.07%. This indicates that 60.07% of all exchangeable cations present are Mg^{2+}. As Beckedahl (1996) and Walker (2007) stipulated upon dealing with RSA soils, especially in cases where high concentrations of exchangeable Mg^{2+} is present, the international threshold values indicating soils with a poor structure should be lowered. In light of the high concentration of exchangeable Mg^{2+} present, it was deduced that the soil analysed at the gully heads was dispersive in nature and prone to erosion in the presence of water.

5.4 DISCUSSION

From the soil data acquired from the wet chemical analyses (from both Malansdam and Kasteelberg) the ESP values are low when compared to the MS%. The ESP values are also below the international standards to classify a soil as dispersive. However, as Beckedahl (1996) and Walker (2007) found the international classification system might be ill suited to RSA conditions, especially in an environment with high exchangeable Mg^{2+}, as this would cause soil to deflocculate in the presence of water (Mcneal *et al* 1968, Emerson & Smith 1970). With the pH being slightly acidic and the EC being

relatively low it would seem as if the exchangeable Mg^{2+} cation is a major role player in gully erosion in the Malansdam area. It would cause the soil to have a dispersive nature due to the large amount of exchangeable Mg^{2+} cations occupying exchange sites on the clay fraction (Refer to Figure 5.7 and Table 5.2). This is in accordance with other RSA studies like Rienks *et al* (2000) and Sonneveld *et al* (2005) who also found soil to be dispersive at a lower ESP than the international classification system.

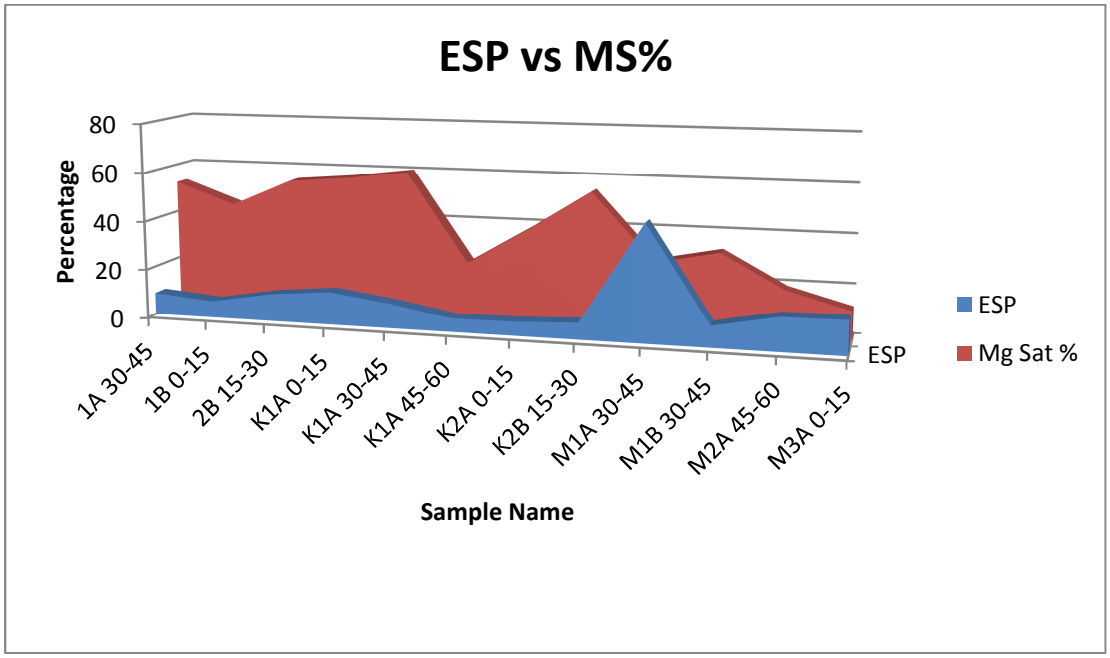

Figure 5.7 Comparison of ESP and MS% values obtained from soil samples collected from gully systems in the Sandspruit catchment

Similarly, the SAR results attained low results. This might be due to the close relationship SAR and ESP values have where the cations in solution mimics the cations on the exchange sites. Since the SAR values are also indicative of the amount of exchangeable Na^{+} cations in solution, it further accentuates the above notion that the exchangeable Mg^{2+} cations are the key constituents causing dispersion.

A and B samples were taken, the former 2m away from the gully head in the direction of the gully head retreat and the latter from the gully wall. The SAR values for the A and B samples are plotted in Figure 5.8. In both samples the majority of SAR values in the 0 – 15cm depths are the highest. This would be indicative that the surface soil would erode first, as this is the area with the most Na^{+} cations. At this point the combined interaction of Na^{+} and Mg^{2+} with water would be greatest and cause soil to disperse. Since the sampling occurred at V shaped gully channels this agrees with Imeson & Kwaad (1980), who found that this gully shape mostly develops from runoff and not piping.

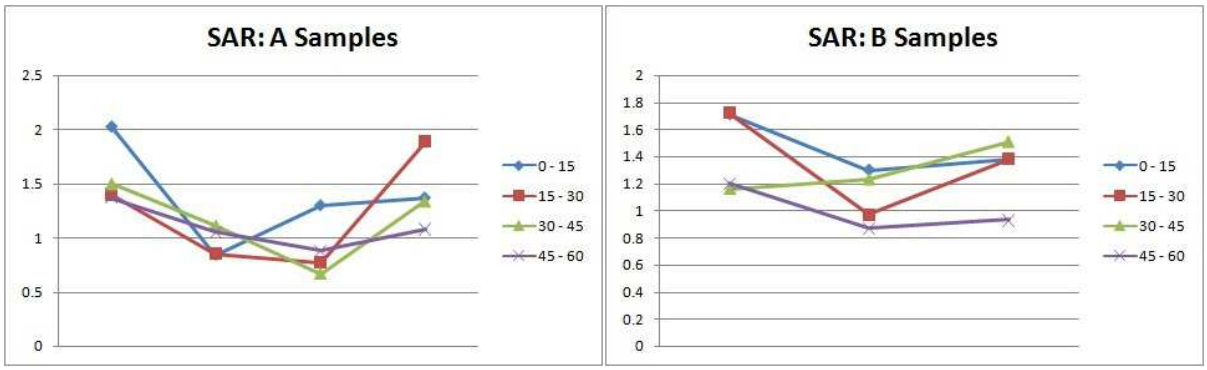

Figure 5.8 SAR values of the A and B samples collected from the active gully sites within the Sandspruit catchment

In below Figure 5.9 the SAR A and B samples were plotted against each other at the various sampled depths.

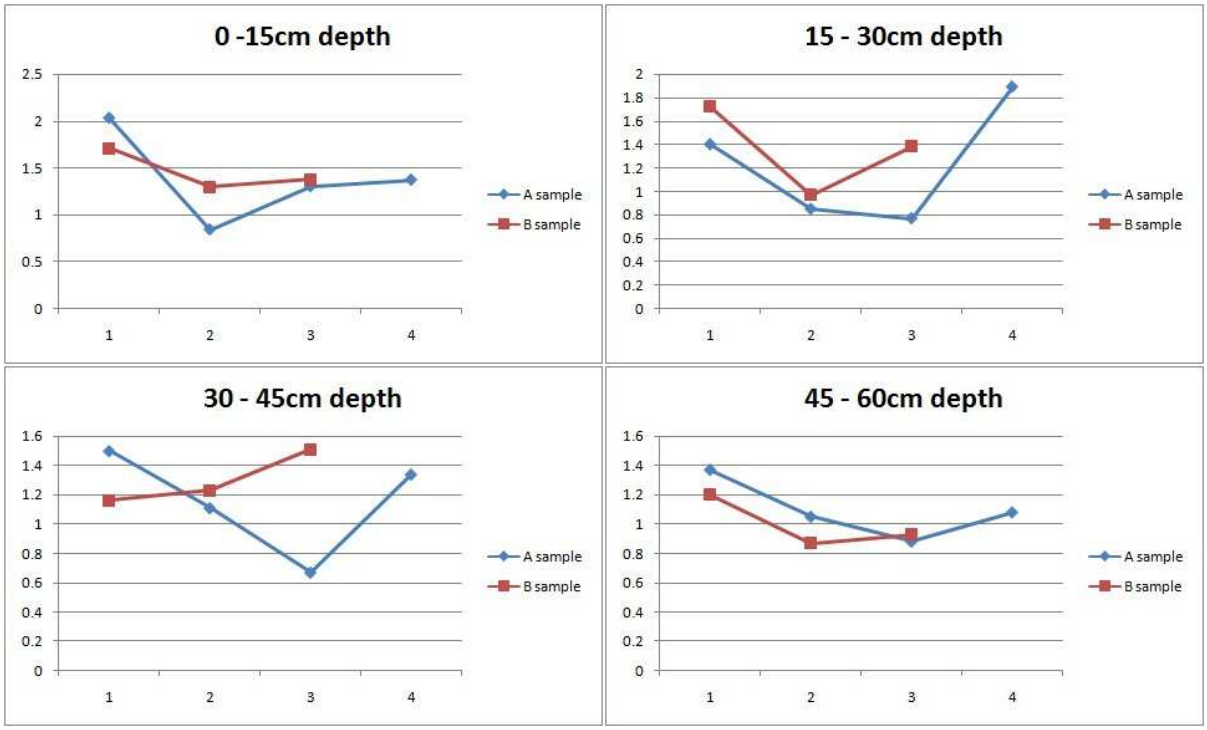

Figure 5.9 SAR values of the A vs B samples plotted against the depths at which it was taken at the gully sites within the Sandspruit catchment

The SAR values measured for the B samples are higher in almost all cases when compared to their comparative A sample. This could be due to the movement of the Na^{+} cation along the hydraulic gradient contributing to salt precipitation on the gully walls as indicated in Figure 4.5b. This could have an enhancement of erosion on the gully walls and head.

5.5 CONCLUSION

The desktop study relating to the impact of the farming practises and gully system on the landscape hydrology, as well as the physical characterisation process both indicated land use as having a determinant impact on gully erosion. The study was however furthered to investigate soil properties as well, after field observations with regards to formation processes shown this to be a possible driving factor contributing to gully erosion.

This investigation followed a more analytical approach instead of a mere soil classification procedure. The intrinsic properties of the soil were investigated by way of CEC analysis to determine the cations occupying exchange sites on the clay fraction. This data was also used to determine soil dispersion indices, ESP and SAR, which were closely related to gully erosion by previous work (Rienks *et al* 2000; Faulkner *et al* 2004; Sonneveld *et al* 2005). The MS% was also calculated from the CEC data as Beckedahl (1996) and Walker (2007) found soils containing high amounts on Mg^{2+} adversely affected soil dispersion in their respected RSA studies. The last index used was that of EC as Sparks (2003) found this to be the best index to determine soil salinity.

The soil chemistry results obtained from the CEC analysis and the indices pointed out that the soil structure was weak and dispersive in the presence of water. It was however not due to excessive amounts of Na^{+} as low values were obtained for both the ESP and SAR indices. The EC values, which is also closely related to Na^{+} was similarly low. The investigation also explored the amount of exchangeable Mg^{2+} in the soil. High values were returned leading to a similar conclusion to that of Beckedahl (1996) and Walker (2007); the main cause resulting in soil structure problems in the Malansdam area is the percentage of exchangeable sites on the clay fraction occupied by exchangeable Mg^{2+}. Although low EC, ESP and SAR values were recorded, the high amount of exchangeable Mg^{2+} in the soil was verification that soil also played a significant role in gully erosion in the Malansdam area. This would enhance the structural weakness of a soil causing it to deflocculate in the presence of water, even with lower amounts of exchangeable Na^{+}present.

Due to this being an Masters project there were time and more importantly cost constraints which led to a limited amount of soil samples being sent for the traditional wet chemical analysis. This directed to project to a search for an analysis method that returns rapid and inexpensive yet, accurate results.

6 NIR PREDICTABILITY OF SOIL PROPERTIES AND DISPERSION INDICES

6.1 SOIL DISPERSIBILITY MEASURES – A NEED FOR COST-EFFECTIVE RAPID ASSESSMENT

Soil is the substance in which gully erosion occurs. Despite this relatively few studies have focused on soil as a major factor playing a role in gully formation with the ripple effect being that "little is known about the properties of soils and the associated processes that control its resistance to gully erosion" (Poesen *et al* 2003: 112). For the complete discussion surrounding soil as a driving factor in gully erosion please refer to Chapter 2, with specific attention on Section 2.5.3.

Section 2.5.3 identified indicators which could be used to identify areas where soil is likely to occur due to dispersion. Normally, these indicators would be determined with the traditional wet chemical analysis as presented in Chapter 5. These methods, however reliable, is time consuming and expensive. NIR diffuse reflectance spectrometry is an economical non-destructive technique that has the potential to make multiple conclusions with a singular scan. This results in rapid analysis of soil samples, as one scan could produce reliable data on soil properties and dispersion indices without having to use the wet chemical analyses. The indicators linked with gully erosion, presented in Chapter 2 and 5, can thus be assessed with one scan.

If NIR diffuse reflectance spectrometry is successful in developing models to determine these indicators a further possibility exist to link these models to satellite sensors capturing the NIR region. This would not only benefit soil erosion, but more specifically gully erosion research, as well as various soil science studies and land management practises such as precision farming. Figure 6.1 indicates the current and ideal situations if these two methods were to be successfully merged (indicated by the dark red arrow). The model has a horizontal flow that defines remote sensing precision and a vertical flow which accounts for soil sampling and analysis, showing its influence on overall precision.

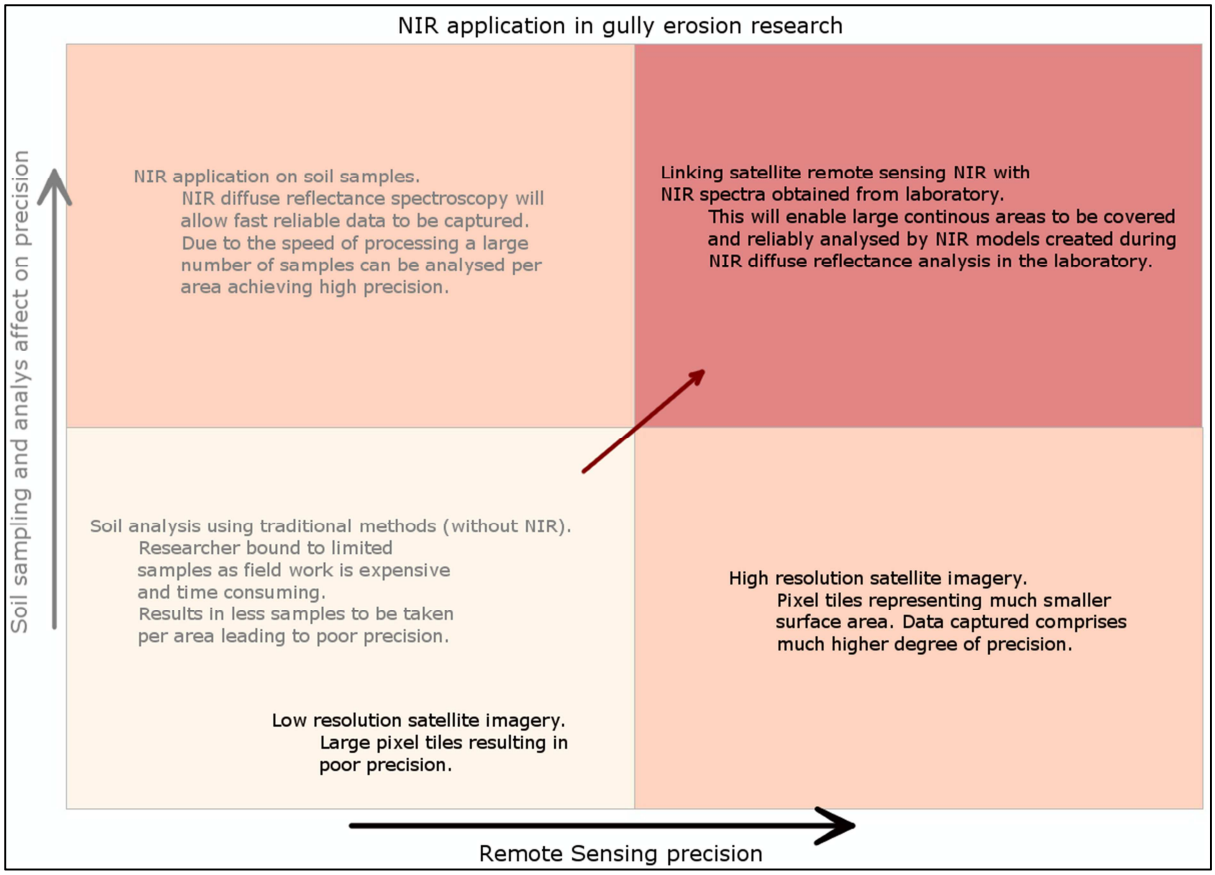

Figure 6.1 Current vs Ideal analyses scenario and the NIR link

The current situation is depicted as the lightest shade block in the left bottom corner in Figure 6.1. Firstly, with regards to studying gully erosion, a limiting factor is the amount of soil samples that can be subject to analysis due to time and cost constraints. As a result of these constraints the density of samples per area under investigation would be low, consequentially having a negative impact on the precision of the work output. This is largely due to uncertainty, because a large area would be left unanalysed due to low sample coverage. If the vertical flow is followed where soil sample analyses can be conducted by means of NIR spectroscopy the precision will increase dramatically. The reason for this is that analyses through NIR diffuse reflectance spectroscopy is inexpensive and rapid (Viscarra Rossel *et al* 2006) and produces accurate results if model calibration is done effectively during model development. NIR diffuse reflectance spectroscopy therefore provides the capability of analysing a greater volume of samples, consequently improving the precision of results obtained. Secondly, remote sensing, applied soil erosion research is currently focussing on sensors on satellites with a large spatial resolution. The sensors of choice for these studies are the Landsat TM, Landsat ETM+ and SPOT 1-4 sensors with spatial resolutions from 10m to 30m (excluding the panchromatic image). Most often these sensors are used to determine land use as a aid to investigate soil erosion (King *et al* 2006; Ning *et al* 2006, de Asis & Omasa 2007). It can also be used to reveal areas of incision, therefore identify areas of erosion, but only on large scale due to the low spatial resolution

(King *et al* 2006). Although being able to indicate areas of erosion features and potential high risk areas, the precision is compromised due to its low spatial resolution. The horizontal flow needs to be followed to sensors containing a higher spatial resolution in order to improve precision. This will improve, because of the pixel size representing areas would be finer resulting in more detailed data.

The possibility exists of combining the two higher precision blocks with the answer being in the NIR region. If the models created during the NIR diffuse reflectance process under laboratory conditions can be integrated with the NIR region of a remote sensing sensor with a high spatial resolution, dispersion indices and measures could be determined by means of readily available satellite images. This will result in copious high precision data which is rapidly and economically obtainable.

6.2 METHODOLOGY

The same soil samples that were discussed in Chapter 5 were used for the purposes of the NIR diffuse reflectance investigation.

6.2.1 Soil sampling

The same soil samples that were collected as per Section 5.2.1 were used for NIR fingerprinting.

6.2.2 Laboratory analysis

The laboratory analyses that the collected soil samples underwent are detailed in Section 5.2.2.

6.2.3 Spectral analysis

The pre-treated soil samples were used for spectral analysis. The dry samples were sub sampled into three equal parts. Of each part approximately 30g were sampled for spectral analysis. Each 30g constituted of six 5g scoops taken in an anti-clockwise rotation of each soil part spread in a petri dish as shown in Figure 6.2. This composite method of sampling was used in order to reduce bias-related errors (Bellon-Maurel *et al* 2010, Mashimbye *et al in press*), thus improving the PLSR calibration models.

Figure 6.2 Composite soil sampling method consisted of taking six anti-clockwise 5 gram scoops which was added to a quartz window sample holder for spectral diffuse reflectance analysis

This method was also used by Mashimbye *et al* (*in press*) whom received good results in terms of Mg^{2+}, Ca^{2+}, Na^{+} and pH predictions. Each scoop was placed in a 51mm diameter sample holder that had a quartz window. The spectral diffuse reflectance of the samples were measured with a Bruker multi-purpose FT-NIR Analyser (MPA; Bruker Optik GmbH, Germany) with a spectral range of 12 500cm^{-1} to 4000cm^{-1} which is equivalent to a wavelength of 700 – 2500nm. Each sample was scanned for diffuse reflectance each consisting of 128 scans. These scans were averaged into one singular graph displaying the diffuse reflectance properties of the particular sample. As each sample was divided into three equal parts this process was done three times for each sample. 12 samples were selected to be scanned which totals to 36 scans with the resultant being 36 diffuse reflectance graphs.

The CEC data obtained by the wet chemical analysis was used as an indicator in order to determine which soil samples to be selected for wet chemical and NIR analyses. From the total of 56 soil samples obtained, the four with the highest total CEC, the four with the lowest total and lastly the four samples found between the extremes (middle averaged amount) were used. This was the only criterion for selection. Whether the soil was sampled from the surface or sub-surface was not taken into consideration upon selection. Within the selected 12 samples, 4 were sub-surface of origin whilst the rest were surface samples. All four samples taken from the gully head wall were classified as surface samples.

6.2.4 Data Management: Model Construction and Selection

Once diffuse reflectance spectra graphs were attained for each sample it underwent spectroscopic pre-processing, PLSR model calibration and building as well as validation with windows based software OPUS 6.5 (MPA; Bruker Optik GmbH, Germany). The QUANT 2 utility was applied as this uses "various mathematical approaches to optimise the calibration model" (Xie *et al* 2011: 55). These mathematical approaches include: 1) No spectral pre-processing, 2) Constant offset elimination, 3) Straight line subtraction, 4) Vector normalisation (SNV), 5) Min-Max normalisation, 6) Multiplicative scattering correction (MSC), 7) First derivative, 8) Second derivative, 9) First derivative and Straight line subtraction, 10) First derivative and SNV and 11) First derivative and MSC. Several results (in most cases above 400) following the different approaches (different approach and spectral range combinations were used) were listed and ranked according to the lowest Root Mean Square Error of Prediction (RMSEP). In each case the approach ranked with the lowest RMSEP was used to build the calibration model.

Within this calibration model certain parts of the spectra were excluded. This could be due to it being insensitive and thus not being adequate to pick up any trends therefore making it ill-suited for prediction purposes. The mathematical approach was applied to the selected area/s only. This was done in order to remove any artefacts that may have occurred during the scanning process hence "reducing optical interference not related to the chemical composition of the sample, such as

variations caused by different sample particle size" (Blanco & Villarroya 2002 in Mataix-Slera *et al* 2012: px).

6.2.5 Model Validation

The performance of each model was measured according to five criteria. These consisted of the four standard criteria used in NIR, namely the coefficient of determination (r^2), the Root Mean Square Error of Cross Validation (RMSECV), the Ratio of performance to deviation (RPD) and Bias but also one new validation technique namely Ratio of Performance of Quartiles (RPIQ) proposed by Bellon-Maurel *et al* (2010) for specific use in soil science.

r^2 indicates the variance in the known measured quantity and the predicted quantity. As the value obrained for r^2 approaches 1 the predicted value approaches the measured value (Bruker Optik GmbH, Germany). Chang *et al* (2001) proposed the following threshold values to be applied to soil prediction NIR: 0.80 – 1 as excellent, 0.50 – 0.80 as fair, and lower than 0.50 as poor and thus unreliable. r^2 is calculated as follows:

$$r^2 = \left[1 - \frac{SSE}{\sum(y_i - y_{m)}{}^2}\right] * 100$$

Equation 6.1

where SSE is the Sum of Squared errors and y_i is the known measured quantity and y_m is the predicted quantity.

Since a leave one out cross validation method was used, the RMSECV would be used instead of the RMSEP which is used for T Test validation. Using the leave one out cross validation method, each sample is left out once and predicted. The RMSECV gives an indication of the quality of the model by looking at its ability to predict the quantities of new samples (Özgür & Göktas 2002). RMSECV values of below 1 is the sought after value. RMSECV is calculated by:

$$RMSECV = \sqrt{\frac{1}{n}\sum_{i-1}^{n}(Differ_i)^2}$$

Equation 6.2

where

$$Differ_i = y_i - y_m$$

Equation 6.3

RPD is the "ratio between the standard deviation (SD) of the measured data and the RMSECV" (Mataix-Solera *et al* 2012:3) and indicates the overall accuracy of the model. RDP is determined by:

$$RPD = \frac{SD\ of\ measured\ data}{RMSECV}$$

Equation 6.4

The threshold values for successful models vary according to different authors. Dunn *et al* (2002) classified the accuracy of models as follow: where RPD > 2 it indicates an excellent model, RDP of 2 > RPD > 1.6 as acceptable and 1.6 > RPD as poor when dealing with a site within the same agricultural field. Chang *et al* (2001) developed a different set of thresholds the year before. This set of thresholds have been cited and reported by more authors (Bellon-Maurel *et al* 2010; Volkan Bilgilli *et al* 2010; Mashimbye *et al in press*). These consist of excellent models having a RPD > 2, fair models with a range of 2 > RPD > 1.4 and non-reliable models having a 1.4 > RPD values. There is no statistical basis for the range of these threshold values suggested and used by different soil scientists. This is one of the reasons why Bellon-Maurel *et al* (2010) has suggested the use of RPIQ in conjunction with RPD to fully assess the accuracy of a model. A further reason for using RPIQ for soil samples, is that RPD might give an artificially high threshold value for samples that have a skewed distribution as is the normally the case with soil, but RPIQ is not affected by this. The larger the RPIQ number the better the model accuracy become (McDowell *et al* 2012). RPIQ is calculated with:

$$RPIQ = \frac{(Q3-Q1)}{RMSECV}$$

Equation 6.5

Where Q3 is the value derived from wet chemical analyses under which 75% of the sample population occur, Q1 is the value from the same analyses under which 25% of the sample population occur and RMSECV is the prediction error upon doing a full cross validation.

For the purpose of this study the RPD threshold values from Chang *et al* (2001) were used. The reason for this is that the soil samples that would be subject to analyses were obtained from different agricultural fields spanning approximately 10km and also that these RPD values have been cited and thus reported more, making this work more comparable to other studies. RPIQ (Bellon-Maurel *et al* 2010; Mashimbye *et al* 2012; McDowell *et al* 2012) was used as a supplementary measure. Due to it still being a relatively new measurement index, few researchers have used it to evaluate their respective predictive models. Therefore, the amount of work that it can be compared to is limited.

"Bias is a measure of the difference between the average value of a distribution (i.e. NIR predictions) and the true value (reference method)" (Bellon-Maurel *et al* 2010 in Mashimbye 2012 *et al*: 5). The closer the number is to zero the less bias the model will be.

6.3 RESULTS

In order to enhance the flow of this chapter, the results achieved during the wet chemical analyses from Chapter 5 are briefly discussed below.

6.3.1 Wet and Wet Chemical Analyses

The data returned after the wet chemical analysis is given in the below Table 6.1. The exchangeable Na^+ values were lower than expected with the values at the Malansdam site being the highest with values between 0.45 – 15.09 (samples: Dag1_1 and M samples). Due to the low values the ESP index for soil dispersion was affected and thus fell below international proposed thresholds. The exchangeable Mg^{2+} were high with values ranging between 0.23 – 8.83. To put this into perspective, the high percentage can be seen as calculated by the MS% with the highest being 60.07% of exchangeable cations being Mg^{2+}.

Table 6.1 Resulting measurements obtained from wet chemical analyses

Soil Sample	EC	pH	Exch Ca^{2+}	Exch K^+	Exch Mg^{2+}	Exch Na^+	ESP	SAR	MS %
Dag1_1A30-45	5	7.1	3.66	1.34	5.17	0.87	8.89	1.05	52.54
Dag1_1B0-15	4	6.6	2.92	0.37	2.92	0.45	6.8	1.45	43.85
Dag1_2B15-30	5	7.5	3.21	0.45	5.88	1.19	11.1	1.72	54.76
K1A0-15	4	7.3	3.33	0.51	7.36	1.73	13.38	1.27	56.91
K1A30-45	5	8.3	1.21	0.58	3.58	0.6	10	0.6	60.07
K1A46-60	7	8.7	0.86	0.49	0.45	0.1	5.48	0.72	23.74
K2A0-15	4	6.7	1.39	0.62	1.39	0.2	5.69	0.81	38.57
K2B15-30	9	6.4	1.39	0.47	2.66	0.33	6.73	1.24	54.83
M1A0-15	3	3.4	4.8	3.27	8.83	15.09	47.15	0.84	27.59
M1B30-45	4	6.5	0.98	0.12	0.61	0.16	8.63	1.23	32.64
M2A45-60	7	6.5	2.43	0.26	0.76	0.54	13.53	0.88	18.99
M3A0-15	3	5.9	1.16	0.22	0.23	0.26	13.79	1.37	12.16

6.3.2 NIR analyses

The 36 diffuses reflectance graphs are indicated in an overlaid manner in Figure 6.3 below. The raw soil spectra are typical of any soil. It is quite monotonous without any dramatic differences occurring between the obtained spectra from the various soil samples. Three distinct absorbance peaks are prominent in the NIR spectra. Two absorbance peaks occur at 7 142cm^{-1} and 5 128cm^{-1} (nanometers equivalent of 1 400 and 1950 respectively) as a result of the bending and stretching of the O-H bands from free water within the soil whilst a third peak occur at 4 545cm-1 (nanometer equivalent of 2 200) due to absorbance of lattice minerals. It is especially this area between 7 142cm^{-1} to 4 545cm^{-1} that is best suited to obtain trends to acquire a “fingerprint” for the various soil properties.

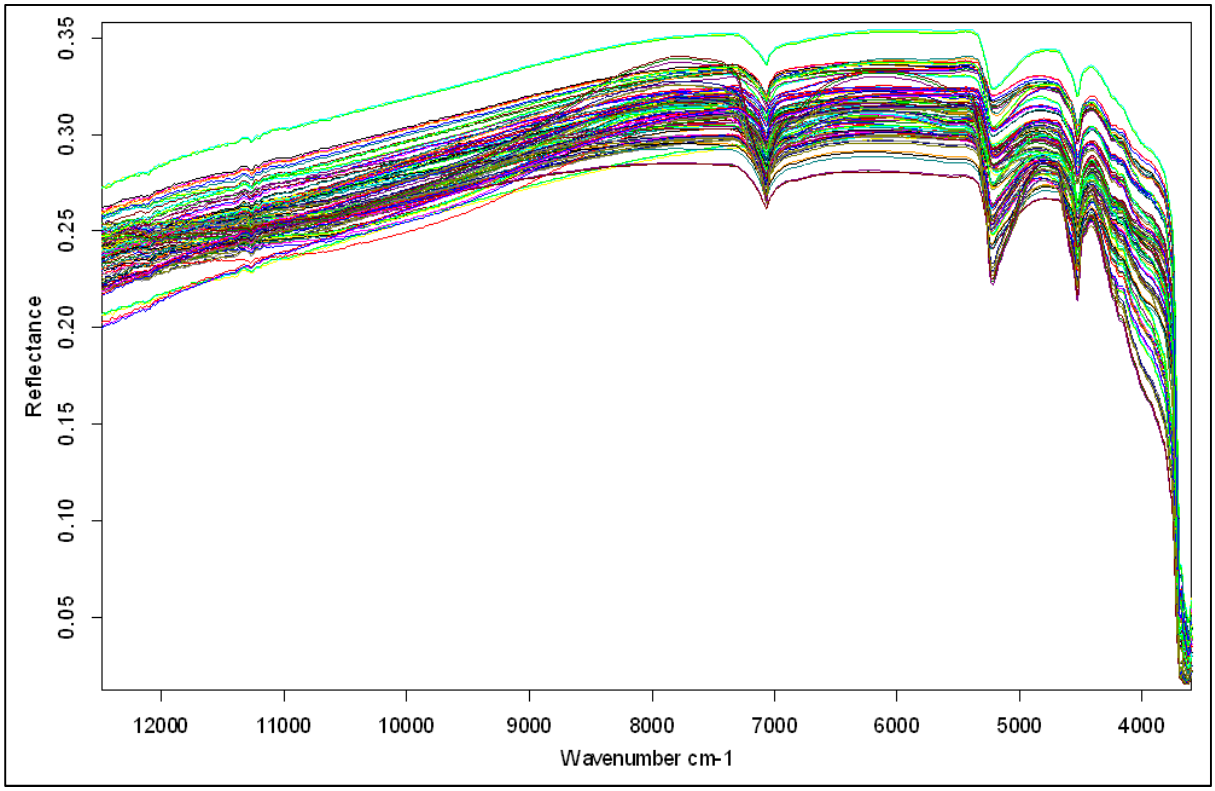

Figure 6.3 Overlaid diffuse reflectance spectra of the 36 soil samples that were scanned

After the raw spectra were obtained it was pre-processed using various mathematical approaches as in the Quant 2 utility in order to provide the best possible calibration model. The mathematical approaches were combined with various regions in the NIR spectral range to further enhance the calibration model. The mathematical approaches as well as the region selection for each soil property are given in Table 6.2. Furthermore, the region selections as well as the pre-processed spectra are given in Appendix C.

Table 6.2 Pre-processing and prediction statistics

Soil Property	Spectral Range (cm^{-1})	Pre-processing Method	r^2	Root Mean Square Error (RMSECV)	Ratio of Performance to Deviation (RPD)	Bias	Ratio of Performance of Quartiles (RPIQ)
Exch Ca^{2+}	6102-544.6; 4605.4-4242.8	First Derivative and Vector Normalisation	0.66	0.648	1.72	0.0683	1.21
Exch K^{+}	5454-4597.7	First Derivative and MSC	0.67	0.171	1.75	-0.014	2.64
Exch Mg^{2+}	7506-6094.3; 5454-4597.7	MSC	0.85	0.871	2.62	0.038	5.06
Exch Na^{+}	7506-6094.3; 5454-4242.8	Min-Max Normalisation	0.79	0.233	2.18	0.0262	2.62
EC	6804-6094.3; 5454-5022	Multiplicative Scattering Correction	0.85	0.674	2.66	-0.171	2.97
ESP	6804-6094.3; 5454-4844.6	Min-Max Normalisation	0.86	1.08	2.69	-0.189	6.09
MS%	5029.7-4597.7	Min-Max Normalisation	0.10	15.9	1.06	-1.4	15.9
pH	12481,7-4242.8	First Derivative and MSC	0.84	0.338	2.51	0.0496	2.66
SAR	7506-4242.8	Constant off-set elimination	0.84	0.149	2.62	0.0377	2.68

The statistics for the cross validation for the models are also given in Table 6.2. These consist of the r^2, RMSECV, RPD, Bias and RPIQ. The performances of all soil properties with regards to r^2 were good, each scoring high values except for the MS% with a value of 0.10. Exchangeable Ca^{2+} and exchangeable K^+ also had high values, but were below the threshold value of 0.80 which is considered as excellent. However, it was far above the value of 0.5 which is considered to be fair with 0.66 and 0.67 respectively. The other soil properties had values above and lingering around the excellent threshold mark with values ranging from 0.79 for exchangeable Na^+ and 0.86 for ESP. In terms of RMSECV all values were below the threshold value of 1 except for the MS% and ESP properties. The RMSECV value for the MS% was 15.9 whilst ESP was only marginally above the threshold value of 1 with a value of 1.08. The RMSECV value for ESP can thus still be considered as acceptable. The values for the other properties ranged from 0.149 for SAR as the best performance to 0.871 for exchangeable Mg^{2+}. The RPD values were used in conjunction with RPIQ as a supplementary value. Only the MS% fell below the 1.4 threshold value which is indicative of a non-reliable model. The RPIQ value for this was calculated as 15.9, which is the highest. A higher RPIQ number indicates a good model, but in this case it only serves as an indication of the variability in the data (values from 0.23 to 8.83) and not a model of good fit. The model for exchangeable Ca^{2+} and K^+ was fair with values of 1.72 and 1.75 respectively. Their RPIQ values for both were also close to the RPD values at 1.21 for Ca^{+2} and 2.64 for K^+ indicating a fair model performance. All the other soil properties had good statistics with regards to model accuracy with ESP performing the best with a RPD value of 2.69 (RPIQ value was 6.09) ranging down to a RPD value of 2.18 (RPIQ value of 2.62) for exchangeable Na^+ in the excellent model category. The RPIQ values closely resembled the RPD values, thus lending support to the model fit predicted by RPD. The values for Bias for all the soil properties were extremely low with values ranging from exchangeable K^+ performing the best with a value of -0.014 and ranging up to -0.189 for ESP. The only exception is the MS% value which is -1.4. The low values obtained for Bias is indicative of the closeness of the average NIR predicted values and the real values as well as a good distribution of prediction errors being below and above the mean. The composite sampling method that was used may be the reason for this result.

Scatter plots for the predicted versus real values are given in Figure 6.4. Outlier values were detected by OPUS 6.5 for exchangeable Mg^{2+} (Figure 6.3c) and Na^+ (Figure 6.3e) as well as pH (Figure 6.3f) and SAR (Figure 6.3g). The outliers are indicated in red. None of these outliers were removed as there was no scientific evidence to support this action. None had a detrimental effect on the model accuracy, although the model statistics for exchangeable Na^+ did decrease significantly upon removal of the outlier sample. Due to this, it was investigated.

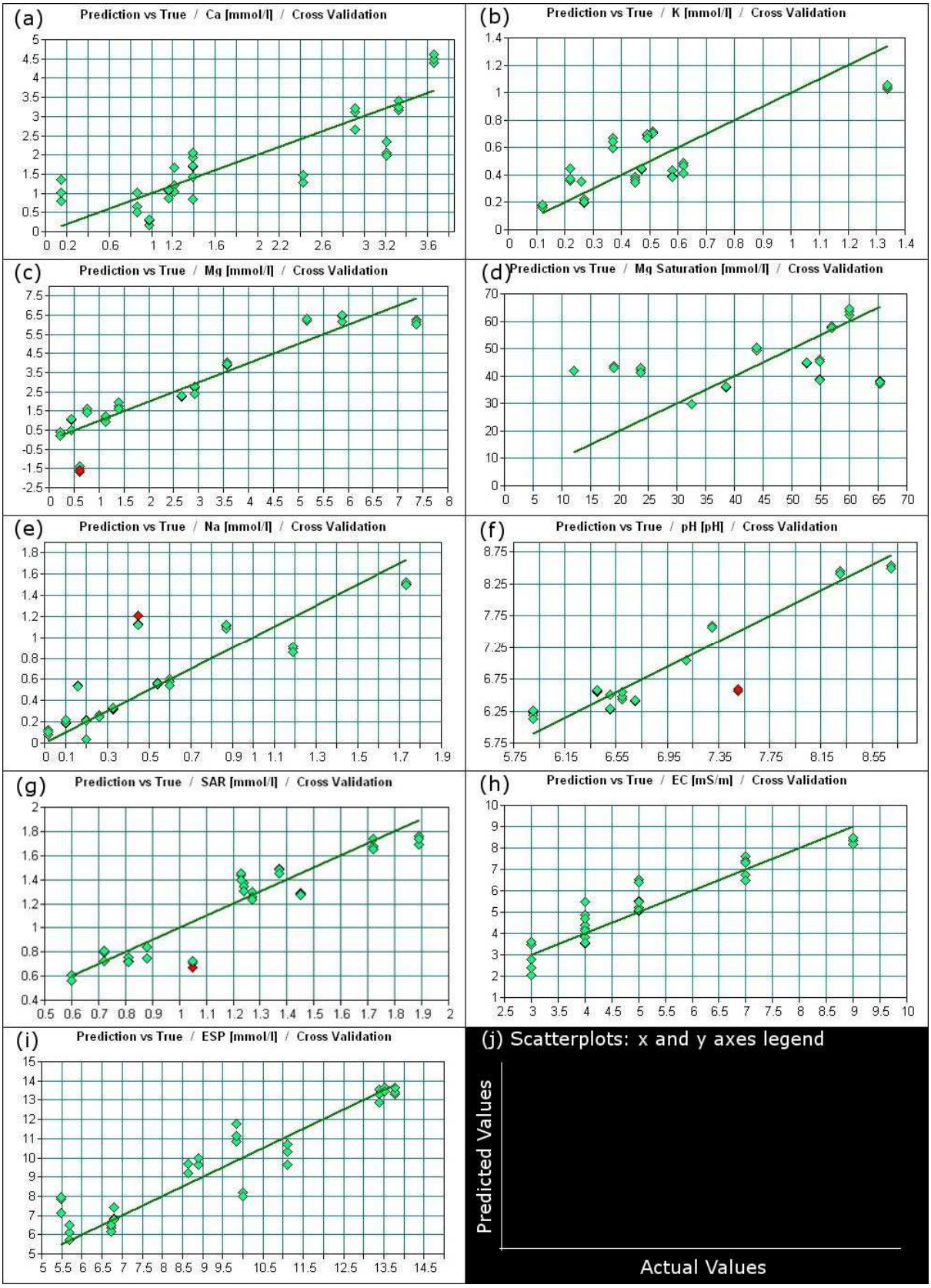

Figure 6.4 Correlation graphs of predicted vs actual values for each of the five chemical soil properties and three dispersion indices

Upon the investigation it was found that the outlier value (sample name: Dag1_1A0-15; second sample name from the left) was not an extreme value as indicated by the diamond shaped symbol in Figure 6.5. Broadening the investigation it was found that the actual measured amount of exchangeable Na^+ was 0.45 whilst the predicted value of NIR was 1.2 as indicated by the squared shaped symbol in Figure 6.5. The reason may be that the total amount of sodium was detected and thus predicted, as NIR would not be able to distinguish between the total amount of Na and the Na^+ on the exchange sites. Even due to this potential "pit-fall" this particular model was still successful and performed fair.

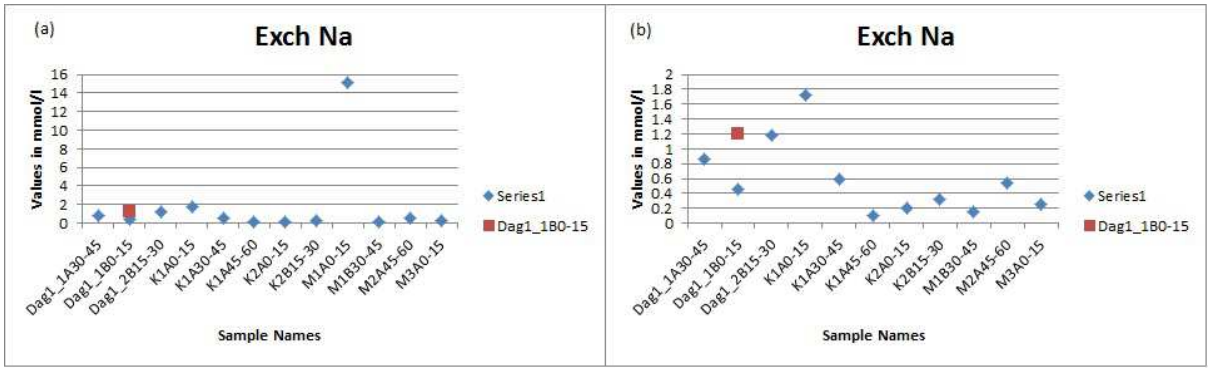

Figure 6.5 Outlier sample for predicted for exchangeable Na^+: a) I*ndicates all the samples; b) indicates the samples without the extreme M1A0-15 sample in order to improve the NIR predicted (square) versus actual (diamond) value for sample "dag1_1B0-15"*

Furthermore, the scatter plots in Figure 6.3 indicate that the values obtained for all soil properties are not a normal distribution. It is a skewed lognormal distribution with a few sample values lying at the bottom section, some at the top section and the majority in the middle section of the mean. The skewed distribution is characteristic of soil, but could also be due to the small amount of samples used in the analysis. If more samples were taken into considerations these "gaps" could possibly be filled resulting in a normal distribution and thus better models. Due to the skewed distribution the newly identified RPIQ index, thus served as a good supplement to RPD in order to see whether the distribution caused an inflation of the RPD value.

6.4 DISCUSSION

Gully erosion research has traditionally overlooked detailed investigation into soil as a factor driving it, due to soil analyses being complex and time consuming whilst also producing hazardous waste. The high accuracy of the NIR diffuse reflectance models indicates that it is a viable option to use when conducting soil analyses. Furthermore it is rapid and easy to use. Investigating whether a soil's intrinsic properties have an impact on gullying no longer has to be overlooked, as this technology can easily be applied. Additionally, the option exists of linking the NIR diffuse reflectance models with

remote sensing sensors that capture the NIR region. This would generate detailed soil data regarding its intrinsic characteristics such as its dispersive nature that would be available from a desktop removing expensive field work activities.

6.4.1 NIR analyses

The statistics for all the soil property predictive PLSR models, except for the MS% was excellent. Considering that few samples were analysed in developing these models and also that these samples were taken at random active gully heads transcending agricultural field units without having any control over the chemistry of the soil involved, the potential for predicting these properties investigated have been found promising.

The models performed well for all four exchangeable cations namely Ca^{2+}, Mg^{2+}, K^{+} and Na^{+}. Success with regards to the prediction for these exchangeable cations in previously conducted studies has been reported as variable.

Exchangeable Ca^{2+} and Mg^{2+} are usually reported as effective with successful predictions. The r^2 and RPD values obtained for exchangeable Ca^{2+} were 0.66 and 1.72 respectively, which would indicate an adequate model since the RMSECV error is small (0.648) and the bias value is negligible (0.0683). The r^2 and RPD prediction statistics are significantly lower than values reported which are mostly in the upper value range such as Malley *et al* (2000) with r^2 of 0.88 and RPD of 3.0 and Zornoza *et al* (2008) with r^2 of 0.94 and RPD of 2.46 both using the 1*M* CH_3COONH_4 buffered at pH7 method. Dunn *et al* (2002) who used the same method distinguished between surface and sub-surface soil establishing a prediction model for both. The r^2 value for surface samples was 0.86 and RPD was reported as 2.7 while the sub-surface samples performed poorer with an r^2 of 0.68 and RPD of 1.9. This may be a reason why exchangeable Ca^{2+} presented a less accurate prediction capability during this work, as both surface and sub-surface samples were intermixed. This is confirmed by Chang *et al* (2001) whom attained a similarly low r^2 value of 0.75 and RPD of 1.94 after constructing a predictive model without making a distinction between surface and sub-surface soil.

The r^2 and RPD values attained for exchangeable Mg^{2+} are excellent with 0.85 and 2.62. The prediction statistics for this is characterised as “excellent”, especially with a small RMSECV (0.871) and negligible bias (0.038). The r^2 and RPD values are comparable with other reported values which indicate that the prediction thereof is highly successful. Other reported r^2 and RPD values which made use of the 1*M* CH_3COONH_4 buffered at pH7 method are Malley *et al* (2000) with 0.79 and 2.25 as well as Zornoza *et al* (2008) with 0.91 and 2.20 respectively, whilst Dunn *et al* (2002) reported an r^2 value of 0.85 for surface samples and 0.74 for sub-surface samples. The excellent prediction of exchangeable Mg^{2+} may be due to its correlation with CEC.

Prediction results obtained for K^+ usually deliver results in the bottom spectrum of the reliable model range with statistics for r^2 around 0.5 and RPD in the region of 1.4. The models consequently border poor and are not always reliable. Predictive statistics returned for validation were r^2 of 0.67 and a RPD of 1.75 which indicate a reliable prediction result, especially when taken into account the small RMSECV and bias statistics of 0.171 and -0.014 respectively. Dunn *et al* (2002) reported similar results with an r^2 of 0.61 and RPD of 1.6 for top soil and r^2 of 0.72 and RPD of 1.4 when using the 1*M* CH_3COONH_4 buffered at pH7 method. Similar high results were obtained in another study with eastern and southern African soils by Shepherd and Walsh (2002) with an r^2 of 0.66, RMSCV of 0.25 and a bias of -0.03 (RPD not reported) by making use of a 1*M* Potassium Chloride (KCl) extraction. Other statistics reported, also border on poor such as Chang *et al* (2001) and Malley & Yesmin (2002) with both reporting r^2 of 0.55 and RPD of 1.44 and 1.5 respectively. Chang *et al* (2001) used a CH_3COONH_4 extraction measure by Perkin-Elmer AA-500 method whereas Malley & Yesmin (2002) used the 1*M* CH_3COONH_4 buffered at pH7 method. The higher statistics in this study might have to do with RSA soils traditionally having fewer exchangeable K^+ and coupling this with the method used for this study obtains respectable results.

Results reported for exchangeable Na^2 are diverse. The majority of published work has conveyed unsuccessful predictive models such as Zornoza *et al* (2008) with 0.13 and 1.08 and Malley and Yesmin (2002) with r^2 of 0.15 and RPD of 1.9 both using the 1*M* CH_3COONH_4 buffered at pH7 method. Authors using different methods have reported similar dire results such as Chang *et al* (2001) with an r^2 of 0.09 and a RPD of 0.92 (CH_3COONH_4 extraction measure by Perkin-Elmer AA-500) and Islam *et al* (2003) with r^2 of 0.34 and RPD of 1.2 (0.01*M* silver-thiourea method). Other reported results have ranged from reliable models such as Dunn *et al* (2002) who used the 1*M* CH_3COONH_4 buffered at pH7 method with an r^2 of 0.64 and RPD of 1.7 for surface samples to excellent models in the same study for sub-surface samples with r^2 of 0.82 and RPD of 2.3. The statistical values found in this study were r^2 of 0.79 coupled with a RPD value of 2.62 constituting an excellent model with a low RMSECV (0.233) and bias (0.0262). The reason for the much higher performance in this study might be due to the fact that NIR cannot distinguish between total Na and exchangeable Na^+. Only one sample was affected by this measurement error in this model, whilst it could have been more pronounce in other work affecting more samples.

The prediction model for EC produced an excellent model with r^2 of 0.85 and a RPD of 2.69 coupled with a RMSECV value of 0.674 and bias of -0.171. These statistics are better than reported statistics for EC which generally is unsatisfactory. In order to establish a comparison, other statistics attained from other authors that used a water:soil slurry are Dunn *et al* (2002) with an r^2 of 0.37 and 0.63 in surface soil and subsurface soil respectively and RPD values of 1.2 and 1.6 for the respected soils and Zornoza *et al* (2008) with r^2 of 0.57 and RPD of 1.73. Zornoza *et al* (2008) put this poor prediction performance down to EC not being correlated to CEC or SOM which is spectrally active, however

there might be a good correlation within the absorbance peaks occurring at 7 142cm^{-1} and 5 128cm^{-1} (nanometers equivalent of 1 400 and 1950 respectively) caused by the O-H bands from free water within the soil. The regions where these peaks occurred were used in order to establish the good prediction data for this model and would therefore serve as evidence of this.

The pH predictive model yielded successful results with r^2 of 83.78, RPD of 2.51 and low values for RMSECV of 0.338 and bias of 0.0496. This is in accordance with other results reported who have also produced successful models with similar statistics for pH such as Reeves *et al* (1999), Chang & Laird (2002), Cozzolino and Morón (2002), Shepherd & Walsh (2002), He *et al* (2007) and Islam *et al* (2003).

ESP, SAR and MS% are derived from the exchangeable cations of a soil. While ESP has received some research attention, though uncommon, the other two indices have not. Dunn *et al* (2002) reported r^2 values of 0.68 and 0.80 for topsoil and sub-soil respectively while achieving a RPD of 1.8 and 2.2 for the two soils respectively. These values are slightly lower than the attained results of r^2 of 0.86 and RPD of 2.69. These statistics are indicative of an excellent model and is coupled with a low bias of -0.189 and marginally large RMESECV of 1.06. The good results are thought to be a result of the good prediction results obtained from the exchangeable cations. For the same reason SAR produced excellent statistics of 0.84 for r^2 and 2.62 for RPD and has a noteworthy low RMSECV and bias values of 0.149 and 0.0377 respectively making this the best model produced. The MS% model was expected to produce equivalent statistics, but unfortunately produced the poorest model with the following statistics: r^2 of 9.8, RPD of 1.06, RMSECV of 15.9 and bias of -1.4. As ESP and SAR both yielded successful models; the mathematical equation used in order to calculate these indices could not have removed it too far from the original chemistry of the soil; hence, the problem with the MS% percentage lies elsewhere. The problem may be that the sample set was not distributed enough with regard to the MS%. Only three samples had small values beneath 25% and when the true versus predicted values are compared these were grossly overestimated. If a larger and more distributed sample set is used, NIR might be able to predict it more successfully.

6.4.2 Remote sensing linkage possibilities

The possibility exists that the trends that were identified to serve as fingerprints during lab spectrometry could be transformed and linked to remote sensing. If proved successful, this will result in a large amount of quality information being generated as the predictive models developed in the NIR region could be applied to remote sensing sensors covering the same region. This information could be utilised to determine areas prone to gully development with the addition of being inexpensive and time efficient.

The Bruker multi-purpose FT-NIR Analyser (MPA; Bruker Optik GmbH, Germany) operates in a spectral range of 12 500cm^{-1} to 4000cm^{-1} (Wavelentgh equivalent: 700 – 2500nm). Figure 6.5

presents each soil property that was subject to NIR diffuse reflectance spectroscopy. The white areas indicate the spectral selection within the NIR region used by OPUS 6.5 (MPA; Bruker Optik GmbH, Germany) to identify trends for predictive purposes for each soil property and index. These were the areas within the NIR region which was used to successfully build the predictive PLSR models. In order for the remote sensing sensor to be of value and possibly aid in predicting values of these properties from reflected spectra it has to consist of a spectral resolution that includes the white areas for each soil property as identified in Figure 6.5.

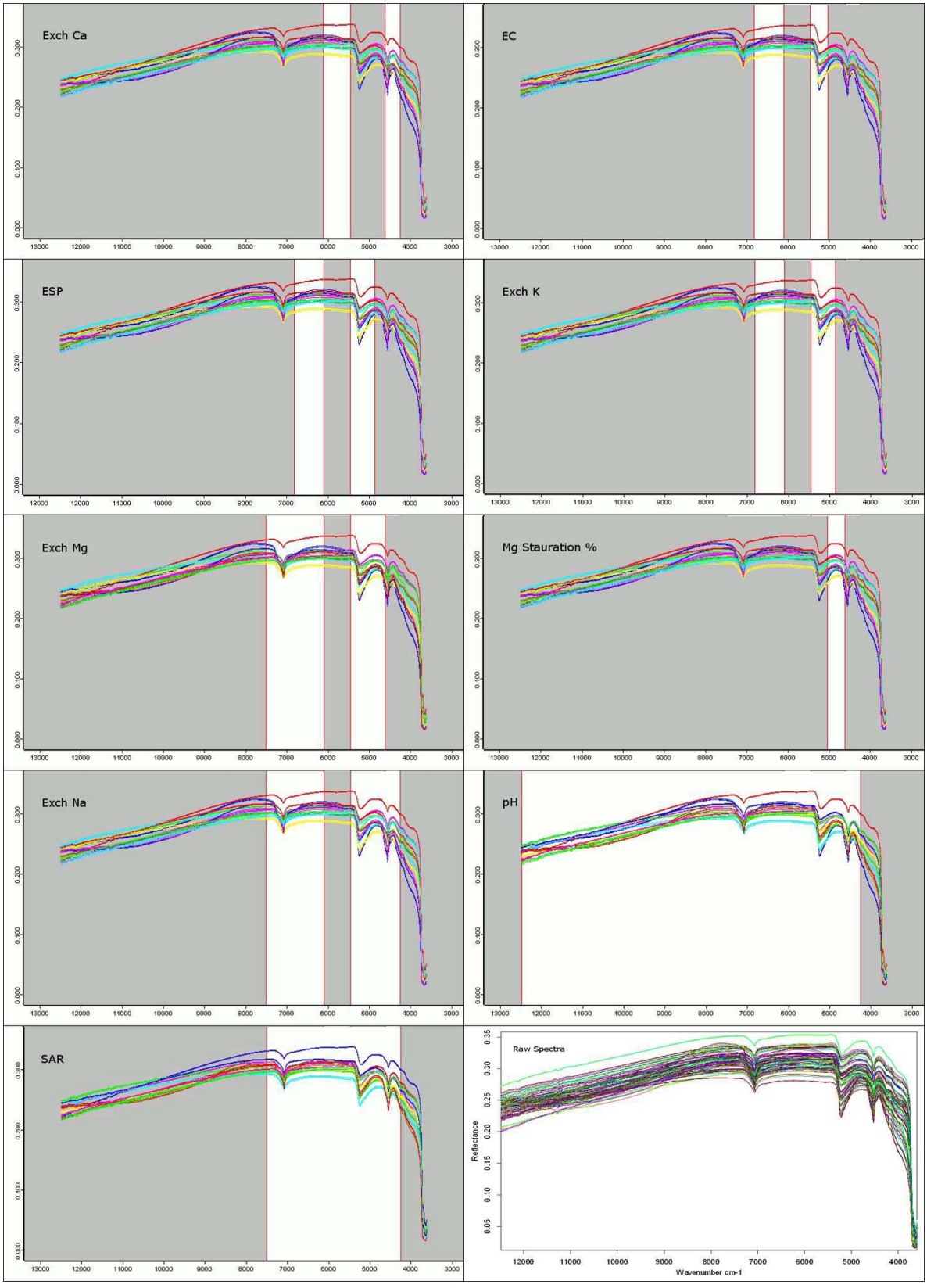

Figure 6.6 Region selection for trend analyses for each of the five chemical soil properties and three dispersion indices that could be used to assess soil dispersion

The Forestry Department at Stellenbosch University has an airborne hyperspectral sensor with a ground resolution of 1m that could be used for this purpose. It is the only one of its kind in RSA. It has 60 spectral bands, and a spectral range of 25 000cm^{-1} – 10 000cm^{-1}. Unfortunately this spectral range would render it ineffective to be used in conjunction with the models produced in this section, except for a small possibility of predicting pH (see Figure 6.5). The National Geo-spatial Information Department (NGI) in RSA which forms part of the Department of Rural Development and Land Reform (DRDLR) also has an airborne sensor consisting of 1 band with a range of 14 814cm^{-1} – 11 764cm^{-1}. It has a ground resolution of 15cm which would make this ideal for investigating the soil properties for gully development, however the spectral resolution will also only allow the possibility of predicting pH and no other soil properties or indices investigated.

Therefore, the search will have to extend to satellite remote sensing. An extensive list of the most popular multispectral remote sensing sensors utilised in RSA are given in Table 6.3 below.

Table 6.3 Satellite Remote Sensing sensors utilised in RSA*

CBERS 2: HRCCD						**CBERS 2: HRCCD**				**CBERS 2: WFI**		**ALOS: AVNIR**			
	Band 1	*Band 2*	*Band 3*	*Band 4*	*PAN*	*Band 1*	*Band 2*	*Band 3*	*PAN*	*Band 1*	*Band 2*	*Band 1*	*Band 2*	*Band 3*	*Band 4*
Spectral Resolution	22 222-19 230	19 230-16 950	15 873-14 492	12 987-11 235	19 607-13 698	6 451-5 715	4 807-4 255	10 405-12 500	20 000-9 090	15 873-14 492	12 987-11 235	23 810-20 000	19 230-16 666	16 393-14 492	13 158-11 235
Spatial Resolution	20m	20m	20m	20m	20m	150m	150m	300m	150m	260m	260m	10m	10m	10m	10m

Landsat 7 ETM+								**SPOT 5: HRV-IR**				**ALOS: PRISM**
	Band 1	*Band 2*	*Band 3*	*Band 4*	*Band 5*	*Band 6*	*Band 7*	*PAN*	*Band 1*	*Band 2*	*Band 3*	*Band 4*	*PAN*	*PAN*
Spectral Resolution	22 222-19 230	19 230-16 666	15 873-14 492	12 987-11 111	6 451-5 714	962-800	4 785-4 255	19 230-11 111	20 000-16 950	16 394-14 705	12 820-11 135	6 330-5 715	19 607-13 698	19 230-12 987
Spatial Resolution	30m	30m	30m	30m	30m	30m	60m	15m	10m	10m	10m	20m	5m	2.5m

ASTER														
	Band 1	*Band 2*	*Band 3*	*Band 4*	*Band 5*	*Band 6*	*Band 7*	*Band 8*	*Band 9*	*Band 10*	*Band 11*	*Band 12*	*Band 13*	*Band 14*	*Band 15*
Spectral Resolution	19 230-16 666	15 873-14 492	13 157-11 628	13 157-11 628	6 250-5 882	4 662-4 576	4 576-4 495	4 475-4 376	4 358-4 228	4 237-4 115	1 230-1 180	1 180-1 134	1 120-1 078	975-914	914-858
Spatial Resolution	15m	15m	15m	15m (Backward)	30m	30m	30m	30m	30m	30m	90m	90m	90m	90m	90m

FORMOSAT 2						**IKONOS-2**					**Quickbird**				
	Band 1	*Band 2*	*Band 3*	*Band 4*	*PAN*	*Band 1*	*Band 2*	*Band 3*	*Band 4*	*PAN*	*Band 1*	*Band 2*	*Band 3*	*Band 4*	*PAN*
Spectral Resolution	22 222-19 230	19 230-16 666	15 873-14 492	13 158-11 111	22 222-11 111	21978-19 230	19 608-16 666	15 873-14 285	13 158-11 765	13 158-11 765	22 222-19 230	19 230-16 666	15 873-14 492	13 158-11 111	22 222-11 111
Spatial Resolution	8m	8m	8m	8m	2m	4m	4m	4m	4m	1m	2.4m	2.4m	2.4m	2.4m	0.61m

WorldView-2									**GeoEye-1**				
	Band 1	*Band 2*	*Band 3*	*Band 4*	*Band 5*	*Band 6*	*Band 7*	*Band 8*	*PAN*	*Band 1*	*Band 2*	*Band 3*	*Band 4*	*PAN*
Spectral Resolution	25 000-22 222	22 222-19 607	19 607-17 242	17 095-16 000	15 873-14 492	14 185-13 422	12 987-11 174	11 628-11 111	22 222-12 500	22 222-19 608	19 608-17 242	15 268-14 492	12 820-10 870	22 222-12 500
Spatial Resolution	1.84m	1.84m	1.84m	1.84m	1.84m	1.84m	1.84m	1.84m	0.46m	1.65m	1.65m	1.65m	1.65m	0.41m
EO-1 satellite: ALI										**PLEIADES-1A or B**				
	Band 1'	*Band 1*	*Band 2*	*Band 3*	*Band 4*	*Band 5*	*Band 6*	*Band 7*	*PAN*	*Band 1*	*Band 2*	*Band 3*	*Band 4*	*PAN*
Spectral Resolution	23 095-22 075	22 222-19 418	19 048-16 528	15 873-14 492	12 904-12 422	8 333-7 692	6 452-5 714	4 808-4 255	20 833-14 492	23 255-18 181	20 408-16 394	16 666-13 888	13 333-10 526	20 834-12 048
Spatial Resolution	30m	30m	30m	30m	30m	30m	30m	30m	10m	2m	2m	2m	2m	0.5m

* Spectral resolution in units of cm^{-1}

All these sensors cover the NIR region (fully or partly) and would thus be suitable candidates to link up with the PLSR models created. Conversely, not all these sensors which cover the NIR region would be suitable for investigating the soil properties relating to gully erosion as the spatial resolution becomes a pivotal element. A high spatial resolution becomes crucial in order to explore gully erosion due to its size variation. Whilst sensors such as Landsat 7 ETM+, SPOT 5, ASTER and ALI contain the whole NIR region, their low spatial resolution will not allow for gully erosion specific research. It could be used to identify trends surrounding an area; a higher spatial resolution would be desirable for gully specific studies. Two options would be available: either use these data sources as it is freely available or use a spectral preserve image fusion technique, in order to improve the resolution of the image without corrupting the integrity of the spectral scale or search for higher spatial resolution sensors. Satellite sensors that capture images with a higher spatial resolution include the GeoEye-1 and PLEISADES-1A/ B. Unfortunately the same problem occurs as with the airborne sensors. It will only be useful in trying to predict pH due to the small area that it covers in the NIR region. The Quickbird and IKONOS sensors would not fare any better as they have the same constraint as the GeoEye-1 and PLEISADES-1A/ B sensors.

The multispectral satellite sensors, although including the NIR region, have broad bands. It might be a difficult exercise to compare the narrow range of spectra obtained from the Bruker multi-purpose FT-NIR Analyser (MPA; Bruker Optik GmbH, Germany) with the broad bands of the multispectral satellites. Therefore, hyperspectral satellites could provide a solution. However, in remote sensing sensors there is a resolution trade-off, because of technical constraints. Hence, satellites with a high spectral resolution are associated with a low spatial resolution and *vice versa* (Satellite Imaging Corporation 2012). The Hyperion sensor on board the EO-1 satellite has a spectral range of 25 000cm^{-1} – 4 000cm^{-1}, with 242 spectral bands which approximates to 10nm per band. This sensor has had positive results with regards to comparing in-situ field measurements with those obtained from the sensor (Gomez *et al* 2008), unfortunately the spatial resolution of 30m might indicate it to be ill suited for gully erosion studies. Similar to the multispectral sensors identified above namely Landsat 7 ETM+, SPOT 5, ASTER and ALI.

Therefore, the multispectral sensors, Landsat 7 ETM+, SPOT 5, ASTER and ALI sensors, as well as the hyperspectral Hyperion sensor should be further explored. Currently, these sensors are best equipped for this application. However, techniques will have to be sought to fuse it with better resolution imagery without altering the integrity of its spectral resolution. Furthermore, it will also need to be determined whether the hyperspectral (narrow bands in the NIR region) or multispectral sensors (broad bands in the NIR region except for ASTER imagery) would work best to link the PLSR models built with the OPUS 6.5 (MPA; Bruker Optik GmbH, Germany) software.

6.5 CONCLUSION

NIR diffuse reflectance prediction potential for five chemical soil properties and three dispersion indices, which are indicative of erosion potential, were investigated. The chemical properties scrutinised, were the basic exchangeable alkaline cations Ca^{2+}, Mg^{2+}, K^{+} and Na^{+}, as well as EC. The three indices measured were ESP, SAR and MS%. Soil sampling occurred in trans-boundary agricultural sites at randomly selected active gully heads. The collected soil samples were minimally pre-processed for NIR diffuse reflectance spectroscopy (only dried, crushed and sieved). The statistics achieved from the PLSR models indicated accurate predictive models for all the above except for the MS% index, that would require further investigation. The results for the other properties and indices were comparable with previous reported statistics and in most cases better. This could be a result of the composite sampling manner followed before subjecting the soil samples to NIR diffuse reflectance spectroscopy. This particular study was limited to a very small amount of samples used, but with the addition of the random sampling at active gully heads, consequently not having any control over the chemistry of the soil, the statistics for the models look encouraging. It would suggest that there is potential to successfully predict all of the above, with the exclusion of the MS%. This would result in fast, reliable and inexpensive analysis of soils and gathering relevant information of a soil's dispersive nature, thus implying whether or not it contributes to gully erosion at a significant level or only minimally.

The possibility also exists that the NIR PLSR predictive models developed for the soil properties and indices can be transposed for use by remote sensing satellite sensors covering the same NIR area. In order for it to be utilised in gully erosion research, the spatial resolution is pivotal. Popular sensors in RSA that covers the NIR area in which the NIR PLSR models were constructed do not currently have sufficient spatial resolution. In order to couple it with remote sensing sensors, it would thus be imperative to research algorithms that can merge the imagery from these sensors with images containing a better spatial resolution in an effort to enhance the spatial resolution, whilst simultaneously keeping the spectral resolution intact.

If the coupling of these two technologies can be successful that is NIR PLSR predictive models employed in conjunction with remote sensing imagery it will greatly improve the precision and surface area that could be covered by researchers in gully erosion studies. This will indicate the movement in Figure 6.1 (dark red arrow to the top right box) to the ideal analysis situation which will lead to large datasets with a high degree of precision that will not only be useful for researchers but also be of great value to land managers.

7 CONCLUDING REMARKS

7.1 MSC REFLECTION

This study involved an investigation on gully erosion within the Sandspruit catchment. Although soil sampling was conducted at various sites, the study was focussed on the split continuous gully system at Malansdam. This gully system was scrutinised remotely via desktop study, physically in the field as well as chemically in the laboratory via traditional wet chemical soil analyses. This was done in an effort to establish the control factors driving gully erosion in the area.

The desktop study had a unique outlook on how the farming methods employed at Malansdam not only influenced the landscape hydrology, but also gully geomorphology. It found that, instead of preventing gully erosion, it spurred it on due to the ploughed contours channelling water into exit points in the gully system higher up in the catchment, where a steep slope occurs. This resulted in an increase of water erosion potential, as it increased the volume as well as the velocity of water flowing higher up in the gully channel. Confirmation of this deduction was the dense dendritic channels that formed behind the ploughed contour where it ends on the crop and natural vegetation boundary. This finding suggested land use as having an impact on gully erosion in the area.

In order to find support for this, a physical gully classification procedure was conducted. This consisted of creating order in the seemingly chaotic gully design by employing the SSO method coupled with the Pierson *et al* (2008) technique. This led to the establishment of a test site where sediment traps were installed to examine sediment movement in the gully. The captured sediment was analysed and linked to stream velocity with the Sunborg diagram (1956). Large flow velocities were deducted from the Sundborg diagram (1956). This supported the desktop study as it required a continuous water source upon rainfall to reach those velocities. This together with the gully channel activity by way of sediment yield implicated the ploughed contours as channels directing water towards the gully system. Land use was again identified as a driving factor behind gully formation in the Malansdam area.

During the physical characterisation process observations related to gully sizes, gully formation systems in action at Malansdam and sidewall processes were made. Both gully formation processes were identified. The piping formation system is related to soil structure; either being indicative of a duplex soil or being the resulting effect of soil chemistry that leads to dispersion in the presence of water. Although land use was already determined as driving gully erosion this avenue was also followed as gully erosion is a systemic threshold phenomenon thus potentially having numerous control factors causing gully erosion at any given time.

During the soil chemistry investigation five soil properties namely the exchangeable Ca^{2+}, Mg^{2+}, K^{+} and Na^{+} as well as EC were explored together with indices linked to soil dispersion and gully erosion

namely ESP, SAR and MS%. The traditional wet chemical analysis procedure was followed in determining the values for each. Low values were recorded for Na^+, EC, ESP, and SAR which meant that the soil was not sodic and Na^+ was not the reason for causing particle deflocculation. However, very high values were obtained for exchangeable Mg^{2+} which resulted in a high MS% index. High amounts of exchangeable Mg^{2+} cause soil to disperse in the presence of water even if there is a low amount of exchangeable Na^+ present as it exacerbates the effect. It was thus deemed that soil was also driving gully erosion in the Malansdam area.

As a result, the split channel discontinuous gully channel at Malansdam was still active and the control factors were a duo between an anthropogenic factor, land use, and a physical factor, soil. This proves why gully erosion investigations should look at both anthropogenic and physical groups as it is a systemic threshold phenomenon with a wide range of possible control factors.

Upon reaching this result, the project took a twist which was categorised as Phase 2. With the project being subject to tight budgetary and time constraints, the amount of soil samples that were sent for traditional wet chemical analysis was severely limited. This led to the seeking of alternative techniques, preferably an inexpensive method that yielded rapid results. It needed to be able to determine the values of the five soil properties and three indices identified as being indicative of a soil's dispersion potential and scrutinised during the soil chemistry investigation (Soil properties: exchangeable Ca^{2+}, Mg^{2+}, K^+ and Na^+ and EC; Indices: ESP, SAR and MS%.). NIR diffuse reflectance spectroscopy showed promise and was investigated to determine whether it could predict the soil properties and indices. The spectra were captured by an FT-NIR Analyser (MPA; Bruker Optik GmbH, Germany) and the OPUS 6.5 (MPA; Bruker Optik GmbH, Germany) windows based software package was used build and validate the PLSR predictive models. The predictive capability of these NIR PLSR models was good for all the soil properties. With regards to the dispersion indices the PLSR models performed well in predicting ESP and SAR, but the MS% returned poor results. MS% would require further investigation. These PLSR models performed well even though samples were only treated minimally (dried, crushed and sieved), the samples were randomly selected at active gully heads from various agricultural field units (not having any measure of control over soil chemistry) and surface and sub-surface samples were intermixed. This indicates that utilising NIR diffuse reflectance spectroscopy in the prediction of soil properties and dispersion indices has the potential of substituting traditional wet chemical analysis or at least serve as a supportive measure. Furthermore, this technology is very attractive as a singular scan in the laboratory could be used to immediately deduct reliable information regarding a soil's dispersive nature indicating whether a soil is a possible driving factor contributing to gully erosion. Furthermore, the probability of combining NIR PLSR predictive models obtained in laboratory and remote sensing sensors that capture the NIR region exists.

7.2 POSSIBLE COMBAT METHODS

In order to cure or stabilise gully formation in the Malansdam area the control factors from both the anthropogenic and physical group requires to be addressed. Firstly, in terms of the anthropogenic group, land use was deemed a driving factor. Alternative cultivation methods to ploughing contours should be looked into. Secondly, with regards to the physical group, improving the soil's structure needs to be examined. Ways should be sought to lessen the amount of exchangeable Mg^{2+} on the exchange sites on the clay fraction, which causes the soil to disperse.

From observation and retrieved sediment data, grass seems to inhibit gully erosion. Grass, as well as wheat, started growing in the gully channels as winter wore on and had an impact on sediment production. It severely decreased it even though rainfall events remained similar to earlier in the winter. Planting and growing grass in the gully channel, or at least at the gully head, might be a good tactic to inhibit gully erosion.

7.3 RESEARCH PROJECT SHORTCOMINGS

The shortcomings of this project have been divided according to the two phases and are written in point form.

7.3.1 Phase 1

- More physical measurements could have been taken e.g. a flow meter could have been installed in the gully channels thus giving more insight into gully dynamics.
- The test site where physical measurements were obtained from was small in comparison to the whole Malansdam gully system. The Southern leg could have undergone the same investigation where upon a comparison could have been conducted between the data of each leg.
- The Sundborg diagram based on grain sizes and flow velocity to determine the erosive nature of water flow was used instead of the more popular threshold method that includes the Shields diagram and many other power function equations. The reasoning behind this is that a methodology to calculate or determine this information for gullies specifically does not exist. All the equations have been developed for rivers. The Sunborg diagram at least had various water heights and therefore thought to be more accurate.
- Only one 3D scan was taken. The potential for its use in gully erosion research looks to be significant but there was not enough time nor enough finances left to do a second scan to use as a layover over the first image.

7.3.2 Phase 2

- Too few soil samples were subject to wet chemical analysis. As a result too few samples were available to analyse with NIR radiation to establish a PLSR prediction model. With the amount of samples accessible only the potential of NIR prediction could be investigated.
- The soil sampling was limited to intervals of 0 – 15, 15 – 30, 30 – 45 and 45 – 60cm. The classical gully system at Malansdam extends much deeper than this.

7.4 RECOMMENDATIONS FOR FUTURE RESEARCH PROJECTS

Recommendations for further study has been given below also in point form:

- Developing a power equation or other means to determine the erosion threshold within a gully system.
- The gully within a gully phenomenon should be investigated as this project found it to have an impact on sediment production. How do these smaller local gully systems affect the larger global gully system especially in sense of sediment production, transport and deposition?
- Ploughed contour cultivation system employed in the Sandspruit catchment was shown to impact the landscape hydrology dramatically causing water to have a higher erosive force as it enters gullies higher up in the landscape where steeper slopes are experienced. This could be mapped over the whole catchment and thereafter the effect could be modelled.
- Sediment fingerprinting should also be looked into. Where does the majority of sediment within an established classical gully system come from?
- Using a 3D scanning equipment to assess sediment loss due to gully erosion over a medium length time period.
- Investigate whether the NIR PLSR predictive models (spectra was capture using the FT-NIR Analyser [MPA; Bruker Optik GmbH, Germany]) developed by the OPUS 6.5 (MPA; Bruker Optik GmbH, Germany) windows based software package can be linked with remote sensing satellites sensors that occupy the same areas in the NIR region.

REFERRENCES

Acocks JPH 1953. Veld types of RSA. *Memoirs of the Botanical Survey of RSA.* 28: 1-192.

Alander J 2011. NIR Spectroscopy notes [online]. Finland: University of Vaasa. Available: http://lipas.uwasa.fi/~TAU/AUTO3220/Umea2handouts.pdf [24 September 2012].

Anderson C, Drennen JK & Ciurczak EW 2008. Pharmaceutical Applications of Near-Infrared Spectroscopy. In Burns DA & Ciurczak EW (eds) *Handbook of Near Infrared analysis. 3rd edition, 585-606.* Florida: CRC Press.

Armstrong JL & Mackenzie D H 2002. Sediment yields and turbidity records from small upland subcatchments in the Warragamba Dam catchment, southern New South Wales. *Australian Journal of Soil Research* 40: 557-579.

Asis de AM & Omasa K 2007. Estimation of vegetation parameter for modelling soil erosion using linear Soectral Mixture Analysis of Landsat ETM data. *ISPRS Journal of Photogrammetry and Remote Sensing* 62: 309-324.

Bakker AC & Emerson WW 1973. The comparative effects of exchangeable calcium, magnesium and sodium on some physical properties of red-brown earth subsoils. II. The spontaneous dispersion of aggregates in water. *Australian Journal of Soil Research.* 11: 151-157.

Batten GD 1998. Plant analysis using near infrared reflectance spectroscopy: the potential and the limitations. *Australian Journal of Experimental Agriculture* 38: 697-706.

Beckedahl HR 1996. Subsurface soil erosion phenomena in Transkei and southern Kwazulu-Natal, RSA. Doctoral dissertation. Pietermaritzburg: University of Kwazulu-Natal, Department of Environmental Sciences.

Bellon-Maurel V, Fernandez-Ahumada E, Palagos B, Roger JM, Mcbratney A 2010. Critical review of chemometric indicators commonly used for assessing the quality of the prediction of soil attributes by NIR spectroscopy. *Trends in Analytical Chemistry*. 29: 1073-1081.

Ben-Dor E & Banin A 1995. Near infrared analysis as a rapid method to simultaneously evaluate several soil properties. *Soil Science Society of America Journal.* 59: 364-372.

Blanco M & Villarroya I 2002. NIR spectroscopy: A rapid-response analytical tool. *Trends in Analytical Chemistry.* 21: 240-250.

Blong RJ, Graham OP & Veness JA 1982. The role of sidewall processes in gully development; some N.S.W. examples. *Earth Surface Processes and Landforms.* 7: 381-385.

Boardman J, Foster I, Rowntree K, Mighall T & Gates J 2010. Environmental stress and landscape recovery in a semi-arid area, The Karoo, South Africa. *Scottish Geographical Journal* 126(2): 64-75.

Boardman J, Parsons AJ, Holland R, Holmes PJ & Washington R 2003. Development of badlands and gullies in the Sneeuberg, Great Karoo, SouthAfrica. *Catena* 50: 165-184.

Bond WJ, Stock WD & Hoffman MT 1994. Has the Karoo Spread? A test for desertification using carbon isotopes from soils. *South African Journal of Science.* 90: 391–397.

Boucher SC & Powell JM 1994. Gullying and tunnel erosion. *Victoria Australian Geographical Studies.* 32: 17-26.

Bradford JM & Piest RF 1985. Erosional development of valley-bottom gullies in the Upper Midwestern United States. In Coates DR & Vitek JD (eds.) *Thresholds in Geomorphology, 75-101*. London: Allen & Unwin.

Brady NC 1990. *The nature of properties and soils. 10th ed*. New York: Macmillan publishing company.

Brown DJ, Shepherd KD, Walsh MG, Dewayne Mays M & Reinsch TG 2006. Global soil characterization with VNIR diffuse reflectance spectroscopy. *Geoderma.* 132: 273-290.

Brubaker SC, Holzhey CS & Brasher BR 1992. Estimating the Water-Dispersible Clay Content of Soils. *Soil Science Society of America Journal*. 56: 1226-1232.

Buchanan 2008. Recent advances in the use of Near IR spectroscopy in the petrochemical industry. In Burns DA & Ciurczak EW (eds) *Handbook of Near Infrared analysis. 3rd edition*, 521-528. Florida: CRC Press.

Carnicelli S, Benvenuti M, Ferrari G & Sagri M 2009. Dynamics and driving factors of late Hoocene gullying in the Main Ethopian Rift (MER). *Geomorphology* 103: 541-554.

Casalf J, Loizu J, Campo MA, De-Santisteban LM, & Alvarez-Mozos J 2006. Accuracy of methods for field assessment on rill and ephemeral gully erosion. *Catena* 67:128-138.

Cerdà A 1999. Parent material and vegetation affect soil erosion in eastern Spain. *Soil Science Society of America Journal*. 63: 362-368.

Champion AM 1933. Soil Erosion in Africa. The Geographical Journal. Vol 82:130-139.

Chang CW, Laird DA, Mausbach MJ & Hurburgh Jr CR 2001. Near-Infrared Reflectance Spectroscopy – Principal Components Regression Analyses of Soil Properties. *Soil Science Society of America Journal.* 65: 480-490.

Chang CW & Laird DA 2002. Near-infrared reflectance spectroscopy analysis of soil C and N. *Soil Science.* 167: 110-116.

Ciurczak 2008. Process Analytical Technologies (PAT) in the pharmaceutical Industry. In Burns DA & Ciurczak EW (eds) *Handbook of Near Infrared analysis. 3rd edition,* 581-584. Florida: CRC Press.

Clark RN 1999. Spectroscopy of rocks and minerals, and princi-ples of spectroscopy. In Rencz N (Ed.) *Remote Sensing for the Earth Sciences: Manual of Remote Sensing*, 3-52. New York: John Wiley & Sons.

Cobban DA & Weaver A van B. A preliminary investigation of the gully features in the Tsolwana Game Reserve, Ciskei, Southern Africa. *RSAn Geographical Journal.* 75:14–21.

Collison AJC 1996. Unsaturated strength and preferential flow as controls on gully head development. In Anderson MG & Brooks SM (eds.) *Advances in Hillslope Processes, 639-709.* London: Wiley.

Collison AJC 2001. The cycle of instability: stress release and fissure flow as controls on gully head retreat. *Hydrological Processes.* 15: 3-12.

Cooke MJ, Stern LA, Banner L, Mack LE, Stafford Jr TW & Toomey III RS 2003. Precise timing and rate massive late Quaternary soil denudation. *Geology* 31: 853-856.

Cozzolino D & Morón A 2010. The potential of near-infrared reflectance spectroscopy to analyse soil chemical and physical characteristics. *Journal of agricultural Science* 140: 65-71.

DERM (Department of Environment and Resource Management) 2010. *Contour bank specifications.* [online]. DERM. Available from http://soils.usda.gov/technical/manual/contents/chapter3.html [Accessed 2 October 2012].

Descrouix L, Gonzáles Barrios JL, Viramontes D, Poulenard J, Anaya E, Esteves M & Estrada J. Gully and sheet erosion on subtropical mountain slopes: Their respective roles and the scale effect. *Catena.* 72: 325-339.

Dunn BW, Beecher HG, Batten GD & Ciavarella S 2002. The potential of near-infrared reflectance spectroscopy for soil analysis – A case study from the Rierine Plain of south-eastern Australia. *Australian Journal of experimental Agriculture.* 42: 607-614.

Emmerson WW & Smith BH 1970. Magnesium, organic matter and structure. *Nature.* 228: 453-454.
Garland G & Broderick D. Changes in the extent of erosion in the Tugela catchment, 1944–1981. *South African Geographical Journal*. 74: 45–48.

Esteves M, Descrouix L, Mathys N & Lapetite JM 2005. Soil hydrfaulic properties in a marly catchment (Draix, France). *Catena* 63: 282-298.

Faulkner H, Alexander R, Teeuw R & Zukowskyj P 2004. Variations in soil dispersivity across a gully head displaying shallow sub-surface pipes, and the role of shallow pipes in rill initiation. *Earth Surface Processes and Landforms* 9: 1143-1160.

Foster 1986. *Understanding ephemeral gully erosion,* Soil Conservation 2. Washington DC: National academy of Science Press, 90-125.

Gardner WD 1980. Field assessment of sediment traps. *Journal of Marine Research.* 38:41-52.

Garland G & Broderick D 1992. Changes in the extent of erosion in the Tugela catchment, 1944-1981. *South African Geographical Journal* 74:45-48.

Ghosh & Rogers, 2008. NIR analysis of textiles. In Burns DA & Ciurczak EW (eds) *Handbook of Near Infrared analysis. 3rd edition,* 485-520. Florida: CRC Press.

Gomez B, Banbury K, Marden M, Trustrum NA, Peacock DH & Hoskin PJ 2003. Gully erosion and sediment production: Te Weraroa Stream, New Zealand. *Water Resources Research.* 39: 1187-1194.

Gomez C, Viscarra Rossel RA, McBratney AB 2008. Soil organic carbon prediction by hyperspectral remote sensing andfield vis-NIR spectroscopy: An Australian case study. *Geoderma* 146: 403-411.

Graaff van de R & Patterson RA 2001. Explaining the mysteries of salinity, sodicity, SAR and ESP. In Patterson RA & Jones MJ (eds) in *Proceedings of on-site '01 conference: Advancing on-site wastewater systems*), 361-368. Amidale: Lanfax Laboratories.

Gyssels G & Poesen J 2003. The importance of plant root characteristics in controlling concentrated flow erosion rates. *Earth Surface Processes and Landforms* 28:371-384.

Hammersley & Townsend, 2008. NIR analysis of wool. In Burns DA & Ciurczak EW (eds) *Handbook of Near Infrared analysis. 3rd edition,* 465-478. Florida: CRC Press.

Hauge C 1977. Soil erosion definitions. *California Geology*. 30:202-203.

He Y, Huang M, Garcıa A, Hernandez A & Song H. Prediction of soil macronutrients content using near-infrared spectroscopy. *Computers and Electronics in Agriculture.* 58: 144-153.

Hessel R 2002. Modelling soil erosion in a small catchment on the Chinese Loess Plateau. Applying LISEM to extreme conditions.Doctoral dissertation. Utrecht. Untrecht University and Koninklijk Nederlands Aardrijkskundig Genootschap, Department of Geographical Sciences.

Hjulstrom F 1935. The morphological activity of rivers as illustrated by river Fyris. Doctoral dissertation. Uppsala. Uppsala University. Geographical Department.

Hoffman MT, Cousins B, Meyer T, Petersen A & Hendricks H 1999b. Historical and contemporary land use and the desertification of the Karoo. In WRJ Dean & Milton SJ (eds.) *The Karoo: Ecological Patterns and Processes,* 257-273. Cambridge: Cambridge University Press.

Hoffman MT & ToddS 2000. A national review of land degradation in RSA: The influence of biophysical and socio-economic factors. *Journal of South African Studies*. 26: 743-758.

Holy M & Cowan M (1982). *Soil Erosion.* Czechoslovakia: Forest Research Insitute.

Horton RE 1945. Erosional development of streams and their drainage basins: hydrophysical approach to quantitative morphology. *Geological Society of America Bulletin* 56: 275-370.

Igwe CA & Udegbunam ON 2008. Soil properties influencing water-dispersible clay and silt in an Ultisol in southern Nigeria. *International Agrophysics.* 22: 319-325.

Imeson AC & Kwaad FJ 1980. Gully types and gully prediction. *Geografisch Tijdschrift.*14: 430-441.

Islam K., Singh B & McBratney AB 2003. Simultaneous estimation of various soil properties by ultra-violet, visible and near-infrared reflectance spectroscopy. *Australian Journal of Soil Research.* 41: 1101-1114.

Janeau JL, Bricquet JP & Planchon O 2003. Soil crusting and infiltration on steep slopes in northern Thailand. *European Journal of Soil Science* 54: 543-554.

Janik LJ, Merry RH & Skjemstad JO 1998. Can mid infra-red diffuse reflectance analysis replace soil extractions? *Australian. Journal of Experimental Agriculture.* 38: 681-696.

Jones JAA 1994. Soil piping and its hydrogeomorphic function. *Cuaternario Geomorfología* 8: 3 – 4.

Kakembo 2001. Trends in Vegetation Degradation in Relation to Land Tenure, Rainfall, and Population Changes in Peddie District, Eastern Cape, RSA. *Environmental Management*. 28: 39-46.

Kakembo V & Rowntree 2003. The relationship between land use and soil erosion in the communal lands near Peddie town, Eastern Cape, South Africa. *Land degradation and Development* 14: 39-49.

Kakembo V, Xanga WW & Rowntree K 2009. Topographic thresholds in gully development on the hillslopes of communal areas in Ngqushwa Local Municipality, Eastern Cape, RSA. *Geomorphology*. 110: 188-194.

Keay-Bright J & Boardman J 2009. Evidence from field-based studies of rates of soil erosion on degraded land in the central Karoo, RSA. *Geomorphology*. 103: 455-465.

King C, Baghdadi N, Lecomte V & Cerdan O 2005. The application of remote sensing data monitoring and modelling soil erosion. *Catena* 62: 79-93.

Kirkby MJ & Bracken LJ 2009. Gully processes and gully dynamics. *Earth Surface and Process Landforms* 34: 1841-1851.

Knudsen D, Peterson GA & Pratt PF 1982. Lithium, sodium and potassium. In Page AL, Miller RH & Keeney DR (eds) *Methods of Soil Analysis Part 2.* 2nd ed. Madison: Soil Science Society of America.

Kosmas C, Danalatos N, Cammeraat LH, Chabart M, Daimontopoulos J, Farand R, Guitierrez L, Jacob A, Marques H, Martinez-Fernandez J, Mizara A, Moustakas N, Nicolau JM, Oliveros C, Pinna G, Puddu R, Puigdefabregas J, Roxo M, Simao A, Stamou G, Tomasi N, Usai D & Vacca A. The effect of land use on runoff and soil erosion rates under Mediterranean conditions. *Catena* 29: 45-59.

Kosov BF, Nikol'skaya II & Zorina YF 1978. Eksperimental'nyye issledovaniya ovragoobrazovaniya. In Makkaveev NI (ed.) *Eksperimental'naya geomorfologiya 3rd ed,* 113-140. Moscow: Moscow University.

Kradjel & Lee, 2008. NIR analysis of polymers in In Burns DA & Ciurczak EW (eds) *Handbook of Near Infrared analysis. 3rd edition,* 529-568. Florida: CRC Press.

Laflen JM, Watson DA & Franti TG (eds) 1985. *Effect of tillage systems on concentrated flow erosion*. Proceedings of the Fourth International Conference on Soil Conservation held 3-8 November. Maracay, Venezuela.

Lal R 2001. Soil degradation by erosion. *Land degradation and development.* 12: 519-539.

Laker 2004. Advances in soil erosion, soil conservation, land suitability evaluation and land use planning research in RSA. *South African Journal of Plant and Soil.* 21: 345-368.

Le Roux JJ, Morgenhtal TL, Malherbe J, Pretorius DJ & Summer PD 2008. Water erosion prediction at a national scale for RSA. *Water RSA.* 34: 305-314.

Lesschen JP, Kok K, Verburg PH & Cammeraat LH 2007. Identification of vulnerable areas for gully erosion under different scenarios of land abandonment in Southeast Spain. *Catena.* 71: 110-121.

Macvicar CN & De Villiers JM 1991.*Grondklassifikasie: n Taksonomiese sisteem vir Suid Afrika*. Republiek van Suid Afrika: Die Departement van lanbou-ontwikkeling.

Malley DF, Hauser BW, Williams PC & Hall J 1996. Prediction of organic carbon, nitrogen and phosphorus in freshwater sediments using near infrared reflectance spectroscopy..In Davies AMC,

Williams P. (eds) *Near Infrared Spectroscopy: the Future Waves,* 691-699. Chichester: NIR Publications.

Malley DF, Martin PD & Ben-Dor E 2004. Analysis of soils in Near-Infrared Spectroscopy in Agriculture. In (eds) Al-Amoodi L, Barbarick KA, Dick WA, Roberts CA, Workman Jnr J, Reeves III JB Publishers (eds) *Near-Infrared Spectroscopy in Agriculture,* 729-784. Wisconsin: American Society of Agronomy Incorporated, Crop Science society of America Incorporated & Soil Science Society of America Incorporated.

Malley DF, Martin PD, McClintock LM, Yesmin L, Eilers RG, & Haulschak P 2000. Feasibility of analysing archived Canadian prairie agricultural soils by near infrared reflectance spectroscopy. In Davies AMC & Gaingiacomo R (eds) *Near infrared spectroscopy,* 579-585. Proceedings of the 9th International Conference, Chicester: NIR publications.

Malley DF & Yesmin L 2002. Unpublished data. In (eds) Al-Amoodi L, Barbarick KA, Dick WA, Roberts CA, Workman Jnr J, Reeves III JB Publishers (eds) *Near-Infrared Spectroscopy in Agriculture,* 729-784. Wisconsin: American Society of Agronomy Incorporated, Crop Science society of America Incorporated & Soil Science Society of America Incorporated.

Martinez-Casasnovas JA, Anton-Fernandez C & Ramos MC 2003. Sediment production in large gullies of the Mediterraneanarea (NE Spain) from high-resolution digital elevation models and geographical information systems analysis. *Earth Surface Processes and Landforms.* 28: 443-456.

Martinez-Casanovas JA, Ramos MC & Garcia-Hernandez D 2009. Effects of land-use changes in vegetation cover and sidewall erosion in a gully head of the Penedes region (northeast Spain). *Earth Surface Processes and Landforms.* 35: 1927-1937.

Martinez-Casasnovas JA, Ramos MC & Poesen J 2004. Assessment of sidewall erosion in large gullies using multi-temporal DEMs and logistic regression analysis. *Geomorphology*. 58: 305- 321.

Mashimbye ZA 2013. Remote sensing of salt-affected soils. Doctoral dissertation. Stellenbosch: University of Stellenbosch, Soil Science Department.

Mashimbye ZA, De Clercq WP, Van Niekerk A & Nieuwoudt H (*in press*). Near-infrared spectroscopic and chemometric modelling of saline soils.

Mataix-Solera J, Arcenegui V, Tessler N, Zornoza R, Wittenberg L, Martínez C, Caselles C, Pérez-Bejarano A, Malkinson D & Jordán MM (*In press*). Soil properties as key factors controlling water repellency in fire-affected areas: Evidences from burned sites in Spain and Israel. *Catena. In press*

Mcbride MB 1994. *Environmental Chemistry of soils*. New York: Oxford University Press.

McCarty GW, Reeves JB, Reeves VB, Follett RF & Kimble JM 2002. Mid-Infrared and Near-Infrared Diffuse Reflectance Spectroscopy for Soil Carbon Measurement. *Soil Science Society of America Journal*. 66: 640-646.

McCarty GW & Reeves III JB 2006. Comparison of Near-Infrared and mid infrared diffuse reflectance spectroscopy for field scale measurement of soil fertility parameters. *Soil Science*. 171: 94-102.

McDowell ML, Bruland GL, Deenik JL ,Grunwald S, Knox NM 2012. Soil total carbon analysis in Hawaiian soils with visible, near-infrared and mid-infrared diffuse reflectance spectroscopy. *Geoderma*. 189: 312–320.

McNeal BL, Layfield DA, Norvell WA & Rhoades JD 1968. Factors influencing hydraulic conductivity of soils in the presence of mixed salts solutions. *Soil Science Society of America Proceedings.* 32: 187-190.

Meadows ME 2003. Soil erosion in the Swartland, Western Cape Province, RSA: implications of past and present policy practices. *Environmental Science and Policy.* 6: 17-28.

Meadows ME & Hoffman MT 2003. The nature, extent and causes of land degradation in RSA: legacy of the past, lessons for the future? *Area*. 34: 428-437.

Mian L, Wenyi Y, Wenfeng D, Yang J & Jingnan 2009. Effect of grass coverage on sediment yield in the hill-slope gully side erosion system. *Journal of Geographical Sciences.* 19: 321-330.

Miller CE 2001. Chemical principles of near unfrared technology. In Williams P & Norris K (eds) *Near infrared technology in the agricultural and food industries*, 10-39. Minnesota: The American Association of Cereal Chemists Incorporated.

Morgan RPC 2005. *Soil Erosion and Conservation*. 3rd ed. Oxford: Blackwell.

Morgan RPC, McIntyre K, Vickers AW, Quinton JN & RJ Rickson 1997. A rainfall simulation study of soil erosion on rangeland in Swaziland. *Soil Technology.* 11: 291-299.

Newgard EC 2005. Near-Infrared Spectroscopy for Analysis of Agricultural Material [online]. Illinois: University of Illinois at Urnama-Champaign. Available from http://online.physics.uiuc.edu/courses/phys598OS/fall05/FinalReportFiles/EricNewgardTermPaper.pdf [Accessed 16 June 2012].

Ning S, Chang N, Jeng K & Tseng Y 2006. Soil erosion and non-point source pollution impact assessments with the aid of multi-temporal remote sensing images. *Journal of Environmental Management* 79: 88-101.

Noguras P, Burjachs F, Gallart F & Puigdefàbregas J 2000. Recent gully erosion in the El Cautivo badlands (Tabernas, SE Spain). *Catena*. 40: 203-215.

Nordstrom K 1988. *Gully erosion in the Lesotho lowlands, UNGI Rapport 69*. Uppsala: Uppsala Univeristy.

Oostwoud Wijdenes DJ, Poesen J & Vandekerckhove L 2000. Spatial distribution of gully head activity and sediment supply along an ephemeral channel in a Mediterranean environment. *Catena*. 39: 147-167.

Øygarden L 2003. Rill and gully development during an extreme winter runoff event in Norway. *Catena* 50: 217 – 242.

Özgür Y & Göktas A 2002. A comparison of partial least squares regression with other prediction methods. *Hacettepe Journal of Mathematics and Statistics*. 31: 99-111.

Pasquini C 2003. Near Infrared Spectroscopy: Fundamentals, Practical Aspects and Analytical Applications. *Journal of the Brazilian Chemistry Society*. 14: 198-219.

Piest RF, Bradford JM & Spomer RG 1975. Mechanisms of erosion and sediment movement from gullies. In *Present and Prospective Technology for Predicting Sediment Yields and Sources*, 162-176. Washington DC: United States Department of Agriculture.

Pierson SM, Rosenbaum BJ, Lucinda DM & Dewald TG 2008. Strahler Stream Order and Strahler Calculator Values in NHDPlus [online]. United States Geological Survey. Available from ftp://ftp.horizon-systems.com/nhdplus/NHDPlusV1/NHDPlusExtensions/SOSC/SOSC_technical_paper.pdf. [Accessed 2 September 2012]

Podwojeski P, Poulenard J, Zambrana T & Hofstede R 2002. Overgrazing effects on vegetation cover and properties of volcanic ash soil on the paramo of Llangahua and La Esperanza (Tungurahua, Ecuador). *Soil Use and Management*. 18: 45-55.

Poesen J 1993. Gully typology and gully control measures in the European loess belt. In: Wicherek S (Ed) *Farm Land Erosion In Temperate Plains Environment and Hills, 221-239*. Amsterdam: Elsevier.

Poesen J & Hooke JM 1997. Erosion, flooding and channel management in Mediterranean environments of Southern Europe. *Progress in Physical Geography*. 21: 157-199.

Poesen J, Nachtergaele J, Verstraeten G & Valentin C 2003. Gully erosion and environmental change: Importance and research needs. *Catena*. 50: 91-133.

Poesen J, Vandaele K & Van Wesemael B 1996. Contribution of gully erosion to sediment production on cultivated lands and rangelands. In DE Walling & Webb BW (eds) *Erosion and Sediment Yield: Global and Regional Perspectives,* 251-266. Wallingford: IAHS Press.

Poesen, J, Vandekerckhove L, Nachtergaele J, Oostwoud Wijdenes DJ, Verstraeten G & Wesemael van B 2002. Gully erosion in dryland environments. In Bull LJ, Kirkby MJ (eds.) *Dryland Rivers: Hydrology and Geomorphology of Semi-Arid Channels,* 229-262. Chichester: Wiley.

Prosser JP, Chappel JMA & Gillespie R 1994. Holocene valley aggradation and gully erosion in headwater catchments, southeastern highlands of Australia. *Earth Surface Processes and Landforms* 19: 465-480.

Rahman AW & Rowell DL 1979. The influence of magnesium in saline and sodic soils: a specific effect or a problem of cation exchange? *Journal of soil science.* 30: 535-546.

Rayment, GE & Higginson FR 1992. *Australian Laboratory Handbook of Soil and Water Chemical Methods*., Australia: Inkata Press.

Reeves III JB, Follett RF, McCarty GW & Kimble JM 2006. Can Near or Mid-Infrared Diffuse Reflectance Spectroscopy Be Used to Determine Soil Carbon Pools? *Communications in Soil Science and Plant Analysis.* 37: 2307-2325.

Reeves III JB, McCarty GW 2001. Quantitative analysis ofagricultural soils using near infrared reflectance spectroscopyand fibre-optic probe. *Journal of Near Infrared Spectroscopy*. 9: 25-34.

Reeves III JB, McCarty GW & Meisinger JJ 1999. Near infrared reflectance spectroscopy for the analysis of agricultural soils. *Journal of near infrared spectroscopy.* 7: 179-193.

Rengasamy P, Greene RSB & Ford GW 1986. Influence of magnesium on aggregate stability in sodic red-brown earths. *Australian Journal Soil Research.* 24: 229-237.

Rey F 2003. Influence of vegetation distribution on sediment yield in forested marly gullies. *Catena.* 50: 549-562.

Rienks SM, Botha GA & Hughes JC 2000. Some physical and chemical properties of sediments exposed in a gully (donga) in northern KwaZulu-Natal, RSA and their relationship to the erodibility of the colluvial layers. *Catena*. 39: 11-31.

Rooyani F 1985. A note on soil properties influencing piping at the contact zone between albic and argillic horizons of certain duplex soils (Aqualfs) in Lesotho, southern Africa. *Soil Science* 139: 517-522.

Ross RS 1995. Recommended Methods for Determining Soil Cation Exchange Capacity. In Sims JT & Wolf A (eds) Recommended soil testing procedures for the northeastern United States. 2nd edition, 62-69. Denver: University of Delaware Press.

Rustomji P 2006. Analysis of gully dimensions and sediment texture from southeast Australia for catchment sediment budgeting. *Catena*. 67: 119-127.

Samani NAA, Hasan A, Mohammed J & Jamal G 2009. Sediment sourcing of gully erosion and factors affecting it in small catchments. *Physical Geography Research Quaterly* 69: 19-34.

Satellite Imaging Corporation 2012. Characterisation of satellite remote sensing systems. Available from http://www.satimagingcorp.com/characterization-of-satellite-remote-sensing-systems.html [Accessed 2 July 2013]

Seilsepour M Rashidi & BG Khabbaz 2009. Prediction of Soil Exchangeable Sodium Percentage Based on Soil Sodium Adsorption Ratio. *American-Eurasian Journal of Agriculture and Environmental Science*. 5: 1-4.

Shepherd KD & Walsh MG 2002. Development of Reflectance Spectral Libraries for Characterization of Soil Properties. *Soil Science Society of America Journal*. 66: 988–998.

Shibusawa S, Imade Anom SW, Sato S, Sasao A & Hirako S 2001. Soil mapping using the real-time soil spectrophotometer.In Grenier, G, Blackmore S (Eds.) *European Conference on Precision Africulrure. 1st edition,* 497-508. Third European Conference on Precision Agriculture. France: Agro Montpellier.

Sidorchuk A 1999. Dynamic and staticmodels of gully erosion. *Catena*. 37: 401-414.

Sidorchuk A, Märker M, Moretti S & Rodolfi G 2003. Gully erosion modelling and landscape response in Mbuluzi River catchment of Swaziland. *Catena* 50:507-525.

Siesler HW 2008. Basic Principles of Near-Infrared Spectrometry. In Burns DA & Ciurczak EW (eds) *Handbook of Near Infrared analysis. 3rd edition, 7-21*. Florida: CRC Press.

Skjemstad JO, Clarke P, Golchin A & Oades JM 1997. Characterisation of soil organic matter by solid state NMR Spectroscopy. In Gadish G & Miller KE (eds) *Driven by Nature: Plant litter quality and decomposition*, 53-271. Wellington UK: CAB International.

Soil Science Society of America 2013. Glossary of soil science terms. Available from https://www.soils.org/publications/soils-glossary/1872 [Accessed 20 July 2013]

Soms J 2006. Regularities of gully erosion network development and spatial distribution in south-eastern Latvia. *Balitica.* 19: 72-79.

Sonneveld MPW, Everson TM & Veldkamp A 2005. Multi-scale analysis of soil erosion dynamics in Kwazulu-Natal, RSA. *Land Degradation and Development.* 16: 287-301.

Souchère V 1995. Spatial model for overland flow in the aim of the development of talweg protection against erosion; application for small cathments in Pays de Caux (upper Normandie). Doctoral dissertation. Paris: Institut National Agronomique Paris-Grignon.

Sparks DL 2003. *Environmental Soil Chemistry*. 2nd edition. United States: Elsevier Science Academic Press.

Sternberg B, Viscarra Rossel RA, Mouazen AM & Wetterlind J 2010. Visible and near infrared spectroscopy in soil science.In Sparks L (ed) *Advances in Agronomy, 1*07: 163-215. Burlington: Academic Press.

Steudel T, Bugan R, Kipka H, Pfenning B, Fink M, De Clercq WP, Flügel WA & Helmschrot J (*in press)*. Implementing contour farming practices to improve hydrological and erosion modelling in semi-arid South Africa.

Strahler AN 1964. Quantitive geomorphology of drainage basins and channel networks. In Chow VT (ed.) *Handbook of applied hydrology* Section 4. New York: McCaw Hill Book Company.

Sundborg A. 1956. The River Klaralven. A Study of Fluvial Processes. *Geografiska Annaler*. 38: 165-221.

Svoray T & Markovitch H 2009. Catchment scale analysis of the effect of topography, tillage direction and unpaved roads on ephemeral gully incision. *Earth Surface Processes and Landforms*. 34: 1970-1984.

Talbot 1947. *Swartland and Sandveld: A survey of the land utilization and soil erosion in the western lowland of the cape province.* Cape Town: Oxford University Press.

Tanji KK 1990. *Agricultural Salinity Assessment and Management (Asce Manual and Reports on Engineering Practice).* New York: American Society of of Civil Engineers.

USDA (United States Department of Agriculture) 2003. *Soil Survey Manuel 2003.* [online]. USDA. Available from http://soils.usda.gov/technical/manual/contents/chapter3.html [Accessed 30 September 2012].

Valentin C, Poesen J & Yong L 2005. Gully erosion: Impacts, factors and control. *Catena*. 63: 132-153.

Vandaele K, Poesen J, Govers G & Van Wesemael B 1996. Geomorphic threshold conditions for ephemeral gully incision. *Geomorphology*. 16: 161-173.

Vandekerckhove L, Poesen J, Oostwoud Wijdenes DJ, Nachtergaele J, Kosmas C, Roxo MJ & Figueiredo de T 2000. Thresholds for gully initiation and sedimentation in Mediterranean Europe. *Earth Surface Processes and Landforms*. 25: 1201-1220.

Vanwalleghem T, Poesen J, Nachtergaele J & Verstraeten G 2005. Characteristics controlling factors and importance of deep gullies under cropland on loess-derived soils. *Geomorphology*. 69: 76-91.

Van Zijl M 2010. An investigation of the soil properties controlling gully erosion in a sub-catchment in Maphutseng, Lesotho. Master's thesis. Stellenbosch: University of Stellenbosch, Soil Science Department.

Verster E, Du Plessis W, Fuggle RF & Schloms BHA 2009. Soil. In Strydom HA & King ND (eds) *Fuggle and Rabie's Environmental Management in RSA*, 313-342. Cape Town: Juta.

Verstraeten G, Poesen J, Vente de J, Koninckx X 2003. Sediment yield variability in Spain: a quantitative and semiqualitative analysis using reservoir sedimentation rates. *Geomorphology*. 50: 327-348.

Volkan Bilgili A, Es va HM, Akbas F, Durak A & Hively WD. 2010. Visible-near infrared reflectance spectroscopy for assessment of soil properties in a semi-arid area of Turkey. *Journal of Arid Environments*. 74: 229-238.

Viscarra Rossel, R.A. & McBratney, A.B 1998a. Soil chemical analytical accuracy and costs: implications from precision agriculture. *Australian Journal of Experimental Agriculture*. 38: 765-775.

Viscarra Rossel RA & McBratney AB 1998b. Laboratory evaluation of a proximal sensing technique for simultaneous measurement of soil clay and water content. *Geoderma*. 85: 19-39.

Viscarra Rossel RA, Walvoort DJJ, McBratney AB, Janik LJ & Skjemstad JO 2006. Visible, near infrared, mid infrared or combined diffuse reflectance spectroscopy for simultaneous assessment of various soil properties. *Geoderma*. 131: 59-75.

Wakindiki IIC, Mochoge BO & Ben Hur M 2007. Assessment of indigenous soil and water conservation technology for smallholder farms in semi-arid areas in Africa and close spaced trash lines effect on erosion and crop yield.In Bationo A, Waswa B, Kihara B & Kimetu J (Eds.) *Advances in Integrated Soil Fertility Management in sub-Saharan Africa: Challenges and Opportunities*, 805-814. Netherlands: Springer.

Walker DJH 1997. Dispersive soils in Kwazulu-Natal. Master's thesis. Pietermaritzburg: University of Kwazulu-Natal, Department of Environmental Sciences.

Watson HK 2000. Land reform implications of the distribution of badlands in the Mfolozi Catchment, Kwazulu-Natal. *RSAn Geographical Journal*. 79: 27-34.

White RE 1969. On the measurement of soil pH. *Journal of the Australian Institute of Agricultural Science.* 35: 3-14.

Wikipedia 2012. Hjülstrom curve [online]. Wikipedia. Available from http://en.wikipedia.org/wiki/Hjulstr%C3%B6m_curve [Accessed 21 September 2012].

Workman JR 1996. Interpretive Spectroscopy for Near Infrared. *Applied Spectroscopy Reviews.* 31: 251-320.

Xie HT, Yang XM, Drury CF, Yang JY & Zhang XD 2011. Predicting soil organic carbon and total nitrogen using mid- and near-infrared spectra for Brookston clay loam soil in Southwestern Ontario, Canada. *Canadian Journal of Science*. 91: 53-63.

Zornozaa R, Guerreroa C, Mataix-Soleraa J, Scowb KM, Arceneguia V & Mataix-Beneyto J 2008. Near infrared spectroscopy for determination of various physical, chemical and biochemical properties in Mediterranean soils. *Soil Biology and Biochemistry.* 40: 1923-1930.

APPENDICES

Appendix A. Hjülstrom curve

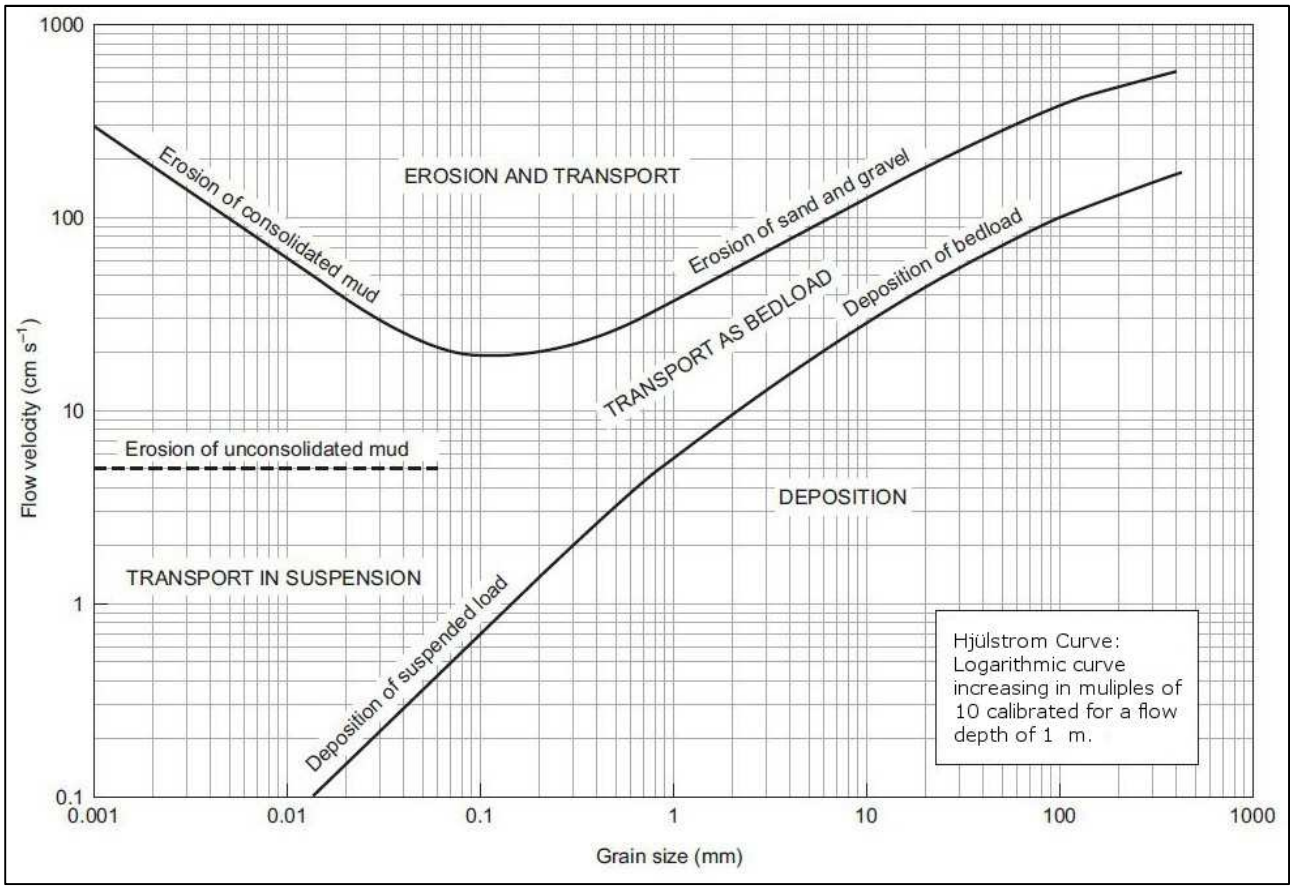

Appendix B: Malansdam gully system. Srahler stream order

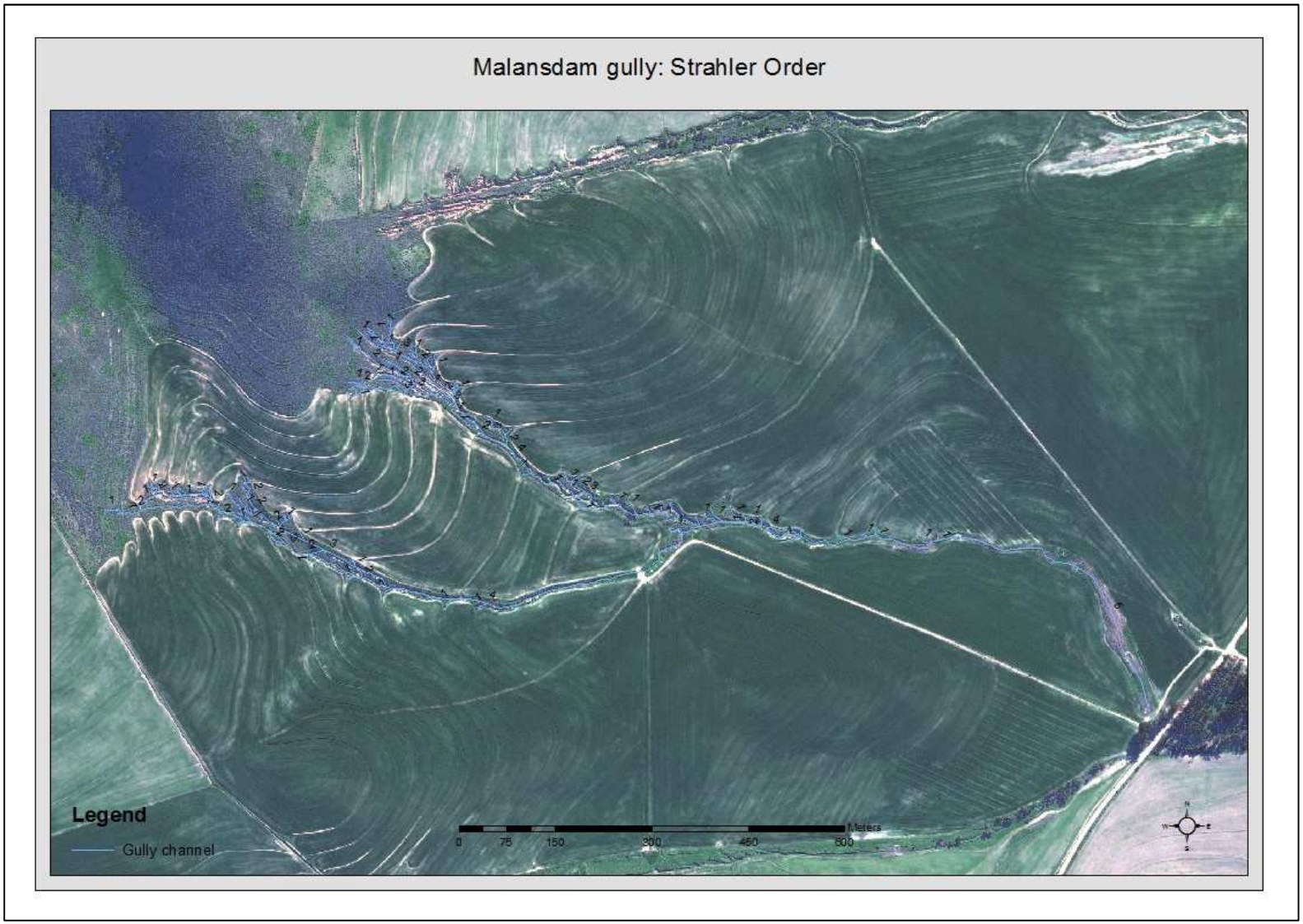

Appendix C: Pre-processed spectra within region selection